Stabilization of Aqueous Template-Based Functionalized Magnetic Nanoparticles

by
Sahar Rahmani

A thesis
presented to the University of Waterloo
in fulfillment of the
thesis requirement for the degree of
Master of Applied Science
in
Chemical Engineering

Waterloo, Ontario, Canada, 2011

Author's Declaration

I hereby declare that I am the sole author of this thesis. This is a true copy of the thesis, including any required final revisions, as accepted by my examiners.

I understand that my thesis may be made electronically available to the public.

Abstract

Magnetic particles have attracted increasing attention in fields ranging from separation processes to electromagnetic information storage an medical application. Various approaches for their synthesis have been developed and studied to satisfy the criteria of production. Improvement and optimization of size, stability, and functionality is of vital importance in biological applications.

The main aspect of project, initially, was to study the application of aqueous functionalized magnetic nanoparticles coupled with high gradient magnetic separation technique for the removal of trace residue of organic contaminants from drinking water. However, the importance of synthesizing stable ferrofluid for this purpose became clear later and took precedence over the initial objective. Different approaches were adopted, such as the incorporation of poly(ethylene glycol) methacrylate, ethylenediamine, and chitosan, to enhance the stability of magnetic particles. However, these surface modifications had unfavorable effect on the stability of initial particles.

In accord with the initial objective of the project, the possibility of utilization of β-cyclodextrin, as organic pollutant entrapment agent, was investigated in preliminary studies conducted on its interaction with a model compound, procaine hydrochloride. The outcomes of these experiments suggest its potential as a

biocompatible removal agent for the elimination of organic pollutant in drinking water system, or other applications that require selective separation of organic compounds.

Acknowledgements

I would like to take this opportunity to convey my deepest appreciation to my supervisor, Dr. K. C. Tam, who gave me the opportunity of explore new possibilities and patiently guided me at every step of this research. Through his invaluable assistance, guidance, and sponsorship I was able to carry out this study to the best of my knowledge and ability.

Special thanks to Dr. Croiset and Dr. Yu for taking the time to review this thesis and provide me with their constructive criticism. Many thanks to Dr. Simon and Dr. Penlidis for giving permission to use their instruments, as well. I am, also, indebted to Ravindra and Yasaman for providing me with the necessary technical training and watched over me as I worked my way to master sample preparation.

I am grateful to all my colleagues and friends, Angela, Fanny, Zhaoling, Neha, Saleem, David, Baoliang, and Yan Nan, who were always there to help me through the vicissitudes of research life and provided an energetic and encouraging environment. Most of all I like to thank Sara, my sister and colleague who never stopped supporting me.

Dedication

I would like to present this thesis to my parents as a small token of appreciation for being by my side during the vicissitudes of these past years, their forgiving hearts, and unconditional love. I am forever grateful and indebted to them for their patience and encouraging attitude as they watch me grow and become who I am today.

Table of Contents

List of Figures

Chapter 1 – Introduction

1.1 Project Motivation

Contamination of freshwater resources has been the subject of extensive researches. The effects of such pollution on living organisms have also been extensively studied. Among them, there is a category that includes trace quantities of ubiquitous natural or synthesized organic compounds. They are referred to as priority organic contaminants. Presence of these contaminants has been noticed only about 70 years ago. This late acknowledgement was due to their low concentrations, making them previously undetectable. In 1965, the first report on their presence in water was published when a steroid ware detected in effluents of wastewater treatment plants (Stumm-Zollinger and Fair, 1965). In the following decades, others reported the presence of similar compounds in aquatic environments (Hignite and Azarnoff, 1977; Tabak *et al.*, 1981; Aherne *et al.*, 1985; Richardson and Bowron, 1985; Aherne and Briggs, 1989; Aherne *et al.*, 1990; Heberer and Stan, 1997).

Priority organic contaminants are associated with toxicological impacts observed on some aquatic organisms (Aherne *et al.*, 1990; Purdom and Mistry, 1994; Henschel *et al.*, 1997; Desbrow *et al.*, 1998; Raloff, 1998; Bart *et al.*, 2006). They contain pharmaceutically active ingredients that are designed to create certain response(s) on targeted species. Hence, they have the potential to cause adverse side effects on non-targeted organisms. The majority of them can interfere with endocrine system

function[1]. Small disturbances in this system's functionality, especially during certain periods, can lead to severe prolonged effects. This group of organic contaminants is referred to as endocrine disrupting compounds (EDCs). Consequently, the presence of EDCs in various aquatic environments, such as wastewater, surface water, sediments, groundwater, and drinking water is of considerable importance (Chang *et al.*, 2009). They include a vast array of compounds that can be divided into several subcategories:

1. hormones, i.e. natural or synthetic estrogens and steroids,
2. pharmaceuticals, i.e. anti-inflammatory, antibiotics, anticancer drugs,
3. personal care products, i.e sun screens, disinfectants, repellents, etc.,
4. herbicides and pesticides,
5. combustion by-products and surfactants.

[1] Normal functions of all organ systems, such as homeostasis, reproduction, metabolism, development, and/or behavior, are regulated by hormones like estrogen, testosterone and/or thyroid.

Over the years, as detection methods have improved, more and more EDCs are being detected. Figure 1-1 illustrates potential pathways that lead to the presence of EDCs in water bodies and Figure 1-2 shows different classes of EDCs that have been reported in aqueous environment. Their presence have been reported in surface and drinking waters in Germany (Heberer and Stan, 1997; Heberer *et al.*, 1997; Heberer *et al.*, 1998; Ternes *et al.*, 1999; Ternes and Hirsch, 2000; Ternes, 2001a; Ternes, 2001b; Jux *et al.*,),

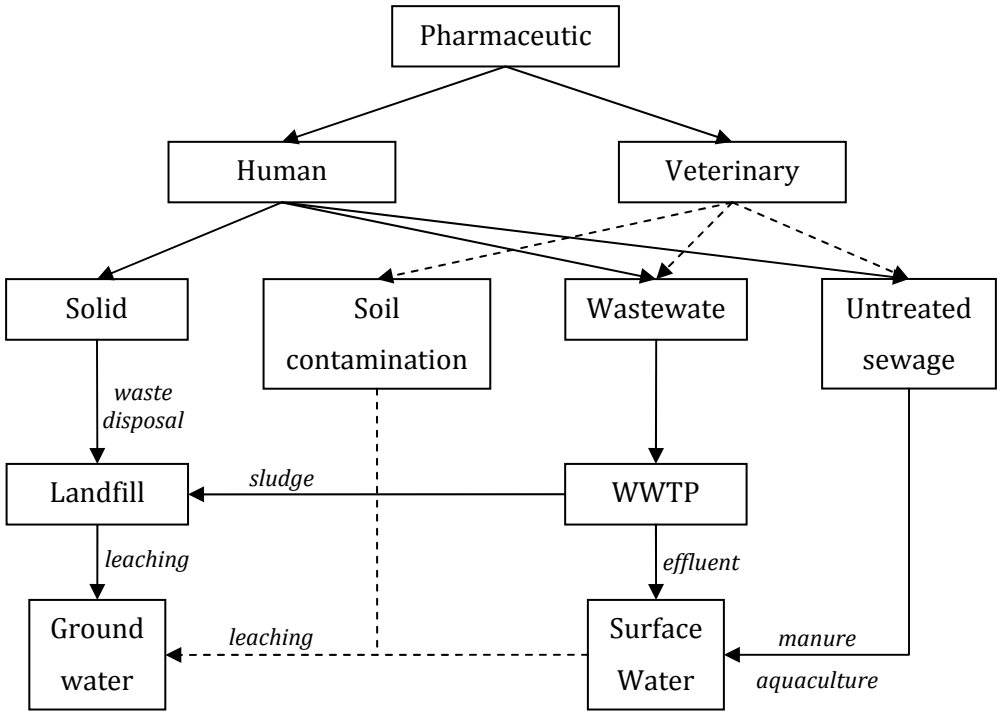

Figure 1-1 Representation of various pathways, from point of consumption to water bodies, for pharmaceuticals. EDCs are primarily released via excretion or disposal to drains, wastewater treatment plant (WWTP) and hospital effluents and runoffs from agricultural, animal, and fish farms or even rain and storm. Insignificant sources such as individual household disposal can also be considered for long term contribution. Urban regions are the major source due to high population density and proximity medical facilities and industries.

Greece (Koutsouba *et al.*, 2003), Brazil (Stumpf *et al.*, 1999; Ternes *et al.*, 1999), Italy (Heberer and Stan, 1997; Perret *et al.*, 2006), South Korea (Kim *et al.*, 2007; Choi *et al.*, 2008; Kim *et al.*, 2009), India (Fick *et al.*, 2009), Austria (Himmelsbach *et al.*, 2003), the UK (Hilton and Thomas, 2003), the US (Boyd *et al.*, 2003; Kumar and Xagoraraki, 2010), Greece (Tsipi *et al.*, 1998; Koutsouba *et al.*, 2003), Spain (Camacho-Muñoz *et al.*, 2010),

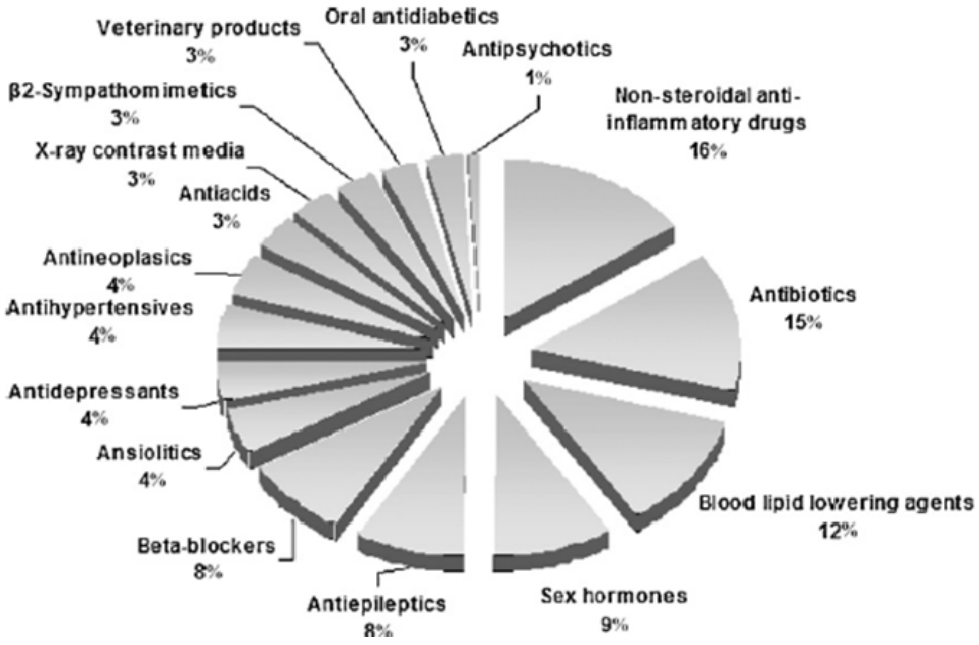

Figure 1-2 Relative percentage of different therapeutic class of pharmaceticals idenified in aquatic environment (Santos *et al.*, 2010)

and Canada (Ternes *et al.*, 1999; Boyd *et al.*, 2003; Metcalfe *et al.*, 2003; Kormos *et al.*, 2006a; Kormos *et al.*, 2006b; Servos *et al.*, 2007a; Servos *et al.*, 2007b; Smyth *et al.*, 2008; Robinson *et al.*, 2009).

Due to the low concentration of EDCs and their metabolites, removal by common treatment methods, i.e. flocculation, coagulation, and sand filtration, is extremely difficult (Nakada *et al.*, 2007). Detection of several EDCs in wastewater treatment plant (WWTP) effluents, groundwater, and drinking waters show that the current treatment protocols are incapable of removing these contaminants effectively (Heberer and Stan, 1996; Ternes *et al.*, 1999). The polar nature of most EDCs not only makes adsorption inefficient but it also results in leakage of these compounds into groundwater aquifers from contaminated sources (Heberer *et al.*, 1998). Though some contaminates are slightly volatile, i.e. musk fragrances, loss by volatilization is insignificant (Larsen *et al.*, 2004). Although in a few case studies, the detected compounds in effluents of WWTP were quantifiable downstream (McDowell *et al.*, 2005; Nakada *et al.*, 2007), most often they passed undetected, which is mainly due to dilution effect. Only advanced treatment processes such as oxidation, activated sludge (Koutsouba *et al.*, 2003; Clara *et al.*, 2005; Miège *et al.*, 2009), activated carbon (Ternes *et al.*, 2002; Liu *et al.*, 2009), and membrane filtration (Yoon *et al.*, 2006) have shown some promises for the partial removal of some EDCs from wastewater effluents. However, some, such as reverse osmosis and nanofiltration, cannot be devised for large scale treatment due to their high cost.

Although EDCs are found in even lower concentrations in distribution systems, their identifications suggest their persistence to treatment processes. Furthermore, these contaminants are not present as individual compounds, but as mixtures. Hence, their

interaction with each other before and during treatment requires comprehensive studies. Additionally, treatment processes, such as ozonation, activated sludge, and UV, apply degradation as a means of removal. Therefore, they transform the known compound into other compound(s), with different nature. These new compounds are invisible to detecting instruments. Thereby, the actual removal efficiency of such processes is questionable. These degradation products, along with unknown metabolites of EDCs, encompass a broad range of chemicals; henceforth, making the determination of all these chemicals and their adverse effects on target and non-target organisms a tedious process which requires lots of time, effort and funding.

At the rate at which these compounds are being introduced to water systems and at which new ones are being developed, such thorough knowledge cannot be gained in time to prevent potential irreversible effects. Beside, drinking contaminated water is not the only exposure route for humans. We can also be exposed by adsorption via skin, for example when swimming, or consumption of contaminated marine products, fish, mussels, oysters, etc. It is suggested that the overall dose of EDCs human can be exposed from fish and drinking water is still lower than the acceptable daily intake value (Cunningham *et al.*, 2009). Hence, it is concluded that the presence of trace concentration of EDCs does not pose appreciable risk to public health (Christensen, 1998; Webb *et al.*, 2003). However, long term exposure to minute concentrations of certain pharmaceuticals, like antibiotics or cytotoxic drugs, may have serious consequences (Oetken *et al.*, 2005; Santos *et al.*, 2010).

Due to the presence of these types of uncertainties and absence of any conclusive health risk report, EDCs occurrence in water is of foremost concern. In view of that, implementation of a method that can effectively remove the majority of EDCs from water bodies, without modifying them and introducing any other unknown contaminants, will assist in reducing the overall toxic load in aquatic environment and their adverse effects. Magnetic separation has shown potentials for purification in many areas, when magnetic particles with proper coating and functionality are devised to bound to desired compounds. Tailoring such particles so that they can couple with a wide range of EDCs and later be separated from water appears to be a sound approach to address this problem.

1.2 Project Objective

Ferrofluids, which are discussed in detail in the next chapter, are colloidal suspension of magnetic nanoparticles (MNPs) and their clusters. They have shown potentials for a range of applications, especially medical applications and separation fields. The majority of ferrofluids consist of magnetite (Fe_3O_4) nanoparticles, coated either with surfactant or polymers. These coatings stabilize the nanoparticles. They also provide a platform for additional surface modification. They possess a large surface-to-volume ratio, which are available without internal pores, avoiding pore diffusion limitation. This makes them more suitable candidates for many adsorption applications compared to porous materials. Aqueous ferrofluids studied in this research consist of magnetite nanoparticles incorporated inside a polymeric template. Surface modification enables

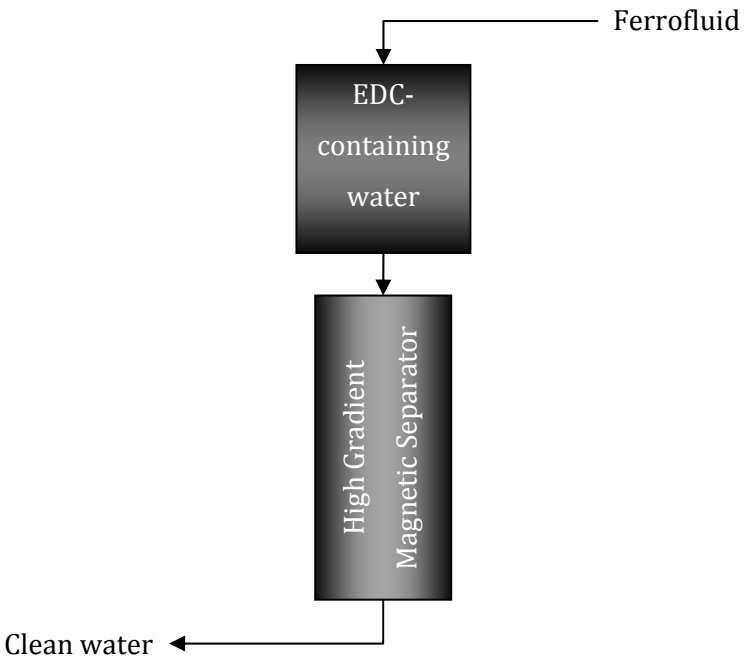

Figure 1-3 Magnetic filtration of EDCs from water with the aid of functionalized magnetic nanoparticles

MNPs to bind with EDCs. When the ferrofluid is introduced to contaminated water, the MNPs bind to the contaminants. Afterward, a simple magnetic filteration through a high gradient magnetic separator leads to the retention of bonded contaminants in the separator while purified water exits the separator (Figure 1-3).

1.3 Organization of Thesis

Chapter 2 provides a background on ferrofluids. Their development, preparation, and various applications are provided through a literature review. More attention is given to the synthesis step selected for the research.

The background and theory behind characterization methods are presented in Chapter 3.

Chapter 4 discusses the synthetic steps for functionalizing the MNPs. Various approaches taken for improving their stability, with or without the introduction of a functional group, are described.

The focus of Chapter 5 is on the results of various analytical studies performed on the MNPs. The most successful products were characterized for their chemical nature, size and surface charge.

Chapter 6 introduces β-cyclodextrin and highlights its potential for removing EDCs by describing its inclusion complexation ability. The procedures for the preparation of drug selective electrode are presented. Then, the results of preliminary studies on β-cyclodextrin inclusion with the sample pharmaceutical, procaine hydrochloride, are reported.

In the last chapter, an overview of the whole research is presented and the final conclusions are summarized. In addition, possible future steps that can be taken towards the preparation of stable template-based aqueous ferrofluids tailored for water treatment and EDC removal are proposed.

Chapter 2 – Magnetic Nanoparticles

2.1 Introduction to Ferrofluids

Ferrofluids are homogenous colloidal suspension of coated magnetic nanoparticles (MNPs), typically 5% v/v (Willard *et al.*, 2004). Figure 2-1 illustrates the schematic of a coated magnetic colloid. The small size of MNPs gives rise to interesting properties that make them particularly suitable for applications in various fields. First of all, it is because of their nano size that the Brownian motion of individual particles and smalls enough colloids can overcome the gravitational, drag, and moderate magnetic field forces; hence maintaining the dispersion of the nanoparticles under most conditions.

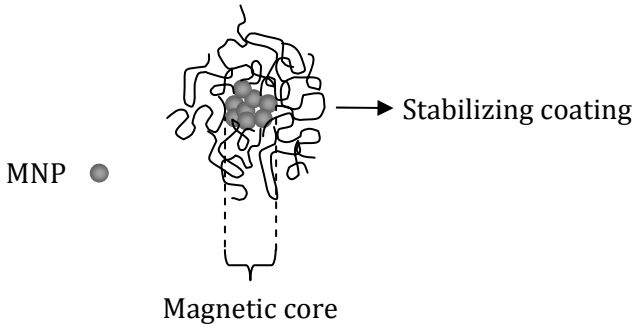

Figure 2-1 The common structre of MNPs colloids in ferrofluids

Furthermore, each of these particles possesses only few domains of randomly oriented magnetic dipole and therefore, has weak magnetization. Hence, the bulk mixture demonstrates superparamagnetism. In other word, ferrofluids show zero magnetization in the absence of magnetic field. Yet, alignment of dipoles leads to

magnetization of the suspension if subjected to strong enough magnetic field. When all the dipoles are aligned their magnetization, saturation magnetization, is often comparable to ferromagnetic materials. Quick demagnetization of particles upon field removal makes this process reversible. Therefore, it offers a straightforward technique for separation applications which require further processing of removed particles, such as in protein and DNA separation.

Moreover, MNPs have surface-to-volume ratio several orders of magnitude larger than their micron-sized siblings, as a result of their size. This non-porous surface eliminates the pore diffusion limitation encountered in many adsorption applications employing porous adsorbent, making MNPs suitable for performing quick adsorption. Nonetheless, it also leads to high surface energy in aqueous medium. Thus, their tendency to coagulate increases.

High saturation magnetization, biocompatibility, better resistance to oxidation, and cheap production cost have made magnetite (Fe_3O_4) the most common magnetic material used in the preparation of MNPs. Nonetheless, other magnetic compounds, such as maghemite (γ-Fe_2O_3), iron, cobalt, zinc, their oxides and alloys ($CoFe_2O_4$), etc. have also been devised.

2.2 Synthesis of Aqueous Ferrofluid

Production of MNP suspensions is an old procedure that has been developed and enhanced over the years. Despite a plethora of techniques that can be utilized to

produce ferrofluids, the principle mechanism for most of them is still the same: the magnetic core is synthesized in the presence of proper stabilizing agent in the desired medium.

MNPs are required to meet several criteria. They have to demonstrate good magnetic response to reduce the intensity of necessary magnetic field and to cause less interruption in process dynamic. In addition, they are required to have zero to low remanence for quick redispersion after the field is removed. Moreover, in many applications they should be considerably small in order to increase available interaction sites or ease their transport. Size, distribution, and many other characteristics of MNPs can be adjusted by process parameters. What follows describes and reviews the methods for the production of water-based ferrofluids.

2.2.1 Wet-grinding:

This mechanical production method is the primary technique for the production of magnetic particles. In this technique, coarse magnetic particles are grounded in the presence of stabilizer in a dispersion medium untill they are in a colloidal state and most of the grounded particles reach the required size. Afterwards, centrifugation separates the larger particles (Hong *et al.*, 2008). However, such procedure is not only very time consuming and demands excessive amount of energy for grounding and separation steps (Odenbach, 2002), but it also yields particles with wide size

distribution and with a variety of morphology. Beside, centrifugation promotes further coagulation.

2.2.2 Chemical Methodologies:

Due to the disadvantages of the grinding technique, chemical reactions have become more common. They offer enhanced homogeneity and cost-effective high-volume production of aqueous ferrofluids in a considerably shorter time. Moreover, they offer easier control over particle size, size distribution, morphology, composition, and structure, simply by manipulating reaction parameters that affect nucleation, growth and coalescence stage, such as temperature, oxidant, concentration, and stirring rate. These techniques commonly incorporate a form of thermal (Barrera *et al.*, 2009) or reductive decomposition of magnetic compound (Willard *et al.*, 2004; Li *et al.*, 2011).

Precipitation reactions are the oldest and most widespread methods for synthesis of nano-size aqueous magnetic particles. In this method magnetic nuclei are formed initially in the aqueous solution of metal salts. Later, addition of a precipitant leads to formation of a supersaturated solution of MNPs. Therefore, they precipitate out of the solution in order to reach thermodynamic equilibrium. When metal oxide is desired, a reducing agent is also added during or after precipitation. Stoichiometric co-precipitation of ferrite and ferric salts, in a basic medium, is most commonly practiced to produce magnetite nanoparticles:

$$Fe^{2+} + 2Fe^{3+} + 8OH^- \xrightarrow{H_2O} Fe_3O_4 + 4\,H_2O$$

However, other procedures and metals, such as cobalt, zinc, nickel, and etc, are also devised to obtain MNP through precipitation reactions (Bacri *et al.*, 1990; Zins *et al.*, 1999).

The size and nature of MNPs depend on the type and concentrations of salts, base, and the rate of addition. The temperature of the reaction also affects the particle size (

Table 1) while its duration influences magnetic parameters, such as magnetic moment and magnetization of particles (Table 2). At ambient temperature, the amount of product reached its maximum after 24 hours at pH 10.5 (Windle *et al.*, 2002), while demonstrating comparably higher effective magnetic moment at basic conditions.

Table 1 Dependence of Particle size on temperature of coprecipitation reaction **(Shimoiizaka, 1978a)**

Reaction temperature, °C	Particle size, nm
60	7
100	9
180	15
250	22
300	28

Table 2 Change of magnetization parameter after precipitation with time **(Blums *et al.*, 1997)**

Reaction time, s	Magnetization, Gs	Magnetic moment, 10^{-16} erg/Oe
15	0.067	0.77
30	0.14	1.03
45	0.25	1.29
60	0.35	1.48
90	0.49	1.71
120	0.57	1.92
180	0.70	2.05
300	0.93	2.36
600	1.05	2.38
∞	1.25	2.40

Precipitation of magnetite is commonly carried out at 80°C to obtain particles of 8–20nm diameter while the mixture is mechanically stirred. Nonetheless, larger particles, 10 –30nm, are produced at lower temperature (e.g. 50°C) from ferrous hydroxyl in ethanol water mixture using an ultrasonic horn (Dang *et al.*, 2009). Slow oxidation of Fe^{2+} in the presence of nitrate ions has also resulted in larger monodisperse particles, 100nm (De Vicente *et al.*, 2000; De Vicente *et al.*, 2010). Precipitation of magnetite at ambient temperature is less often practiced (Lefebure *et al.*, 1998). Moreover, most aqueous magnetite precipitation experiments are conducted under nitrogen purge due to the sensitivity of iron oxide to oxidation. Yet, water-dispersible MNPs have been synthesized in the absence of nitrogen blanket by microwave irradiation (Yangde *et al.*, 2008).

2.3 Stability of Ferrofluids

As a result of attractive magnetic dipolar, Van der Waals forces, and high surface energy, MNPs have high tendency to agglomerate. Agglomeration reduces the mono-dispersity and is not desirable in applications where particle size and dispersity is of importance, such as biological and medical applications. Therefore, MNP coating has attracted lots of attention as a mean to avoid agglomeration by subjecting the particles to enthalpic and/or entropic repulsion.

In water-based MNPs, stability can be achieved by introducing steric and/or electrostatic hindrance (Figure 2-2). The latter is dependent on the surface charge of bare MNPs and is less desirable as it loses efficiency at high pH and high ionic strength. The former, however, is quite robust when proper coating is devised. One of the main factors that should be considered when choosing a coating is its solubility in the medium. An insoluble coating is deemed useless for stabilizing the particles because it breaks down in the carrier liquid. Another factor worth mentioning is the mechanism by which the coating attaches to the magnetic core. It could bind by hydrophobic interaction to particles surface, as in bi-functional water-soluble polymers (Burke *et al.*, 2002), or electrostatic interactions (Ghosh *et al.*, 2011). However, it is very sensitive to electrolytes. Formation of strong spontaneous chelate bond between MNP surface and carboxylic acid has been devised since the early days of ferrofluid production where MNPs were coated with fatty acids (Mikhailik *et al.*, 1991). This attachment technique

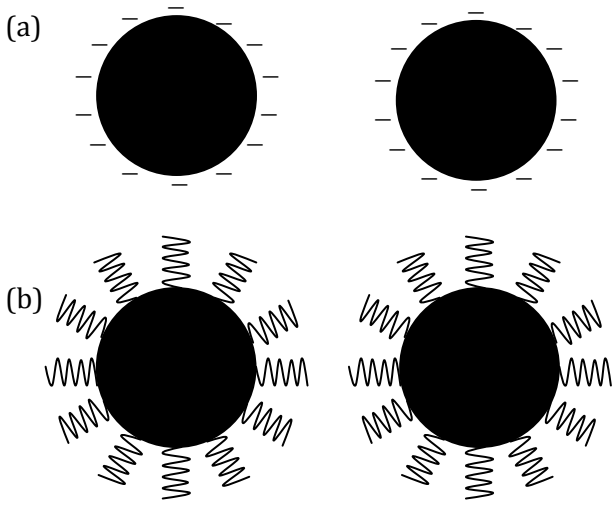

Figure 2-2 Illustration of different approaches to achieve stability (a) electrostatic, and (b) steric

not only is suitable for aqueous condition but also is significantly more persistent to fluctuation in pH and ionic strength.

The oldest and most common method for stabilizing aqueous MNPs is bi-layer surfactant coating (Reimers and Khalafalla, 1972; Shimoiizaka, 1978b; Ramírez and Landfester, 2003). In this approach, the inner layer forms chelate bonds with MNP interface while its hydrophobic interactions with the second layer hold the latter in place. However, these interactions are weak and the outer layer can easily desorb. To overcome this weakness, the two layers can be attached to one another covalently. However, the materials or methods used to achieve such attachment are often too complex or expensive for large scale production. Utilization of phospholipid outer layer enhances the stability as a result of its stronger interaction and adsorption to the inner layer (Horák *et al.*, 2007) compared to organic acids (Ramírez and Landfester, 2003)

and saccharides (Groman and Josephson, 1993; Palmacci and Josephson, 1993). However, even such coatings fail in high electrolyte concentration and are prone to desorption upon the addition of organic compounds that makes them soluble.

In many applications, polymeric coatings have replaced surfactants. They offer a more efficient stabilization and eliminates the need for strong, and yet unstable, non-covalent hydrophobic interaction. The polymer alone can provide simultaneous steric hindrance and electrostatic repulsion. Moreover, it provides a platform for straightforward surface modification to introduce functionality. Dextran (Pardoe *et al.*, 2001; Pankhurst *et al.*, 2003; Carp *et al.*, 2010; Petričenko *et al.*, 2010), poly(vinyl alcohol) (Pardoe *et al.*, 2001; Pankhurst *et al.*, 2003), poly(ethylene glycol) (Hu *et al.*, 2006; Yallapu *et al.*, 2010), poly(methacrylic acid) , poly(styrene) (Ramírez and Landfester, 2003; Tudorachi and Chiriac, 2008; Li *et al.*, 2010), polyacrylamide and poly(acrylic acid) (Jain *et al.*, 2010) are among the most common polymer coatings incorporated on MNPs for the production of stable ferrofluids.

2.4 Coating techniques

There are no ideal or best approaches for stabilizing magnetic colloids. Each approach has its own pros and cons. In every cases, compromises are made between all the desired characteristics, based on their necessity and importance, and the preparation technique is chosen accordingly to obtain the optimal particles that are suitable for the

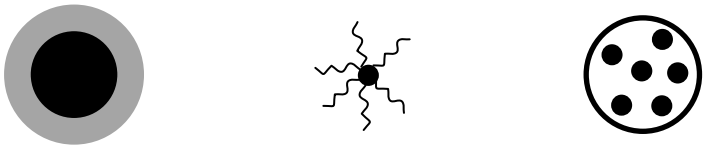

a) Core–shell b) Brush c) Matrix

Figure 2-3 Most common morphology of polymer-coated MNPs

specific application. Here the most common techniques for aqueous stability of magnetic colloids are chosen from a plethora of methods and are described below.

2.4.1 Post-synthesis Coating

Because the presence of monomers and initiators in MNP synthesis reaction mixture affects the nucleation, growth, agglomeration, and precipitation of the particles, many have favored post-synthesis coating of the MNPs. Living radical polymerization techniques are among the most common methods when the polymerization initiates directly on the surface of previously prepared MNPs (Matsuno *et al.*, 2004; Hu *et al.*, 2006; Wang *et al.*, 2006). They yield particles of desired size with narrow size distribution and with core–shell or brush–like structure (Figure 2-3-a and b).

In a different approach, heterogeneous polymerization techniques, like emulsion (Horák and Chekina, 2006), miniemulsion (Ramírez and Landfester, 2003), microemulsion (Liu *et al.*, 2003; Sahingr and Ilsin, 2010), inverse emulsion (Hong *et al.*, 2009; Tataru *et al.*, 2011), inverse microemulsion (Deng *et al.*, 2003; Vogt *et al.*, 2010),

inverse miniemulsion (Yang *et al.*, 2008; El-Sherif *et al.*, 2010), and dispersion (Altintaş *et al.*, 2007; Lu *et al.*, 2008), are carried out in presence of ferrofluids to impregnate magnetic colloids inside a polymer network during its synthesis (Figure 2-3-c).

Nonetheless, the presence of MNPs in polymerization medium, also affects the reaction kinetics and stability of the system. Their affinity to polymer should be strong, while their interaction with other compounds, such as initiator, has to be as low as possible to avoid undesirable side reactions. It is possible to prepare polymer coating and MNPs separately and then in another step incorporate them inside the coating. There are several techniques to do so. In th solvent evaporation technique, synthesized MNPs are emulsified in a polymer solution, till it evaporates (Arica *et al.*, 2000). However, this simple technique produces rather large polydisperse particles. In the phase separation method an emulsion of polymers is formed in the presence of the MNPs. Then, by changing the conditions of the continuous phase, like temperature, pH, ionic strength, or addition of a precipitant, they are precipitated out of the medium,

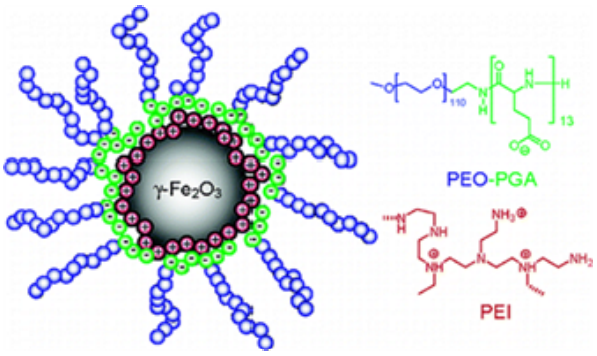

Figure 2-4 Layers of polyelectrolytes conjugated to the magnetic colloid (Thünemann *et al.*, 2006)

coating the MNPs. In layer-by-layer coating, electrostatic interaction between the anionic polymers and the cationic surface of MNPs leads to particles coating (Cabuil *et al.*, 1994; Ghosh *et al.*, 2011). Additional layers are added via electrostatic attraction. Aqueous maghemite colloids were obtained via this scheme (Figure 2-4) (Thünemann *et al.*, 2006). Sonication is also commonly used to conjugate proper coating onto the prepared MNPs (Mizukoshi *et al.*, 2009; Badruddoza *et al.*, 2010; Feng *et al.*, 2011). Proper aging of ferrofluid in the presence of polymer, under proper conditions of temperature and pH, is all it takes to covalently bind the coating to MNPs surface and stabilize the magnetic colloids (Feng *et al.*, 2008). Similar approach has also resulted in stable aqueous dispersion of magnetite nanoparticles, obtained by thermal decomposition, coated with poly(ethylene glycol) (Barrera *et al.*, 2009). Monodisperse water-soluble MNPs bearing hydroxyl functionality was obtained by this technique (Lattuada and Hatton, 2007)

2.4.2 Indirect Approach

In this approach the desired MNPs are produced with proper organic surfactant. Then a simple ligand exchange reaction substitutes the surfactant with hydrophilic coating so that MNPs maintain their stability in an aqueous environment. Oleic acid coated MNPs are common in this approach for ligand exchange reaction, where oleic acid is replaced with water-dispersible coating containing necessary functionality (Lattuada and Hatton, 2007). The MNP size can be tuned via seeded-growth to obtain larger particles (>10nm), while the change in heating rate alone can yield particles of smaller size (6 –

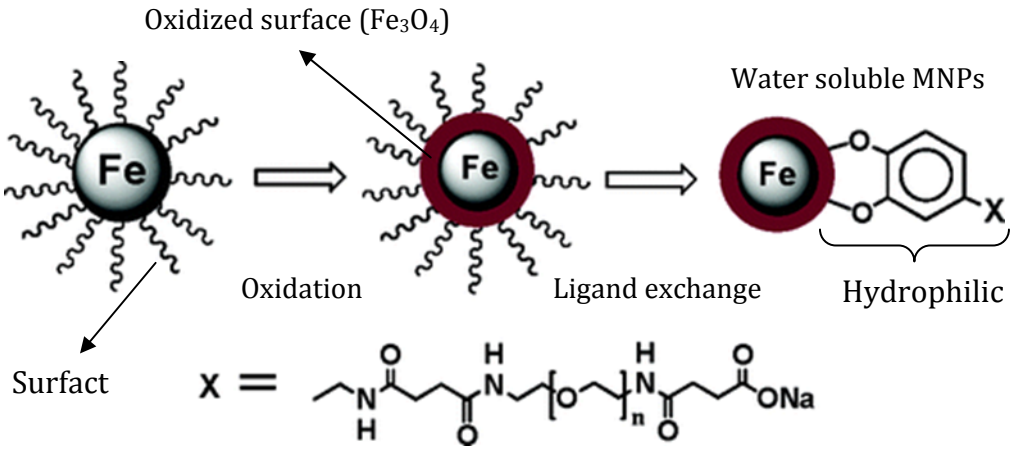

Figure 2-5 Preparation of water-dispersible MNPs (Peng *et al.*, 2006)

11nm). Monodisperse MNPs synthesized via thermal decomposition were also stabilized via ligand exchange (Figure 2-5). Such particles demonstrated considerable stability due to the controlled surface oxidation of iron particles (Peng *et al.*, 2006).

2.4.3 *In Situ* Coating

Polymer-coated MNPs can also be prepared via *in situ* synthesis, in the presence of polymer template. This approach is not as commonly practiced as post-synthesis coating; due to the limiting criteria of solvent and the effect of the presence of polymer on size, polydispersity, structure and nature of the magnetic colloids. In this technique, the reaction medium not only has to diffuse inside the network but it also must not promote MNP agglomeration. Such particles are either monodisperse or have narrow dispersity and can contain high magnetic loading. For example, a temperature-sensitive hydrogel offers a good mean for embedding magnetite nanoparticles (Pich *et al.*, 2004;

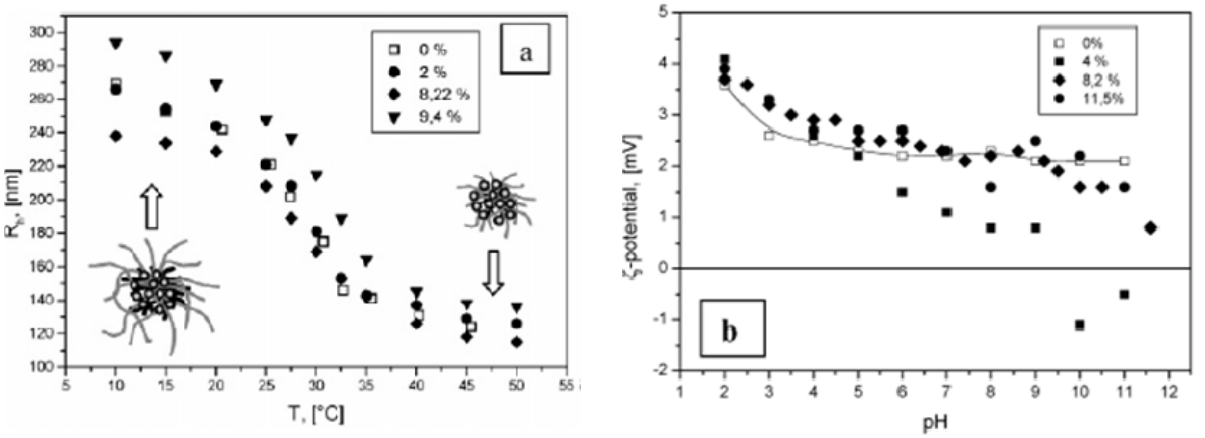

Figure 2-6 Properties of magnetic microgel with different magnetite loading (a) hydrodynamic radii and (b) ζ-potential (Pich *et al.*, 2004)

Lapointe and Martel, 2009; Meenach *et al.*, 2009; Tabatabaei *et al.*, 2009). Such composites inherit the characteristic of the polymer template while demonstrating magnetic behavior (Figure 2-6).

2.5 Applications

The MNPs can be easily tailored for the desired application by means of functional coatings. The magnetic nature of these particles allows for their selective manipulation and separation. Moreover, their superparamagnetic characteristic is favorable in many applications. They have shown potentials in mass-transfer limited processes, by improving the solute exchange between liquid an gas phase upon contact (Olle *et al.*, 2006). Here, only few of their applications are pointed out to avoid lengthy descriptions which are out of the context.

2.5.1 Magnetic recording / storage media

It has been shown that surfactant-coated MNPs have the ability to self-assemble into periodic arrays with equal spacing, which makes them suitable for individually addressable bits in magnetic storage media. Such application requires monodisperse particles with size distribution of less than 10% (Dai *et al.*, 2010; Lin *et al.*, 2010; Ray *et al.*, 2010).

2.5.2 Image contrast agent

MNPs are currently used as contrast agents to enhance magnetic resonance imaging (MRI) (Bulte and Kraitchman, 2004; Horák and Chekina, 2006). MRI is based on the offset between minute magnetic moment of a proton and the exceedingly large number of protons present in biological tissue. Properly synthesized MNPs are at their saturation magnetization under the magnetic field of MRI scanners, which is significantly larger than the one of iron salts currently devised. Moreover, tumors do not adsorb these agents the way healthy tissues do. Therefore, they improve the contrast in final image and assist in the visualization of vascular and central nervous system and in the detection and the identification of unhealthy tissues (Michel *et al.*, 2002; Wacker *et al.*, 2003).

2.5.3 Drug targeting/delivery

In this approach, the behavior desired drug complexes with MNPs. Then, the complex is concentrated in certain tissues (i.e. tumor site, cancerous cells) by means of magnetic

field. Then, it is released to carry out its action(s). However, magnetic particle have to have spherical shape and small size, with distribution lower than 15%, in order to easily transport and reduce their agglomeration risk in blood vessels (Willard *et al.*, 2004).

This application was first suggested in late 70s' (Senyei *et al.*, 1978; Widder *et al.*, 1978). In an *in vivo* application, magnetic drug carriers, localized around a tumor, were able to remiss or reduce its size (Widder *et al.*, 1983). Magnetic drug delivery does not introduce any toxicity and abnormality in subjects and is practically safe (Lubbe *et al.*, 1996). As drug carriers, MNPs have the potential for delivering pharmaceuticals to the specific location. This leads to the confinement of the drug's effect(s) in certain tissue; hence increasing its effectiveness while lowering the side effects, prescribed dosage, and cost.

This application has gained interest in the cancer therapy field. Anticancer agents, such as radionuclides, cancer-specific antibodies, and genes bounded magnetic nanoparticles can be enriched in desired sites, using external magnetic field, thereby enhancing the efficiency of the treatment (Alexiou *et al.*, 2003). Magnetically labeled liposome drug carrier released the drug in desired location upon heating, by alternating magnetic field or laser pulse (Babincová *et al.*, 2002; Chen *et al.*, 2010; Nappini *et al.*, 2010). For a more comprehensive overview of applications of ferrofluids for drug targeting and delivery, reader should refer to Lubbe *et al*. (2001) and Ram *et al*. (2011).

2.5.4 Cell and protein separation

Ferrofluids have provided a fast, feasible, and cost-effective technique in biomedical applications (Pankhurst *et al.*, 2003; Yavuz *et al.*, 2009) such as protein recovery and cell labeling and separation (Zborowski and Chalmers, 2008). Appropriate polymer coating improves the selectivity and the capacity of MNPs for such application. Phospholipid-coated magnetic particles have been successfully used as ion exchange media for the separation and recovery of proteins from fermentation broth (Bucak *et al.*, 2003; Ditsch *et al.*, 2006; Utkan *et al.*, 2011). These particle showed high capacity for protein separation and were recoverable.

In the field of biomedicine MNPs are also applied as biosensors for detecting biological targets such as liposome (Chemla *et al.*, 2000) or measuring binding forces between biological factors (Baselt *et al.*, 1998).

2.5.5 Water treatment

In the early investigation on the implementation of ferrofluids in water purification, they showed potential for adsorbing certain ions and compound on their surface. They reduced the concentration of suspended solid, phosphorus, and removal of iron, aluminum, coliform bacteria, color, and turbidity (De Latour, 1973; De Latour and Kolm, 1975). Moreover, magnetized sludge offers higher separation with larger thickening factor and with lower biological oxygen content in the effluent (Faseur A. *et al.*, 1986). Thus, this technology has significantly gained in popularity in water treatment as a

mean for preserving the aquatic ecosystem, via the reduction and removal of unwanted harmful compounds and species (Sakaguchi *et al.*, 2009; Sakaguchi *et al.*, 2010).

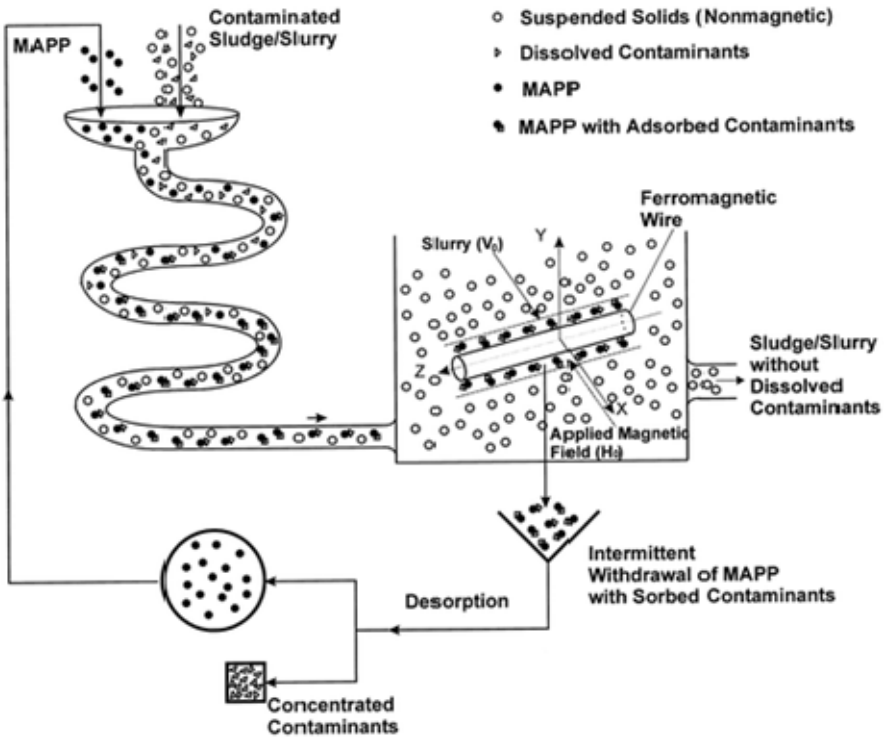

Figure 2-7 Schematic of a suggested magnetic separation process. MAPP represents magnetic polymer (Leun and Sengupta, 2000)

Magnetite nanoparticles have shown potential for full-scale application as an efficient method for the adsorption and removal of phosphate ion, despite their lower saturation magnetization (De Vicente *et al.*, 2010). Introducing superparamagnetic characteristic into nonmagnetic polymeric sorbents by irreversibly depositing magnetite nanoparticles into their matrix can remove dissolved environmental contaminants from

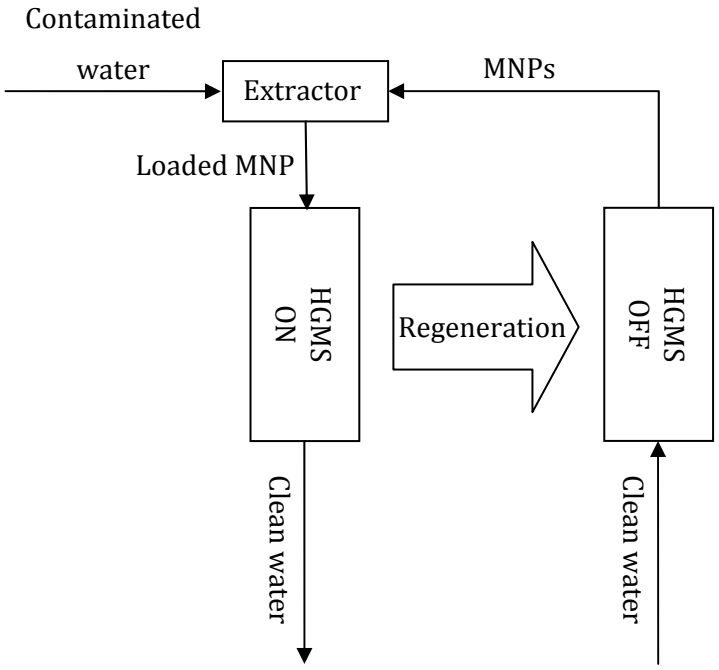

Figure 2-8 Schematic of the proposed process for treatment of water with magnetic nanoparticles

the slurry in one-step magnetic separation (Figure 2-7). In 2002, a process concept for water treatment and regeneration of the particles Figure 2-8based on the one suggested earlier was proposed (Figure 2-8) (Moeser *et al.*, 2002). In this process, after the contact stage between MNPs and contaminants, which happens in the extractor, the contaminant-loaded MNPs mixture passes through a high gradient magnetic separator. The loaded particles are collected inside, when the field is on, while the clean water exits. Afterward, they are regenerated by washing the loaded MNPs with proper solvent to remove the attached contaminants while the magnetic field retains the MNPs inside the separator. After MNPs are completely washed, the magnetic field is turned off so that they could be recycled into the process with clean water. The high gradient

magnetic field inside the high gradient magnetic separator is produced by a bed of 50μm magnetically susceptible steel mesh placed between two poles of an electromagnet, to dehomogenize the field (Figure 2-9). Later, a multistage countercurrent continuous contact process (Figure 2-10) was proposed to improve the treatment capacity (Egashira and Hatton, 2005). This process proved successful under practical operating conditions with better removal yield at higher flow rates.

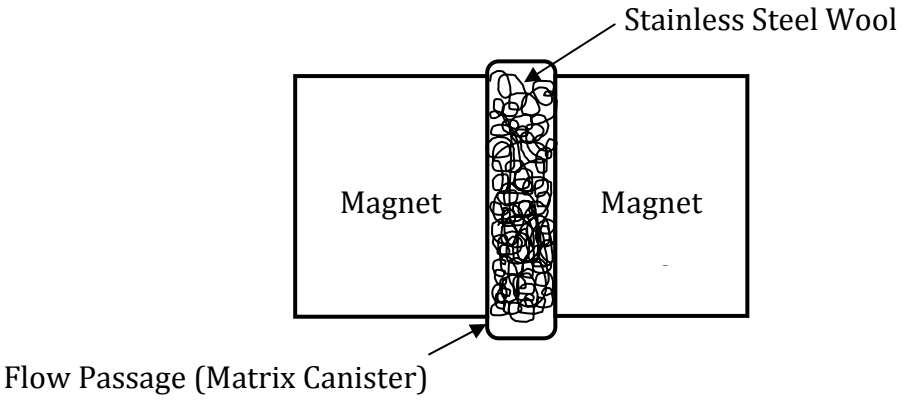

Figure 2-9 Schematic of a high gradient magnetic seperator

Individually coated MNPs are not efficiently captured by the separator compared to their aggregates, even at low flow rates (Moeser *et al.*, 2004). They calculated that the optimal size of polymer-coated MNP for efficient and permanent capture is 70nm, using the single-wire model. However, in the later experimental study, aggregates larger than 50 nm showed significantly high capture efficiency (Ditsch *et al.*, 2005).

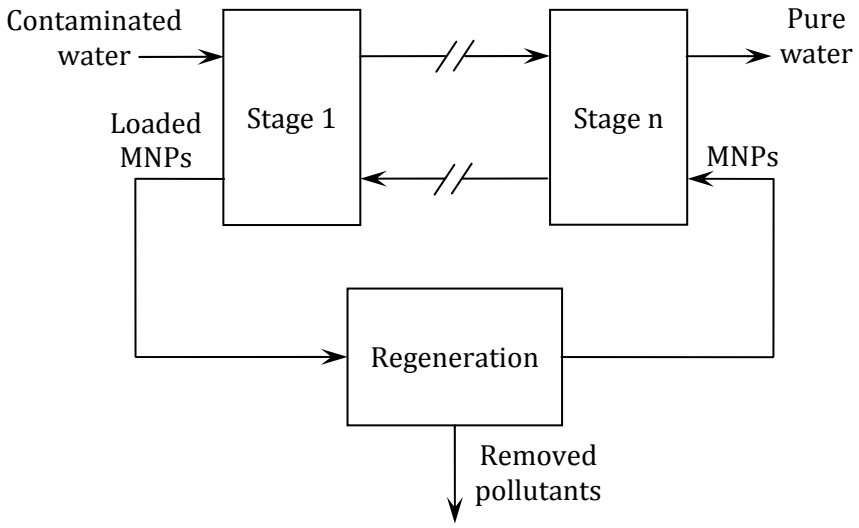

Figure 2-10 Schematic of the propused multistage countercurrent continuous contact process (Egashira and Hatton, 2005)

Panneerselvam *et al.* found that the removal of Ni(II) with magnetic nanoparticle is an endothermic reaction that looses efficiency in high concentration (Panneerselvam *et al.*, 2011). In another study, the application of polyrhodanine encapsulated magnetic nanoparticles deemed effective for the adsorption and removal of metal ion (Song *et al.*, 2011), especially Hg^{2+} (Figure 2-11-a). These particles were easily collected and regenerated with an external magnetic field (Figure 2-11-b). Badruddoza *et al.* took advantage of carboxymethyl-β-cyclodextrin for fabricating magnetic particles with enhanced adsorption toward copper ions (Badruddoza *et al.*, 2010). Although they utilized β-cyclodextrin, the main adsorption mechanism was the formation of surface complex between copper ions and oxygen atoms on carboxyl groups. They reported

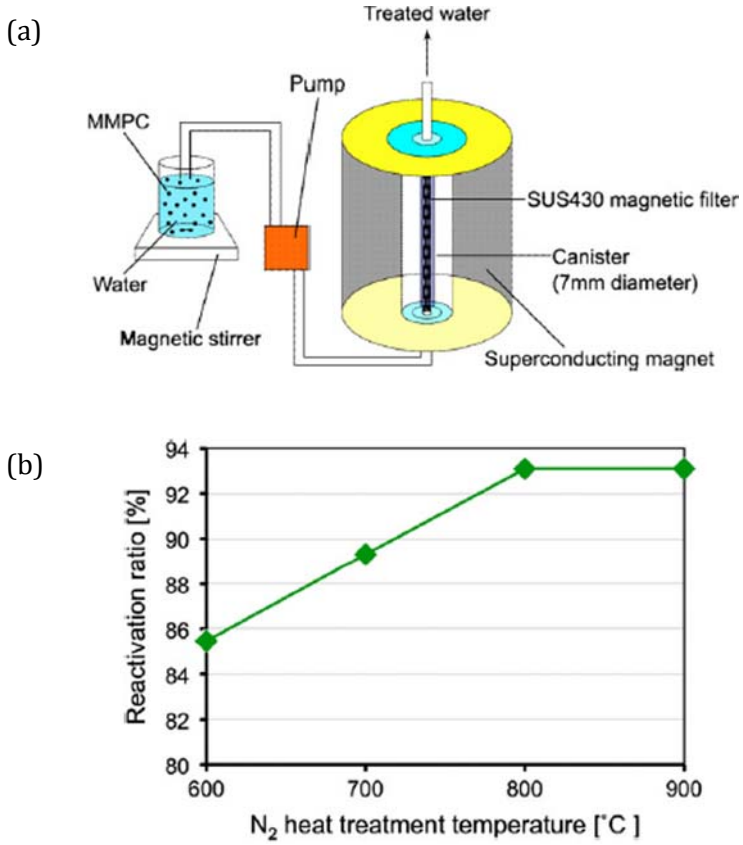

Figure 2-11 (a) Diagram of HGMS process, (b) Temperature effect on regenration of MNP (Kondo *et al.*, 2010)

successful regeneration of their MNPs as well. Magnetic mesoporous carbons were also able to absorb organic pollutants from water (Kondo *et al.*, 2010). These particles were easily captured by the high gradient magnetic separator (Figure 2-11-a), and their high-temperature reactivation further increased their adsorption efficiency (Figure 2-11-b). Suitable MNPs proved to be useful as catalytic agent for the decomposition of toxins for water remediation (Bromberg and Hatton, 2007). These particles showed stability over a wide range of pH in aqueous medium. Their magnetic nature allowed for easy recovery without loss of activity

Chapter 3 – Characterization Techniques

3.1 Neutron Magnetic Resonance Spectroscopy (^{1}H NMR)

NMR spectrum is used not only to study the molecular structure, but also for quantitative estimation of the molecular weight of the polymer chains, as the integration curve of each peak in the spectrum is directly related to the abundance of individual protons in the structure. In order to comprehend the theory behind this technique, one has to look at the relationship between the energy of different states, the magnetic field applied and its frequency.

The presence of an applied external magnetic field will induce nuclei that exist in two nuclear spin states of different energies. Slightly more than half of the nuclei exist in the lower energy state, α, than in the higher one, β. The homogeneous external magnetic field, B_o, is created with a large magnet, commonly a super-conducting solenoid (University Tutorial, 2003). The energy difference between the spin states, ΔE, is directly proportional to the strength of the applied magnetic field (Figure 3-1). The proportionality coefficient is the frequency of the field. ^{1}H NMR spectroscopy records transitions between these spin states, induced by electromagnetic B_o field, for hydrogen atoms in the sample. B_o is typically 7.05T or 70,500 Gauss..

NMR spectroscopy was conducted on a Bruker Bio Spin 300 MHz spectrometer at room temperature. Deuterated dimethylsulfoxide(DMSO-d_6), acetic acid (CH_3COOH-d_4), and deuterium oxide (D_2O) solvents were purchased from Sigma Aldrich.

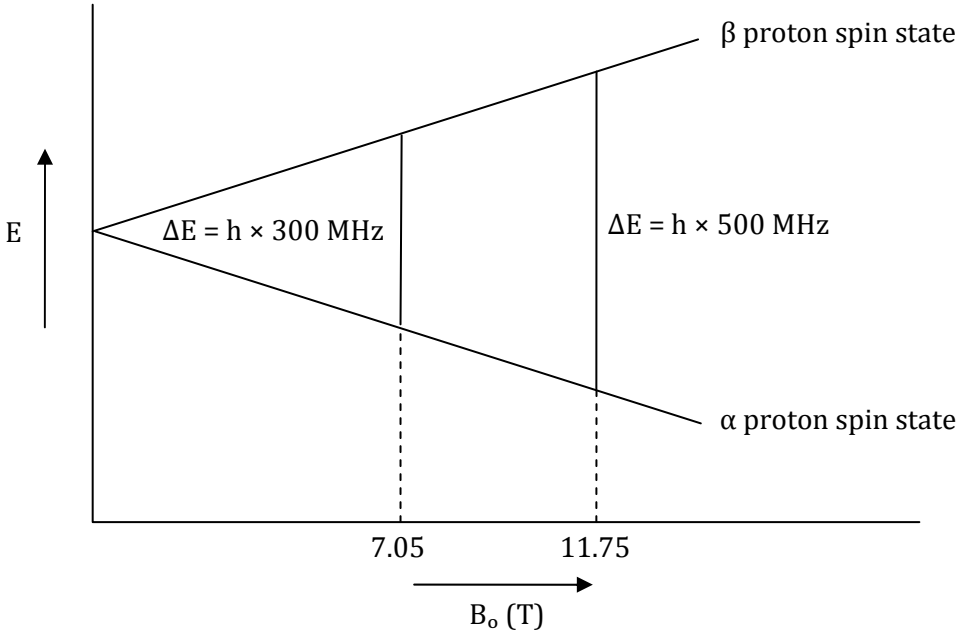

Figure 3-1 Relation between B_o (magnetic field) and frequency (ν) or the energy $\Delta E = h \nu$

3.2 Fourier Transform-Infrared Spectroscopy (FT-IR)

The goal of any absorption spectroscopy, like FT-IR, is to measure how well a sample absorbs or transmits different wavelengths of light. Basically, a FT-IR spectrometer emits a light beam, containing various wavelengths, and measures how much of that beam is absorbed or transmitted while passing through the sample. This technique is repeated several times, depending on the resolution adjustment, with a range of wavelengths. Afterwards, the spectrometer analyzes the collected raw data to infer how much is the amount of the absorption at each wavelength. This process is conducted both in absence and presence of sample in order to obtain the "background " and

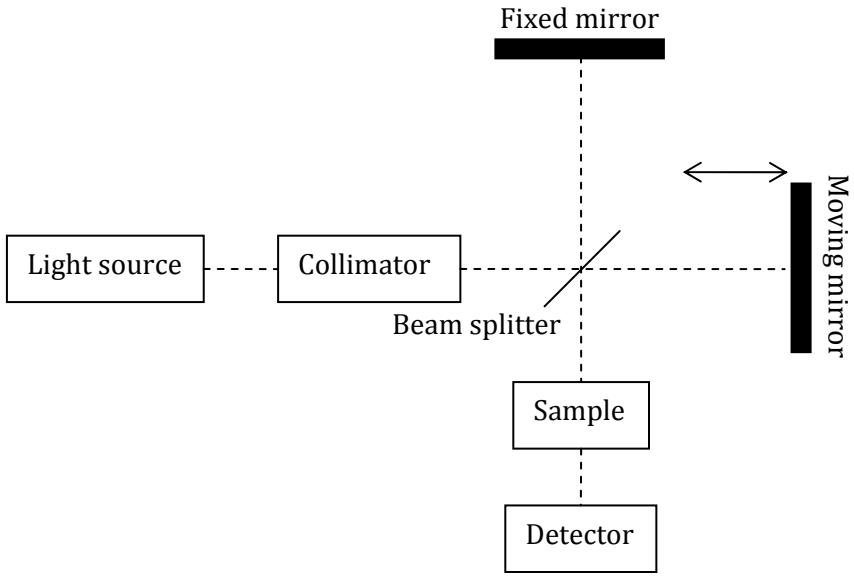

Figure 3-2 Schematic diagram of adopted Michelson interferometer, for FT-IR spectrometry

"sample" spectra, respectively. The latter will be different from the former because the sample will absorb some wavelengths of the incident light.

The current FT-IR spectrometers are based on the Michelson interferometer (Figure 3-2). In this instrument, an infrared light, i.e. LASER, is collimated after radiation and hits the splitter. Here, ~50% of it reflects toward a fixed mirror (beam 1) while the rest is directed toward the moving mirror (beam 2). These mirrors reflect these beams back to the splitter. In an ideal case, only 50% of the original light passes through the splitter, colliding with the sample located in the sample holder before reaching the detector. The motion of the moving mirror leads to different optical path length for beam 2, resulting

in delays, known as retardation, in its detection, compared to beam 1. The final interferogram is acquired by recording the detector's reading for various retardation values.

For the purpose of this study, a Bruker Tensor 27 FT-IR instrument at room temperature was used. All samples were prepared as solid KBr pellet and measurement were performed under nitrogen flow. The spectra were recorded from 4000 to 400 cm^{-1} wavelength with 32 repeat for medium resolution of the spectrum.

3.3 Potentiometric and Conductometric Titration

Analysis of potentiometric and conductometric titration curves of polyelectrolyte solutions leads to quantification of carboxyl group on the polymer.

$$P - COOH \xrightarrow{XOH \rightarrow X^+ + OH^-} P - COO^- + H^+$$

A Metrohm Titrando 809 titration System equipped with Metrohm pH probe coupled with Metrohm Conductometer 712 equipped with Metrohm Pt1000 conductivity probe wwas used to carry out simultaneous pH and conductivity measurements. This instrument is accompanied with Tiamo software capable of controlling the titration process. A 0.1M standard HCl and NaOH solution were prepared from corresponding 1M standard solution (Acros), and subsequently used for the forward acid titrations and backward base titrations.

All titrations were performed 3 times under constant stirring in a 100-ml airtight, jacketed titration vessel (supplied by manufacturer), under continuous N_2 purge. The temperature was set to 25°C, controlled by a water bath. For all the measurements, 50ml solution with 0.1wt% concentrations was prepared. Titration dosage was adjusted to 0.01ml with lag time of 60 seconds between two consecutive dosing to allow for equilibrium in neutralization reaction.

3.4 Dynamic Light Scattering (DLS)

Light scattering can be explained in terms of electromagnetic theory. It is based on the polarization of electron clouds of a molecule due to oscillation of the electron field associated with an incident light wave, which is scattered upon impact in different directions. The intensity fluctuation of scattered radiations, due to Brownian motion, known as Doppler shift, in conjunction with broadening of central time-averaged scattered intensities of static light scattering, also known as Rayleigh scattering, can be used to determine the dynamic properties of a system, such as weight-average molecular weight, second viral coefficient and z-average radius of gyration.

DLS accounts for the frequency broadening of the scattered light and examines the intensity variations with time and correlates them to the scattered properties. In general, the terms of the correlation functions of dynamic variables are always used to describe the response of the scattering molecules to the incident light. The intensity of

scattered light can be determined by photon correlation spectroscopy. The average intensity, *<I>*, over long observation time, *T*, can be expressed by (Brown, 1993):

$$< I >= \frac{1}{T} \lim_{T\to\infty} \left(\int_0^T I(\theta, t) dt \right) \tag{3.1}$$

Consequently, to study the dynamic properties of the scattering system, correlation functions need to be derived from the time dependant measurements (Brown, 1993):

$$G_2(t) =< I(t)I(t+\tau) > \tag{3.2}$$

that could be normalized as:

$$g_2(t) = \frac{< I(t)I(t+\tau) >}{< I(t)^2 >} \tag{3.3}$$

where *I(t)* is an average value of the product of the scattered intensity at time *t*, and *I(t+τ)* is the intensity registered at decay time τ. After applying Siegert relations for simplifications and Fourier transformation, equations (3.2) and (3.3) become:

$$G_1(t) = \sqrt{(G_1(t) - B)} \tag{3.4}$$

$$g_1(t) = \sqrt{\frac{(G_1(t) - B)}{B\beta}} \tag{3.5}$$

where B is the baseline, β is the coherence factor that is generally considered an adjustable parameter in the data analysis procedure, $G_1(t)$, and $g_1(t)$ are the auto-correlation function and its corresponding normalized function , respectively.

For dilute systems that contain non-interacting homogenous monodisperse spherical particles, equation (3.5) can be expressed as:

$$g_1(t) = \exp(-\Gamma t) = exp\left(-\frac{t}{\tau}\right) \tag{3.6}$$

where $\Gamma=\tau^{-1}$ is the decay rate:

$$\Gamma = q^2 D_0 \tag{3.7}$$

where q, particular wave vector, is:

$$q = \frac{4\pi n_0}{\lambda} \sin\left(\frac{\theta}{2}\right) \tag{3.8}$$

with λ being the incident light wavelength, n_0 the refractive index of the sample and θ the angle at which the detector is located with respect to the sample cell. Hence, Stoke-Einstein equation is expressed as follow:

$$D_0 = \frac{kT}{6\pi\eta R_h} \tag{3.9}$$

where k is the Boltzmann constant ($1.380\,6504\times10^{-23}$ J/K), D_0 is the diffusion coefficient, T is the absolute temperature, η is the solvent viscosity and R_h is the polymer hydrodynamic radius (Noggle, 1996).

DLS experiments were conducted using a Brookhaven LASER light scattering system. This system consists of a BI200SM goniometer (Ver. 2.0), BI-9000AT digital correlator and other supporting data acquisition and analysis software and accessories. The goniometer consists of focusing optics, rotating arm (for angle-dependence studies), detector optic, detector, neutral density filter, beam focus, sample cell assembly, and a high voltage power supply for the detector. It is equipped with a 200mW 488nm vertically polarized argon ion LASER, digitally-controlled water bath. The count rate is controlled by adjusting either the detector's pin-hole size, the LASER power, or both in order to achieve the desirable count rate of $2\times10^5 - 5\times10^5$ counts per second (cps).

This count rate leads to good signal to noise ratio. A 30-minutes warm up period was allowed before initiating the data acquisition. Also, in order to improve the acquisition accuracy, filling liquid (decahydronaphthalene) was filtered through a 200nm filter and pumped into the sample holder for 10min prior to measurement, to reduce the beam refraction from possible scratches on sample vial and remove any bubble that it may contain. The acquired data is analyzed by GENDIST program that devises inverse Laplace transformation technique to convert the distribution of decay rate to size distribution.

The concentrations of the nanogels and magnetic nanoparticles solutions investigated by light scattering were kept in the dilute solution regime (~0.001wt%) where the

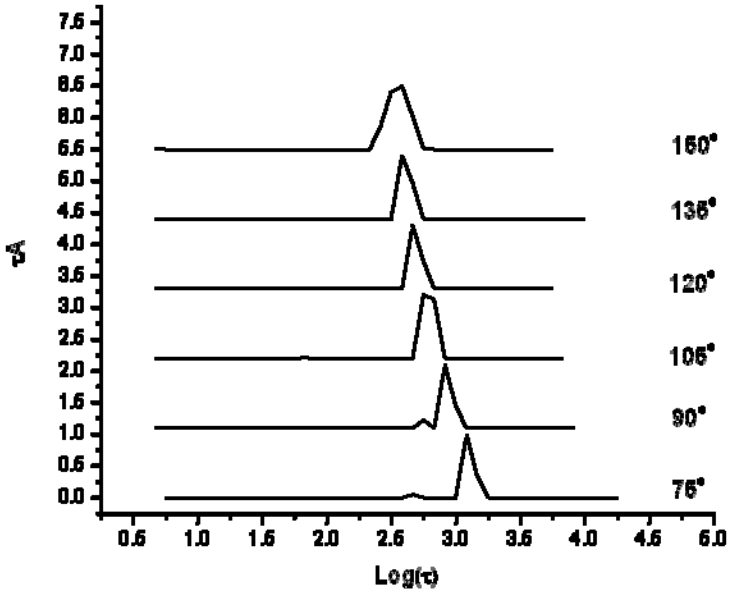

Figure 3-3 Distribution plot of a sample at several angles

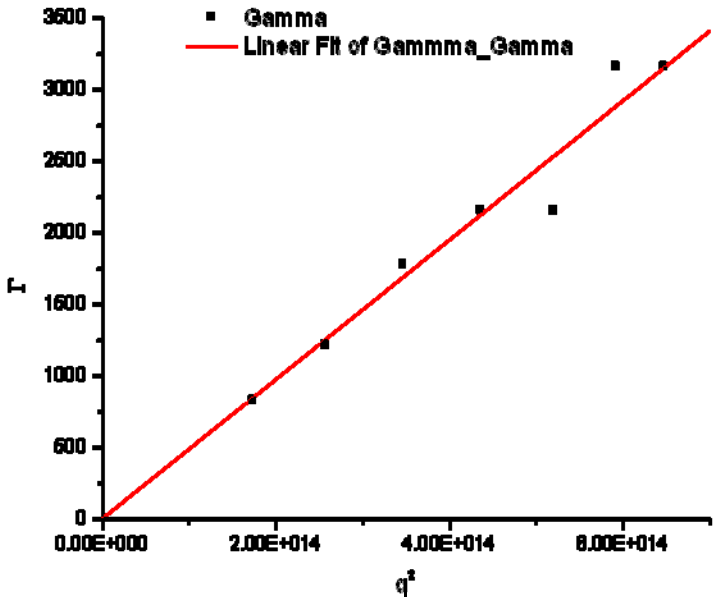

Figure 3-4 Plot of Γ vs. q2. If the data points follow a straight line, the diffusion coefficient will be the slope of the linear trend line that passes through them. Substitution of this value in Stokes-Einstein equation, Eq. (3.9**)**, yields the angular independent.

solution was transparent and inter-particle interactions can be neglected; hence, the scattering behavior of individual particles can be studied. All samples were passed through a 0.8μm nylon filter membrane prior to measurement to remove dust particles.

Here, several measurements were performed at varying scattering angles (75-150) (Figure 3-3) for a given sample to confirm that translational diffusion is the main mode of particle motion that give rise to the observed peak and hence justifying the use of the Stokes-Einstein equation to calculate the average hydrodynamic radius, Eq.(3.9). Depending on the anisotropy and polydispersity of the system, the plot of Γ vs. q^2 may

or may not show an angular dependence. Spherical particles yield angle independence plot like the one in Figure 3-4.

3.5 Zeta Potential (ζP)

Particles commonly carry negative electrostatic surface charge. Hence in a solution, positive ions are attracted to the particles interface by strong electrostatic interaction between opposite charges, forming a positively charged layer around the particle called Stern layer. Consequently, a diffusion layer is created between positively charged Stern layer, and the charge of the bulk solution (Figure 3-5) (Khouri, 2010). The ζP is the difference between the charge at the edge of the Stern layer and the bulk of the suspending liquid. It can be measured by tracking the moving rate of a charged particle across an electric field. Usually, a value less than -15mV represents the start of

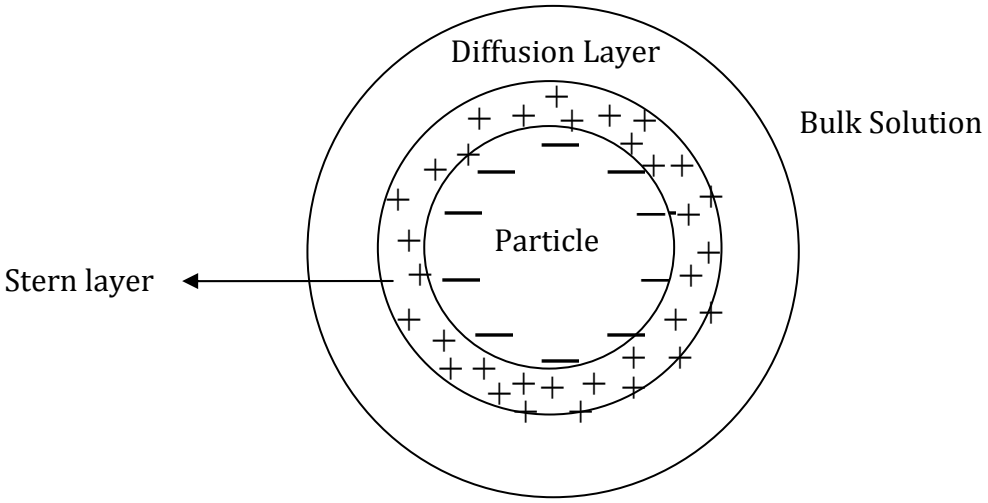

Figure 3-5 Charge arrangement in solution

agglomeration, while values greater than -30mV indicates presence of sufficient repulsion to prevent agglomeration.

The colloidal stability and surface charge of the scaffolds and MNPs were examined using a Brookhaven 90 Plus particle size analyzer, with an attached ZetaPALS phase analyzing light scattering system at ambient temperature. This instrument is equipped with a 35mW diode LASER aligned at a 90° scattering angle. A pair of palladium electrodes, assembled on an acrylic support, performs measurements by applying an electric field inside the sample.

The samples were prepared in polystyrene cuvettes and the measurements were carried out at 25°C. Each run in sample measurements consists of five cycles where the charges on the two electrodes were alternated and an average of the reading from five runs were used to obtain the particle electrophoretic mobility. The samples were diluted to 0.005wt% with 0.1M NaCl prior to measurement. One milliliters of the sample were loaded to the electrode cell. The electrophoretic mobility (μ_e) of the particles measured over 25 electrode cycles was converted to the zeta potential (ζ) using the Smoluchowski equation:

$$\zeta = \frac{\eta}{\epsilon}\mu_e \qquad (3.10)$$

where η and ε are the viscosity and dielectric constant of the dispersion medium, respectively. The quoted zeta potential is an average of five measurements.

3.6 Isothermal Titration Calorimetry (ITC)

Amongst the various methods for the determination of the reaction enthalpy, i.e. electronic absorption (UV-vis), nuclear magnetic resonance (NMR), chromatography (gas or liquid-phase), etc., calorimetry is the only direct method of measurement. In this technique, the equilibrium constant and reaction enthalpy are calculated using the data gathered at a constant temperature. Such direct approach has advantages over other methods, by applying the Van't Hoff equation with the assumption of constant heat capacity over the experimental temperature range.

Calorimetry is the study of the amount of energy exchanged in the form of heat between two systems within a period of time. As the industry has shifted away from commodity chemicals to high-value-added specialty chemicals, calorimetric method is used to enhance the product performance and quality while lowering its production cost. Valuable thermodynamic properties, such as enthalpy (ΔH), entropy (ΔS), Gibbs' free energy (ΔG), and heat capacity (C_p) are obtained from this method and are used to understand the principles behind interaction of different molecules. Depending on targeted application, such as flow, dilution, association/dissociation, titration, etc., various calorimeters are designed and used.

In titration calorimetry thermochemical and analytical applications are combined to determine the enthalpy change of a chemical reaction as a function of the amount of added reactant. When substances interact, heat is either generated (exothermic) or absorbed (endothermic). The enthalpy change of such interaction is a function of the amount of titrant injected into the reaction cell. The measurement of this heat allows the accurate determination of binding affinity (K), change in enthalpy (ΔH) and change in entropy (ΔS), thereby providing a complete thermodynamic profile of the intra-molecular interaction in a single experiment:

$$\Delta G = -RT \ln K = \Delta H - T\Delta S \qquad (3.11)$$

Despite the advantage of calorimetry over other methods for the determination of reaction's thermodynamics, it is not the most widely used approach for studying thermodynamics of the cyclodextrin complexation. One reason could be the combination of the need for a relatively large amount of sample, sophisticated and delicated equipment, and some expertise required to obtain reliable results. Of the various types of calorimetry, i.e. batch microcalorimetry, flow microcalorimetry, titration calorimetry, titration microcalorimetry is the most modern and refined technique currently available. The prefix "micro-" associated with microcalorimetry shows a measurement system with thermal sensitivity of 1μW or higher. This instrument is a power-compensation-based diferential calorimeter (Wiseman *et al.*, 1989) in which the effect of the heat exchange, due to change in temperature, is

suppressed by an input heat source/sink. The advantage of this method lies in its quasi-isothermal conditions during the measurement, where heat loss does not contribute a significant error, and, therefore, precise determination of the electric compensation energy is possible.

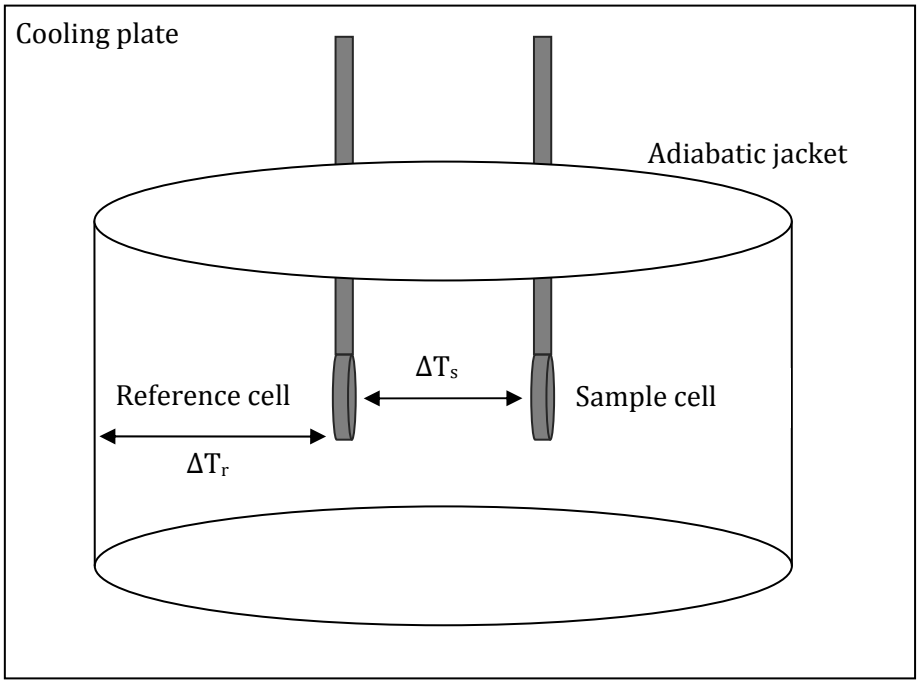

Figure 3-6 The schemcatic of Microcal ITC

In this study, Microcal ITC (Northampton, MA) was used to aquire of micro-calorimetric data. This instrument consists of a reference cell and sample cell of approximately 1.45ml volume (Figure 3-6). Both cells are insulated by an adiabatic shield. Temperature sensors measure the temperature difference in each cell, ΔT_r and $\Delta T_{s,}$ respectively. Using a feedback control system, the instrument is be able to keep ΔT_r

constant (as baseline) by addition or removal of heat from the sample cell. The amount of the power required to maintain ΔT_r constant over time is an indication of the heat generation or consumed resulting from the interaction (VP-ITC Instruction

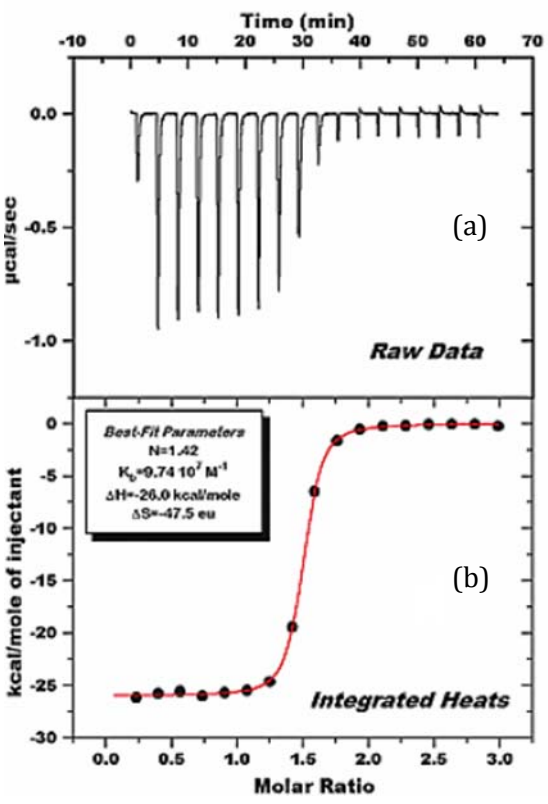

Figure 3-7 a) Heat release data for individual injections, b) processed data (VP-ITC Instruction Manual. 2001)

Manual. 2001). Figure 3-7-a represents the heat released for each injection. After integrating of the area of each injection the complete binding isotherm is obtained (Figure 3-7-b).

All the titrations were carried out at 25.0±0.02°C by injecting different concentrations of aqueous solution of PHC from a 270-µl injection syringe burette into the sample cell filled with β-CD solution. The tip of the syringe is tailored to act as a blade-type stirrer to ensure an optimum mixing and a homogeneous solution inside the cell at all time. Using the supplied software, other injection parameters such as number, volume, and lag time for each injection were controlled.

3.7 Ion–Selective Electrode (ISE)

The ISE system is a relatively simple procedure to perform common analysis in a cost-effective manner. It is a electrochemical sensor that evaluates the activity of a certain ion in the presence of other ions, rather than its concentration. Nonetheless, such electrode can be used for concentration measurement if a constant concentration of an inert electrolyte can be added to all samples so as to fix the relationship between activity and concentration. This constant concentration eliminates minor measurement-related errors resulting from variations in sample composition. The response of ISE developed in this chapter is defined by the Nernst equation:

$$E = E^0 \pm \frac{RT}{zF} \ln a_i \qquad (3.12)$$

where E and E^0 are the potential and the standard potential of the ion, R is the universal gas constant (8.314 J K^{-1} mol^{-1}), T is the absolute temperature (K), z is the number of

moles of transferred electrons, F is the Faraday constant (9.648×10^4 C mol^{-1}), and a_i is the activity of the ion.

Determination of the electromotive force (EMF) is necessary for potentiometric studies in which ion-selective membrane electrodes are utilized. A proper system consists of two solutions separated by a membrane:

Reference Electrode (1)	Test Solution (1)	Selective Membrane	Internal Solution (2)	Internal Reference Electrode (2)

The EMF of such system is determined by following equation:

$$EMF_{cell} = E_2 + \Delta\Phi_{\mathrm{M}} - E_1 \tag{3.13}$$

where E_1, E_2, and $\Delta\Phi_{\mathrm{M}}$ are potential response of electrode 1, 2 and membrane potential. The combination of selective membrane, internal solution, and internal reference electrode constitutes the ISE. Therefore, the potential of the ISE, E_{ISE}, is equal to:

$$E_{ISE} = E_2 + \Delta\Phi_M \tag{3.14}$$

In absence of any other interfering ion, the membrane potential is determined by:

$$\Delta\Phi_M = \frac{RT}{zF}\ln\left[\frac{a_{i,1}}{a_{i,2}}\right] \tag{3.15}$$

where $a_{i,1}$and $a_{i,2}$ are its activity in test solution and internal solution, respectively. Equations (3.12), and (3.15) are identical for a system without transfer. In other words, for internal solution with constant activity of $a_{i,2}$, E_2 must be constant as well. Consequently:

$$E_{ISE} = \text{constant} + \frac{RT}{zF}\ln a_{i,1} \tag{3.16}$$

where

$$\text{constant} = \frac{RT}{zF} ln\, a_{i,2} \tag{3.17}$$

All the quantities in equation (3.17) can be determined independently of i.

ISE is used in food and beverage industries for analysis of ions, i.e. calcium, sulphide, cyanide, nitrate, chloride, fluoride, bromide, sodium, ammonia, in products, such as dairy, wine, beer, bacon, fish, tea. In addition, ISE are utilized in geology and agricultural studies for measurement of various ions present in rocks, clays, and soils. Moreover, environmental quality control and pollution monitoring fields have also taken

advantage of the ISEs ease-of-use in identification and quantification of contaminants in air, water, and soil.

In biomedicine, they are proven valuable for quantification of various ions, i.e. sodium, potassium, calcium, ammonium, chloride, fluoride, etc., in tissues and body fluids. ISE has also found application in quality control of pharmaceutical industries. Other applications of ISEs include end-point detector in complexometric and precipitation titrations, chromatography, organic compounds, biochemical reactions and inorganic systems assay (Xu, 2001).

The electrode system used in this study has the electrochemical arrangement of Ag/AgBr/Internal solution/membrane/test solution/Ag/AgCl reference (Figure 3-8). This electrode measures the electromotive force (EMF) values of the solution relative to reference electrode. This values are, then, converted to drug concentration using calibration data. The internal solution inside the Teflon tubing was 1mM PHC in 10mM NaBr. This ion selective membrane was conditioned for half an hour prior to use. In all experiments, the temperature was kept to 25±0.1°C by circulating thermostated water inside the jacket of the test vessel. The test solution was stirred continuously during the measurement.

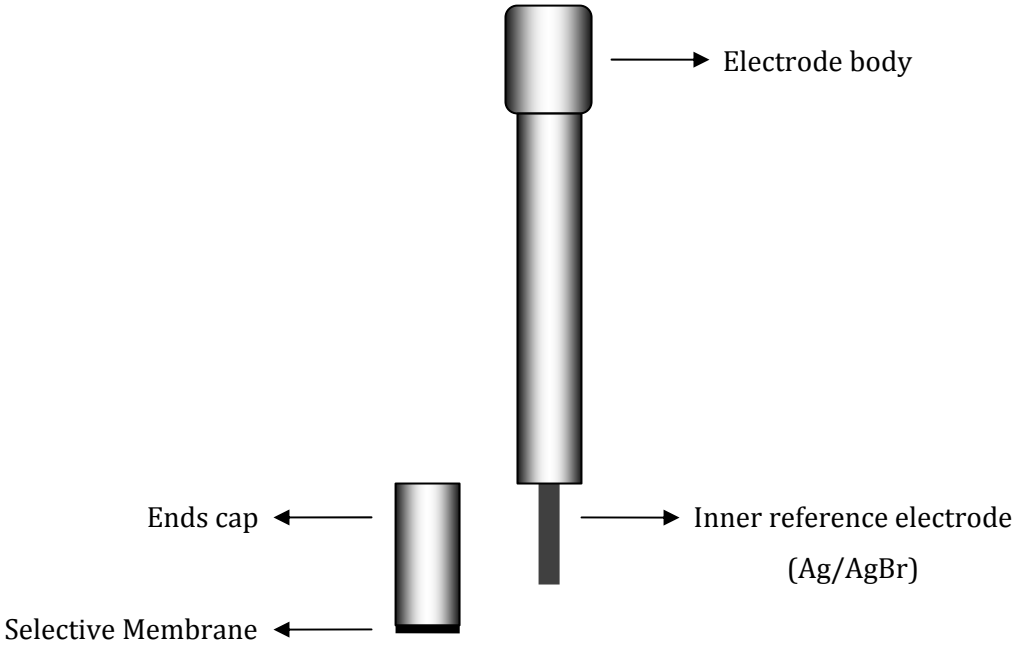

Figure 3-8 Schematic of ISE electrode

Chapter 4 – Stabilizing MNPs

4.1 Considerations

The objective of this research is to prepare aqueous ferrofluid applicable to water treatment for the removal of organic contaminants. Such ferrofluid should contain properly stabilized and functionalized MNPs that are obtained with simple procedures that are cost-effective for large scale industrial applications.

The coating material is one of the key concerns. Various materials are used for bench-scale experiments. However, not all of them are applicable for large scale production. The nature of surfactant attachments to the magnetic particles makes them unsuitable for aqueous environment. Therefore, polymer coatings offer a better alternative. Among various coating mechanisms, electrostatic attachment of coating to charged magnetic surface is very sensitive to ionic strength and pH fluctuation, making it unsuitable for applications in which the pH and ion concentration cannot be closely monitored. Hydrophobically attached coatings easily desorb if their solvent is present in the mixture. Covalent attachment also involves expensive materials and/or instrumentation that make it unacceptable for large scale production. Consequently, only polymers that are able to form chelate attachment with the surface of magnetic particles offer an enhanced coating with a few-step simple procedure. Among chelate forming groups, carboxylic acids are able to easily form strong and sustainable irreversible attachments that will remain under most conditions.

Carboxylic acid is available in a broad range of polymers. However, the suitable polymer should be produced with a simple and economic procedure in large scale. Emulsion polymerization is widely used in industry because of its straightforward approach and setup. It also offers a better control over the size and morphology of the polymers.

Moreover, the techniques that are devised for synthesizing the magnetic nanoparticle should also be scalable for mass production. Chemical precipitation of magnetite is the simplest and most common procedure that requires relatively inexpensive ingredients and instrumentation. However, the magnetite particles obtained via this method are sensitive to oxidation and must be promptly coated. Hence, post-synthesis coating methods, which are widely practiced in bench-scale, are not applicable to large scale production, due to significant aggregation and oxidation that occur during the time lapse between synthesis and coating steps. Therefore, *in situ* coating offers a more reasonable choice. The presence of polymer in precipitation reaction mixture has only a slight effect on the particle size (because deprotonated hydroxyl groups form chelate attachments with the surface of magnetite particles and protect them against aggregation as they are synthesized).

Another key aspect in this research is the selection of a functional group. It is through this functionality that the final product can bind to organic contaminants. The compound chosen for this purpose must have high affinity to organic compounds.

Moreover, it should attach to the polymer coating through an industrially applicable procedure.

4.2 Materials

Methacrylic acid (99.5%), ethyl acrylate (99.5%), diallyl phthalate (97%), Aerosol OT surfactant, poly(ethylene glycol) methacrylate (M_n= 300 and 2080 Da, PEGMA300 and PEGMA2080), N-(3-dimethylaminopropyl)-N′-ethylcarbodiimide hydrochloride (≥98%, EDC), and N-hydroxysuccinimide (98%, NHS), were obtained from Sigma Aldrich. Sodium bicarbonate, ferrous sulphate heptahydrate, sodium nitrate, and acetonitrile (99.9%) were purchased from Fisher Scientific. Sodium persulfate (98+%), ammonium hydroxide (28-30w%), β-cyclodextrin, p-toluenesulfonyl chloride (99+%), sodium hydroxide, ethylenediamine (99+%), N,N-dimethylforamide (DMF), and 1M standard HCl and NaOH titration solutions were obtained from Acros Organics. 2-sulfoethyl methacrylate was purchased from Scientific Polymer Products.

Methacrylic acid, ethyl acrylate, and PEGMA300 and 2080 were purified, by passing through an alumina column twice to remove monomethyl ether hydroquinone and other existing inhibitors from stock solutions prior to their use. A MilliPore Milli-Q Advantage A10 Ultrapure water purification system provided the water for all the reactions. The regenerated tabular cellulose membrane dialysis tubing were purchased from Spectra/Por.

4.3 Synthetic Protocols

The synthetic procedure selected for this research involves the semi-continuous emulsion polymerization of methacrylic acid-co-ethyl acrylate polymeric scaffold, from monomers, using diallyl phthalate as cross-linker to obtain PMAA-EA nanogel. This scaffold is pH responsive and swells as pH reaches neutrality (Rodriguez *et al.*, 1994). Its carboxylic affinities not only offer a suitable coating for embedding MNPs, but they also provide a platform for attachment of functional groups. These scaffolds can easily be magnetized via template–based coating of magnetite nanoparticles prepared via chemical precipitation of ferrous ions in a one-step *in situ* approach. In addition, several procedures for introducing further stability onto the template, as pre- and post-synthesis steps, were also examined.

Afterward, attachment of the β-cyclodextrin (β-CD) functional group onto the magnetic polymer in via $COOH/NH_2$ reaction was studied. This compound was selected due to its ability to form inclusion complex with a wide range of organic compounds and because of its reasonable price. An amide-containing side group could easily attache to activated β-CD in order to prepare it for attachment to MNPs via carbodiimide reaction.

4.3.1 Synthesis of Polymeric Template

Cross-linked polyacids expands upon neutralization, which tends to form a network structure, i.e., microgel or hydrogel, compared to linear polyelectrolytes, if sufficient

cross-linking is introduced to the structure (Eichenbaum *et al.*, 1999a). Poly(methacrylic acid) is a weak polyacid and it exhibits interesting conformational and swelling transition upon an increase in pH. The extent of its transition is dependent on the cross-link type and density, the degree of neutralization, attached functionalities, as well as ionic strength (Rodriguez *et al.*, 1994; Eichenbaum *et al.*, 1998; Eichenbaum *et al.*, 1999a; Eichenbaum *et al.*, 1999b; Tan *et al.*, 2005).

Poly(methacrylic acid – ethyl acrylate) cross-linked with diallyl phthalate, PMAA-EA (Figure 4-1) is a randomly cross-linked hydrophobically modified alkali water-soluble associative polymer nanogel consisting of hydrophilic structure (MAA) with randomly distributed hydrophobic group (EA). Neutralization of carboxyl groups inside the nanogels increases the repulsion and osmotic pressure inside the scaffold against the bulk solution; resulting in its swelling and increased solubility (Tan *et al.*, 2005). The synthesis procedure was a conventional semi-continuous emulsion polymerization that yields a narrow particle size and size distribution. In a typical aqueous emulsion polymerization, emulsification of relatively hydrophobic monomers, in an oil-in-water mixture, with emulsifier is followed by the reaction initiated with a water-soluble initiator. The process that follows is adopted from a previously reported approach (Wang *et al.*, 2000).

In a 500 ml 3-neck reaction vessel 0.3g of 75% Aerosol OT surfactant and 0.6g of 2-sulfoethyl methacrylate were added to 300ml water and were magnetically mixed under nitrogen purge. The monomer feed mixture of total monomer weight of 15g with

1:1 molar ratios was prepared by charging methacrylic acid and ethyl acrylate, together with 1.12g of surfactant and 1.17g of cross linker, diallyl phthalate, into 60ml of water. The monomer solution, monomer feed, was dispersed under vigorous shaking and transferred into a syringe. The initiator mixture, comprised of 0.5g sodium persulfate and 0.15g of sodium bicarbonate dissolved in 60ml of water. This mixture, initiator mixture, was transferred to another syringe. 1g sodium persulfate in 40ml water comprised of the initial initiator mixture. The reactor was heated to 80°C, where upon 10v% of the monomer mixture was added.

When the reactor temperature reached 80°C again, the initiator solution was added to the reactor to initiate the seeding stage of polymerization, in order to form *in situ* seed products. After 30min into the seeding stage, the growth stage was commenced by injecting the remaining monomer and initiator feed mixtures into the reaction vessel for periods of 60 and 90min, respectively, using syringe pumps, under continuous purging and stirring at a reaction temperature of 80°C. After the initiator feed mixture was completely introduced to the reactor, the reaction was left to proceed for another hour for completion of polymerization. The polymer mixture, having a milky color, was then dialyzed in D/I water using a regenerated cellulose tubular membrane (12000-14000 Da molecular weight cutoff). The dialysis process was carried out over a period of one month, where the D/I water was replaced every other day. All the impurities and unreacted compounds were removed during this period. The final solid content of the polymers was approximately 2.92 % by weight.

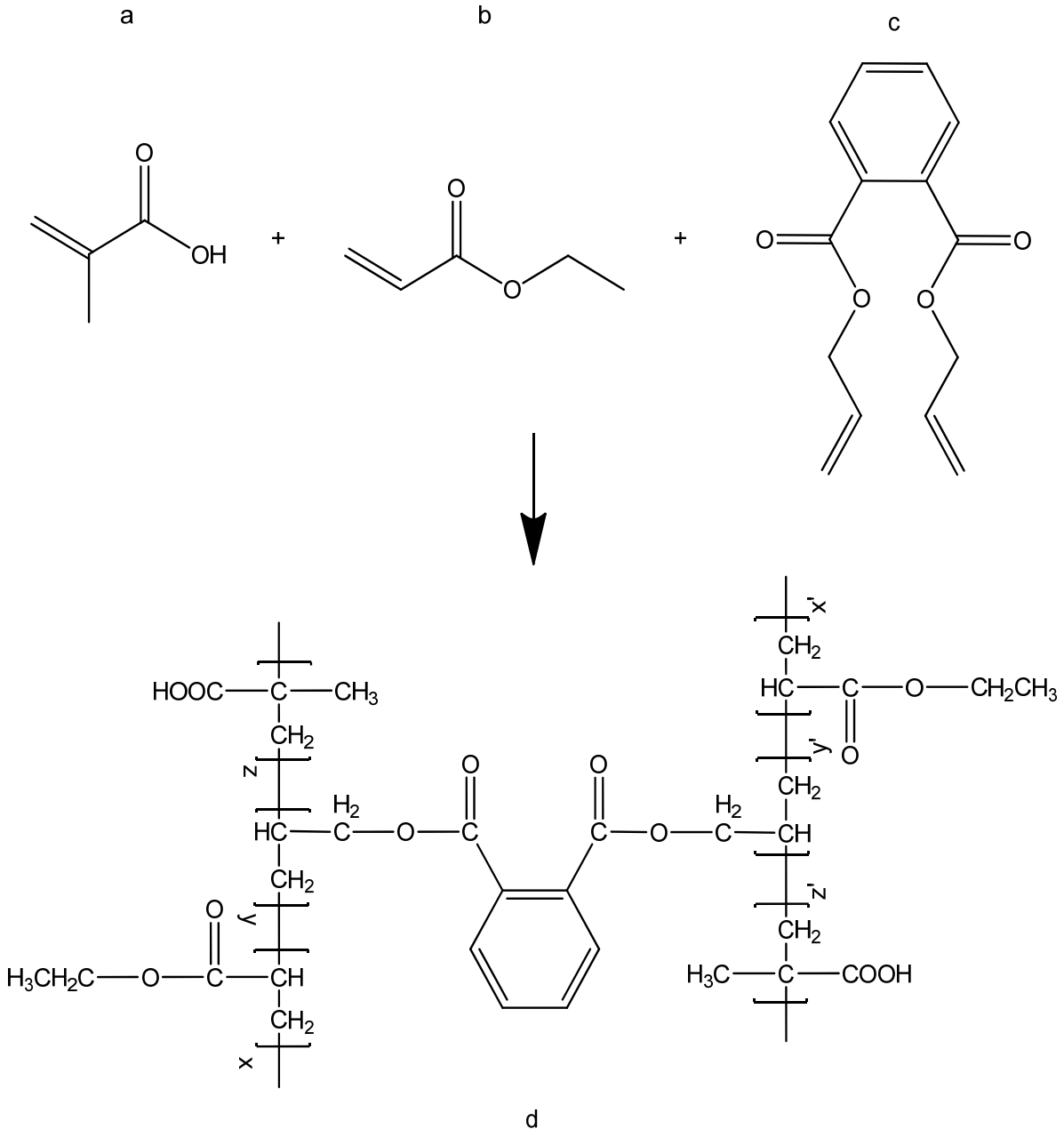

Figure 4-1 Reaction scheme for the synthesis of PMAA-EA polymeric scaffold. a) methacrylic acid, b) ethyl acrylate, c) dially phthalate, and d) crosslinked PMAA-EA

4.3.2 Magnetic Nanoparticles Loading

After the production of polymeric lattice in the previous stage, they were used as colloidal scaffold to load magnetite nano-sized particles (MNPs) into their networks. The purpose of this step is to infuse magnetite (Fe_3O_4) inside the polymer matrix in order to make them magnetic. Magnetite was chosen as it is biocompatible, non toxic, and possesses a higher magnetic saturation compared to other iron oxides. The colloidally-stable products can remain suspended under moderate magnetic fields since the Brownian motion of the nanoparticles is dominant. MNPs possess high surface area to volume ratio that provides high contact surface for adsorption of contaminants. However, it also heightens their tendency to agglomerate, which makes the production of monodisperse particles significantly challenging. One proposed approach to address this problem is to utilize polymeric templates as *in situ* reactors for the synthesis of MNPs as reported by Zhang in 2004 (Zhang *et al.*, 2004). Here, the precipitation technique was utilized to load the MNPs into the polymer nanogels.

A 120ml, 0.5w% solution of polymeric scaffold was prepared and its pH was adjusted to 6.5, using 0.5M NaOH. The solution was then purged for 30min with N_2, after which, 2.5g of $FeSO_4 \bullet 7H_2O$ dissolved in 30ml de-oxygenized water was injected to the reactor, equipped with a mechanical stirrer. This mixture was stirred under nitrogen purge for another 2 hours. Subsequently, the reaction temperature was increased to 35°C, and 0.25g $NaNO_2$ and 15 ml of NH_4OH were added to the reactor, and upon this addition, the milky polymer solution changed to dark green. The content of the reactor was left to stir

for another hour and the color of the reaction mixture gradually changed to dark brown (Figure 4-2). The mixture was then dialyzed for one week in D/I water, where water was replaced every other day (MNP1). The concentration of the solution was 0.44wt %.

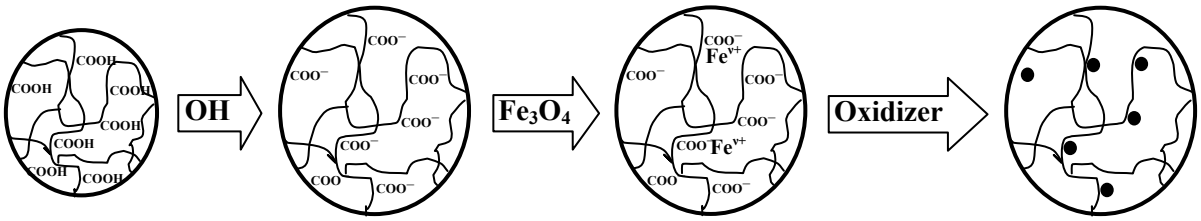

Figure 4-2 Schematic diagram of polymer lattice magnetization

Due to partial instability of MNP1, the magnetic loading approach was modified to a new composition of polymer to iron ratio of 1.25:1 (Moeser *et al.*, 2002). In the adopted procedure, the pH of a 100 ml polymer solution with 0.5wt% concentration was adjusted to ~6.5 using 1M NaOH. After purging the solution for half an hour with nitrogen, 20ml solution of 1.44g of $FeSO_4 \bullet 7H_2O$ in de-oxygenized water was injected into the reaction mixture. The reactor temperature was increased and maintained at 35°C. After 2hrs, 0.15g $NaNO_2$ and 12.5ml of NH_4OH were added to the reaction mixture and stirred for another hour. The mixture was then dialyzed for a week in D/I water, where water was replaced every other day. These particles showed higher stability upon storage (MNP2). The concentration of the solution is 0.68 wt %.

Figure 4-3 A picture of MNP synthesis toward the end of the reaction

4.3.3 Stabilization Experiments

There are two general colloidal stabilization principles that contributed to the stability of nanoparticles: steric and electrostatic stability. The latter is achieved by electrical repulsion of particles with similar surface charges (either positive or negative), while the former is attained by introducing steric hindrances in order to prevent the particles from agglomerating. The introduction of 2-sulfoethyl methacrylate to polymer network increases the negative surface charges of the scaffold and hence the electrostatic repulsion of particles. With regards to steric stabilization, the next section describes the procedures where linear polymeric chains of different molecular weight and

characteristics were examined for their potential to impart physical interference to further increase the stability of MNPs.

PEGMA with different molecular weights and chitosan were investigated for their ability to stabilize the MNPs. These compounds are common as surface coating agents for magnetic particles that are aimed for medical applications, because of their biocompatible characteristics.

4.3.3.1 PEGMA Stabilization

4.3.3.1.1 First Approach:

Conjugating PEGMA branch onto polymer scaffold: about half an hour before the completion of the polymerizaition reaction, two 25ml scaffold solutions were taken from the bulk mixture. A specific amount of PEGMA300 was added to one while PEGMA2080 was added to the other. Both mixtures were left to stir at 80°C for one hour. Afterward, both solutions were purified by dialysis for one week in D/I water, replaced every other day, yielding PMAA-EA-300 and PMAA-EA-2080 respectively.

Magnetic loading of PEGMA grafted polymer network: magnetic nanoparticles particle leading protocol (4.3.2) was carried out for 0.5wt% of PMAA-EA-300 and PMAA-EA-2080. The final solutions were dialyzed again for another week (PEGMA-MNP-300 and PEGMA-MNP-2080, respectively).

4.3.3.1.2 Second Approach:

Grafting PEGMA onto MNPs: in two air-tight containers, under N_2 purge, 50ml solution of MNP1 with 0.1w% concentration, at 70°C, were prepared. Then, appropriate amounts of sodium bicarbonate initiator were added to each one, followed by the required amount of PEGMA300 and PEGMA2080. The reaction mixtures were stirred for an hour. Afterward, both solutions were dialyzed for period of one week in D/I water, which was replaced every other day (MNP-PEGMA300 and MNP-PEGMA2080 respectively).

4.3.3.2 Chitosan Stabilization

Chitosan is a high-molecular-weight linear polysaccharide composed primarily of b-(1,4) linked 2-deoxy-2-amino-d-glucopyranose units, and partially of b-(1,4) linked 2-deoxy-2-acetamido-d-glucopyranose. It has been used in a variety of applications in medical, agricultural and waste treatment fields (Hsu *et al.*, 2002) due to its nontoxic, biodegradable and biocompatible nature. Moreover, the presence of active hydroxyl and amino groups on its backbone has attracted increasing attention in the development of different derivatives. In the following experiments, grafting of chitosan onto the polymeric template was performed.

As the scaffolds containing MNPs possess carboxylic groups on their surface, chitosan can be easily grafted onto the particles, by covalent attachment of amino groups present on chitosan backbone, via carbodiimide activation. Using EDC and NHS, one should keep in mind that the choice of pH significantly influences the coupling efficiency of EDC to

carboxyl group. In EDC assisted NH_2/COOH reactions, acidic environment is a necessity for effective activation of EDC by NHS. However, due to low solubility of chitosan in water, acetic acid (1% w/v) was used as solvent, which protonated the amino groups of chitosan. The presence of EDC in such acidic environment promotes its activation with NHS, resulting in an undesirable reaction of acetic acid with chitosan's deprotonated amines. Hence, to avoid this negative impact, chitosan was dissolved separately in acetic acid, while EDC and NHS were added to ferrofluid solution to activate its surface carboxyl groups. In spite of high stability of ferrofluid under basic condition, it become gradually unstable as the acidity increases. Hence, the pH should be chosen in a way that promotes EDC activation, and not affecting the MNPs' stability considerably.

The pH of a 25ml MNP2 solution was adjusted to 5. To this mixture 0.05g EDC and 0.06g NHS were added and left for 10min for preferential activation of polymer surface carboxyl group of polymer lattice. 0.2g chitosan was dissolved in 20ml acetic acid (1%w/v). The two mixtures were then combined together and were stirred for an additional hour (CTS-MNP).

4.3.4 Functionalization Experiments

In this section the procedure and steps for attachment of β-cyclodextrin to the magnetic scaffold using, chitosan and EDA, are described.

4.3.4.1 Mono-6-tosyl-β-cyclodextrin (TS-βCD)

Most modifications of cyclodextrins take place on their hydroxyl groups. The common cyclodextrins (α, β, and γ) have three hydroxyl groups: one primary and two secondary. The primary OH groups demonstrate stronger basic properties, and hence are considered nucleophilic, while the secondary ones are either acidic or inaccessible. Hence, modifications of cyclodextrins usually take place in one of the primary hydroxyls that has been activated.

A typical activation procedure involves tosylation of one of the primary OH groups on β-CD structure was as followed (Trellenkamp and Ritter, 2010) (Figure 4-4): 10.0g of β-CD was dissolved in 500mL of a 0.4M aqueous solution of sodium hydroxide and cooled to 0°C. Subsequently, 35.0g of p-toluenesulfonyl chloride was added in small portions to the solution under intense stirring over 5min. The resulting suspension was stirred for a further 30min while the temperature was maintained below 5°C and then quickly filtered. The filtrate was neutralized with hydrochloric acid and stirred for 1h. The resultant precipitate was filtered, washed three times with water and dried overnight at 60°C. The yield of the reaction was 25.6%.

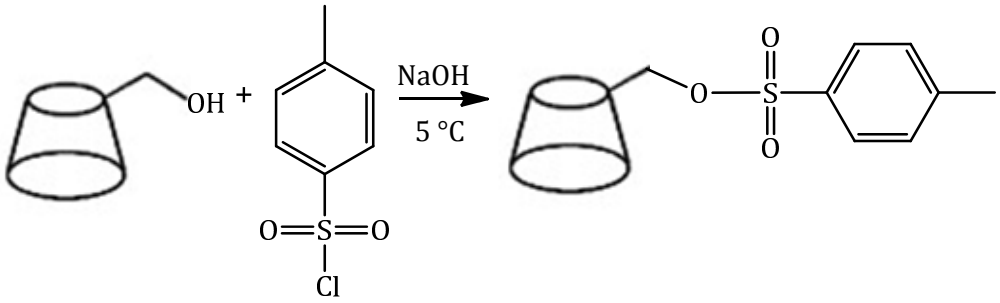

Figure 4-4 Tosylation of β-CD

Due to the low yield, the first method was further modified (Gonil *et al.*, 2011). 25g of β-CD was dissolved in 350mL of NaOH (10%w/v) and stored overnight in the refrigerator. 10g p-toluenesulfonyl chloride was added and stirred at 0–5°C in an ice bath. The reaction mixture was stirred vigorously at 0–5°C for 2h. Subsequently, another 15g of p-toluenesulfonyl chloride was added and stirred continuously at the same temperature for another 3h. The reaction mixture was filtered through a sintered glass funnel to separate unreacted p-toluenesulfonyl chloride. The filterate was treated with hydrochloric acid (pH 1–2) at 0–5 °C and stored overnight in the refrigerator. The precipitated solid was isolated by vacuum filteration, and it was then recrystallized by dissolving in hot water. The solution was then cooled down to room temperature and stored in the refrigerator overnight. The yield was 31.73%.

4.3.4.2 β-cyclodextrin Functionalization

The following functionalization reactions are based on the nucleophilic substitution of mono-6-tosyl-β-cyclodextrin tosyl group with an anion.

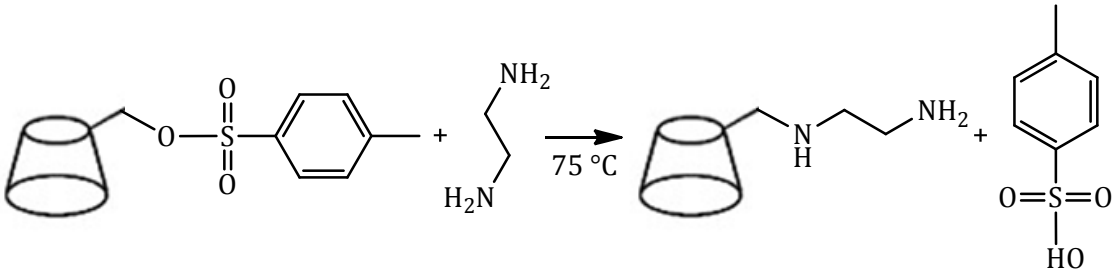

Figure 4-5 Schematic of synthesis route for EDA-βCD

4.3.4.2.1 Synthesis of ethylenediamine-conjugated β-CD (βCD-EDA):

After activating the β-CD on one of its primary hydroxyl groups, conjugation of ethylenediamine can be easily accomplished. For this purpose 5g of TS-βCD was stirred at 75°C in 30ml of ethylenediamine for 4hr (Figure 4-5). The solution was then cooled to ambient temperature. Ethylenediamine-conjugated β-CD was precipitated using cold acetone. Then, it was repeatedly washed and precipitated with water-methanol mixture and cold acetone, respectively, to ensure complete removal of unreacted ethylenediamine. It was then dried at 50°C for three days in vacuum oven.

4.3.4.2.2 Grafting of βCD-EDA onto MAA-EA scaffolds(βCD-POL):

To ensure that β-CD could be grafted onto the polymeric scaffold, the reaction was performed and the chemical composition was analyzed by NMR to ensure successful grafting. For this purpose, 0.2g of βCD-EDA, 0.31g of EDC, and 0.18g of NHS was added to 28ml of polymer solution. The reaction mixture was magnetically stirred and left over night. It was then dialyzed with D/I water for a day.

4.3.4.2.3 Conjugation of βCD-EDA onto MNPs (βCD-MNP1):

0.2g of βCD-EDA, 0.31g of EDC, and 0.18g of NHS was added to a 28ml ferrofluid. The reaction mixture was magnetically stirred and left over night, and it was then dialyzed with D/I water for a day (βCD-MNP1).

4.3.4.2.4 Grafting of β-CD on to chitosan (βCD-CTS):

Different approaches were selected from the literature to perform the nucleophilic substitution on TS-βCD with chitosan (Figure 4-6). The modified procedures are described below:

(1) 0.3g of chitosan was dissolved in 15ml of DMF. To this solution, 0.5g of TS-βCD dissolved in 4ml DMF was added drop-wise, and the mixture left to stir for 48h at 50°C. Afterward, the yellow precipitates were filtered and washed with water (Chen and Wang, 2001).

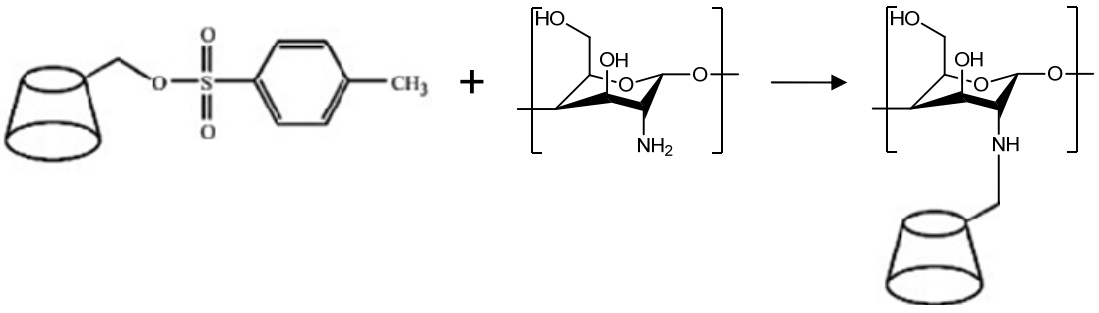

Figure 4-6 Schematic of grafing β-CD onto CTS step

(2) 0.3g chitosan was dissolved in 30ml acetic acid (1%v/v, pH=4). 0.5 g TS-βCD dissolved in 4 ml DMF was added to this solution. The mixture was stirred and refluxed at 100 °C for 24 h. Afterward, it was dialyzed in water for 3 days. It was then freeze-dried to yield a cotton-like powder (Gonil *et al.*, 2011).

(3) To a solution of 0.1g of chitosan in 25ml acetic acid (2%v/v), 0.43g of β-CD, 0.88g of ascorbic acid was added and mixed at 35°C. After half an hour, 0.06g of sodium persulfate was added and left to stir for an additional hour. Then, the pH increased to ~6.5 to separate the unreacted β-CD, and the solution was mixed with acetone to recover the precipitate. The precipitate was repeatedly washed with acetone to remove any residual β-CD and it was then freeze-dried (Sharma and Mishra, 2010).

Although, all these approaches are similar, the first method was the easiest, , with higher yield, and required the least expensive materials, which makes it more suitable for large scale.

4.3.4.2.5 Conjugation of βCD-CTS onto the MNPs (βCD-MNP2):

To attach βCD-CTS onto the MNPs, similar procedures to the one mentioned in section 4.3.3.2 was followed with appropriate amounts of materials.

Chapter 5 – Results and Discussion

In this chapter, the results of characterizations of polymeric scaffold, MNPs and their derivatives are reported.

Although many different synthetic approaches were considered to stabilize and functionalize the MNPs, none of them proved efficient in increasing the stability of any of synthesized MNPs. Despite the sufficient stability of the parent MNPs demonstrated over long time (6 months), all their derivatives demonstrated moderate to high tendency for agglomeration and precipitated or oxidized upon storage as shown in Figure 5-1.

When PEGMAs were used to introduce additional steric hindrance for stabilizing the MNPs, the increase in temperature necessary for the grafting reactions resulted in the oxidation of iron ions from Fe^{2+}/Fe^{3+} to Fe^{3+}, and these particles precipitated out of the polymeric scaffold. When grafting was performed before magnetization the final result was not any better. However, in this case, the presence of PEGMA not only hindered the entrance of iron ions to the PMAA-EA network, but also, it promoted their interaction with oxygen double bonds of methacrylate end group.

EDA proved to be too short to introduce any physical hindrance. Chitosan were too long, even when they were initially functionalized with β-CD to lessen the amounts of

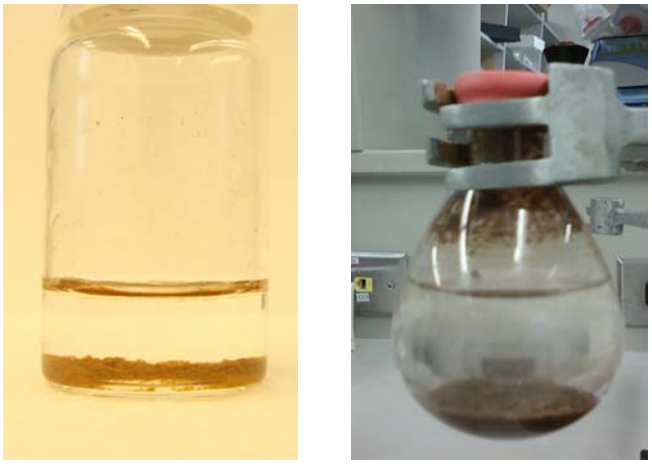

Figure 5-1 Instability of MNPs derivatives EDA-MNP (a) and PEGMA-MNP-2080 (b)

amine group on their backbone. Therefore, extensive agglomeration occurred during the reactions due to bridging. Thus, the results that are described in this chapter mostly focused on the polymeric scaffold and MNP.

5.1 Spectrometry

5.1.1 NMR

Since dried PMAA-EA scaffold are difficult to be solublized in DMSO-d_6, a small volume of the polymer solution was diluted with DMSO-d_6. However, it introduced enough moisture to the sample that led to a significant interference from the large water peak. As a result, the NMR spectra did not yield intense peaks for the functional groups in the polymer network. However, magnification of the spectra revealed the characteristic peaks for protons present in ethyl acrylate and methacrylic acid groups of the polymer

(Figure 5-2). This spectrum is in accordance with the ones reported earlier (Bajaj *et al.*, 1994; Jassal *et al.*, 2003). The multiplet peaks of methyl group proton appeared between 0.75-1.35ppm (*a* and *a'*). The methylene proton on both MAA and EA contributed to the broad signal between 1.4 and 2.0ppm (*b+b'*), and the peck at 2.25ppm was attributed to methine protons of EA (*c*). The signals at 2.5 and 3.5ppm were caused by residual protons of DMSO-d_6.

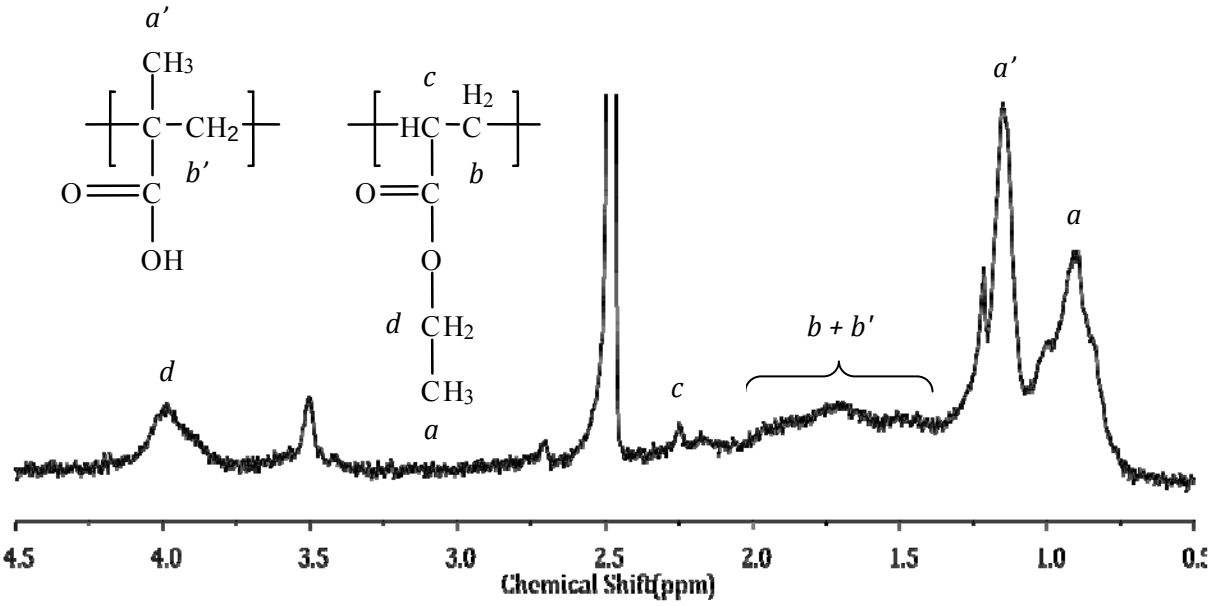

Figure 5-2 ^{1}H NMR spectra of polymeric template in DMSO-d_6

When comparing the NMR spectra of TS-βCD to its parent compounds, p-toluenesulfonyl chloride and β-CD, (Figure 5-3) the broad band of β-CD between 4.0-3.5ppm, related to C—H band at C_2, C_3, C_4, C_5, and C_6, its C_1—H band, at 4.8ppm, and p-toluenesulfonyl chloride characteristic double bands of benzene group, at 7.75 and 7.35

ppm (*a*), proved the successful production of TS-βCD. The binding of β-CD to EDA results in and manifestation of EDA ethylene group peak at 2.06 ppm (Figure 5-3-d).

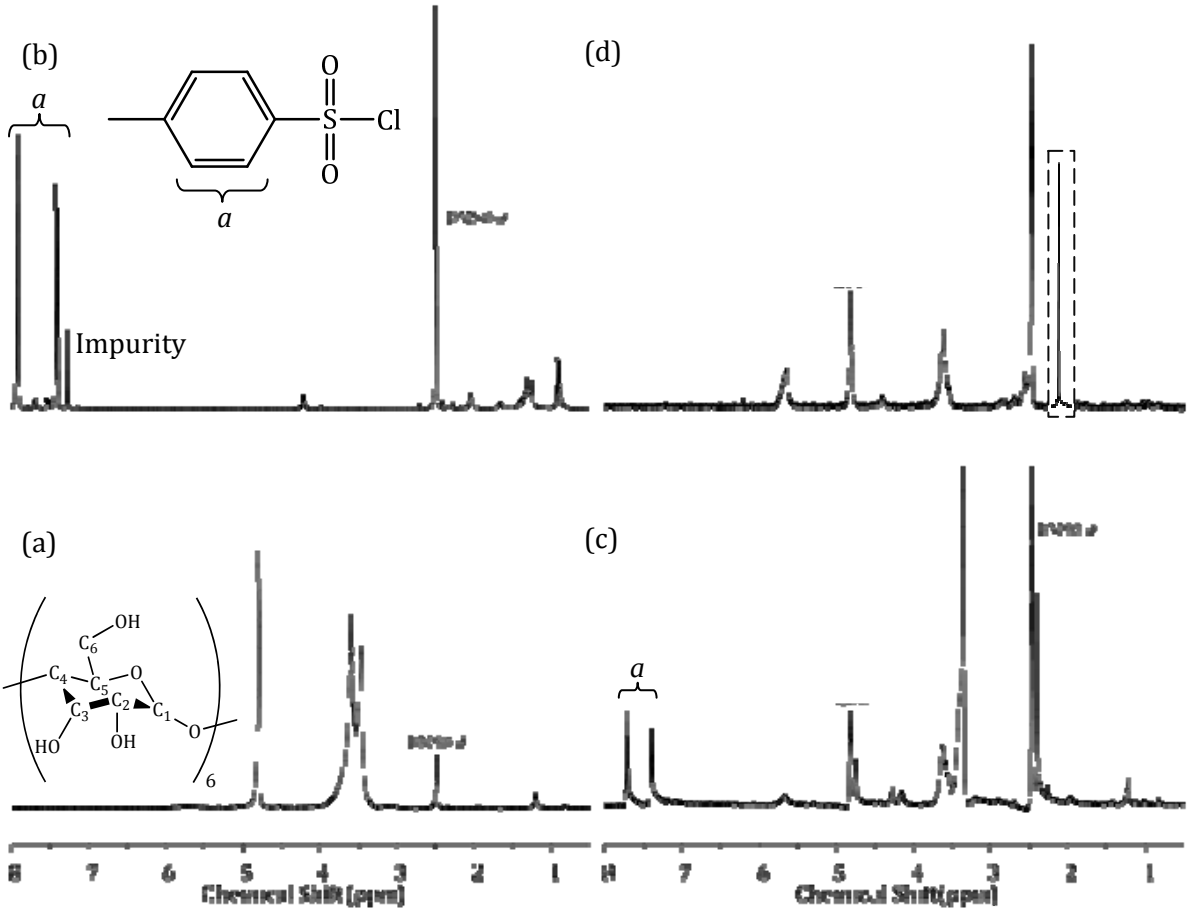

Figure 5-3 ^{1}H NMR spectrum of β-CD (a), TsCl (b), TS-βCD (c), and EDA-βCD (d) in DMSO-d_6

Attachment of β-CD to chitosan also leads to the appearance of β-CD characteristic multiple peaks between 3.7-3.2ppm. This is due to C—H bond on the backbone of chitosan (Figure 5-4). The sharp peak at 1.78ppm (*a*) was from the methyl group of chitosan and the one at 2.90ppm (*b*) was due to its primary amine.

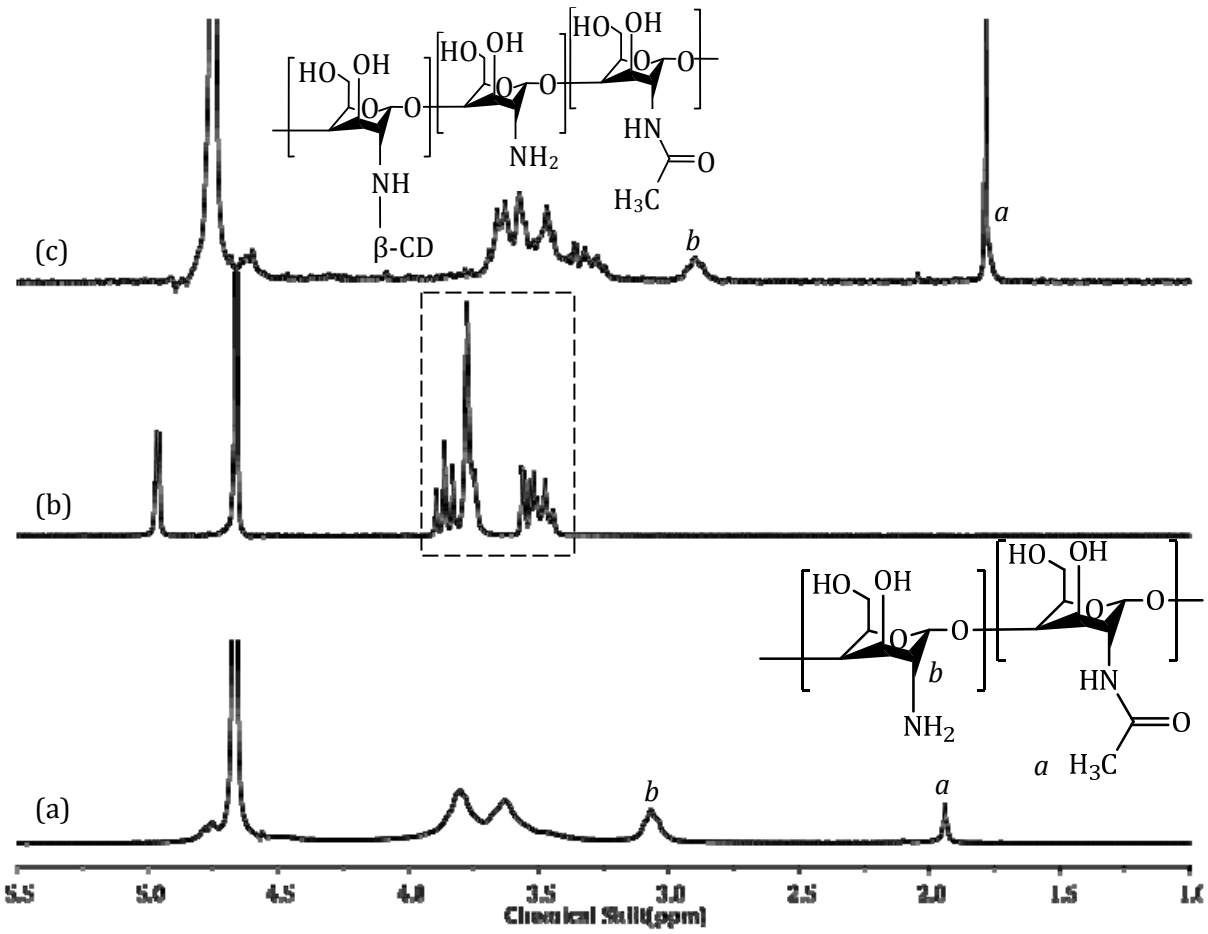

Figure 5-4 ^{1}H NMR spectra of Chitosan (a), β-CD (b), and βCD-CTS (b) in CD_3COOD/D_2O

5.1.2 FTIR

Due to the magnetic nature of MNPs, NMR is not a suitable method to perform characterization studies on them. Therefore, FT-IR was selected as their functional group recognition technique. In the spectra of the polymeric scaffold (Figure 5-5-a), carbonyl stretching of the acid and ester units appeared at 1735 and 1703cm^{-1}, respectively. The broad signal from 3227 to 3425cm^{-1} was due to the O—H stretching

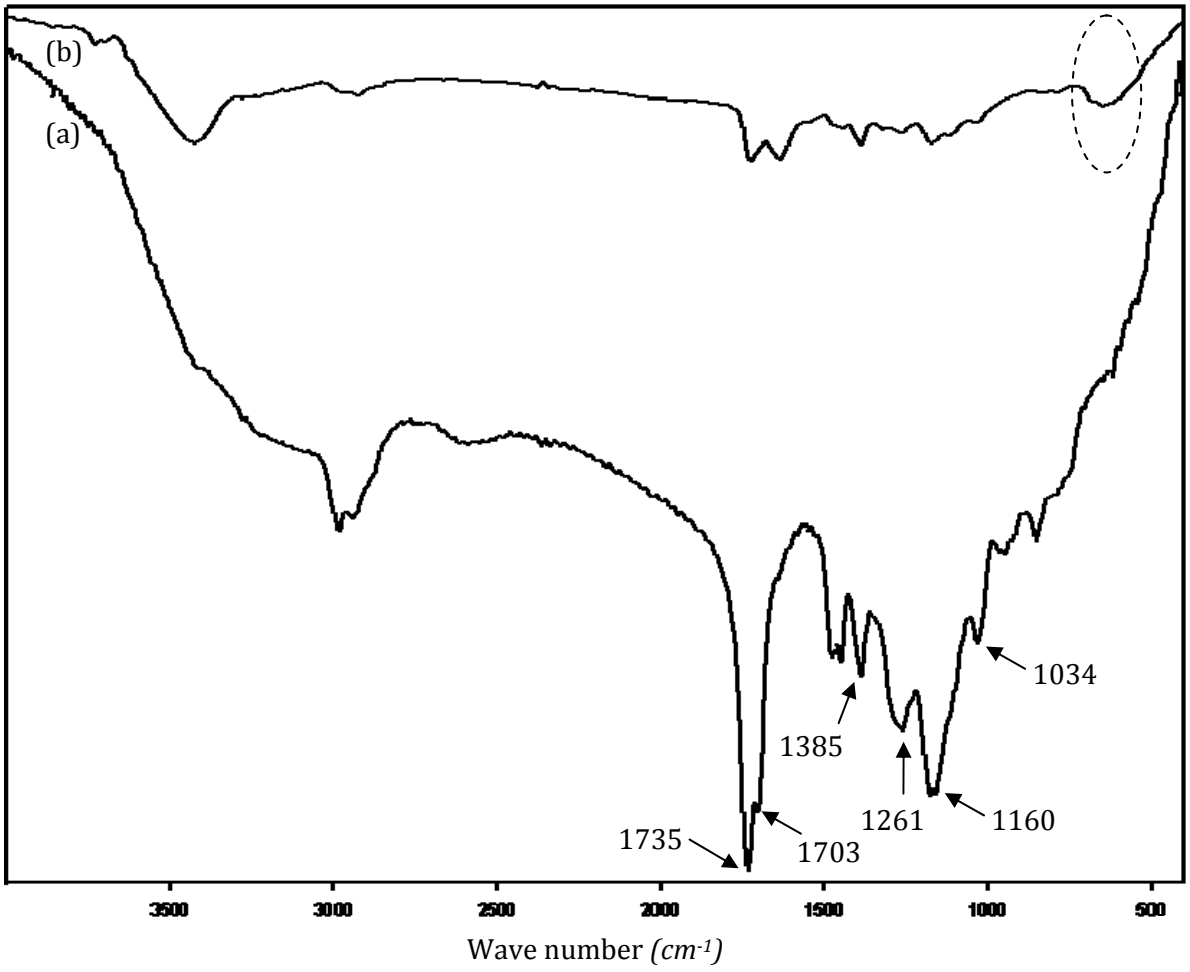

Figure 5-5 FT-IR spectra of PMAA-EA (a) and MNP (b). The appearance of a broad weak adsorption signal at 650 cm^{-1} is the proof of magnetite incorporation inside the polymer

vibration of the carboxyl group of the methacrylic acid portion of the scaffold. C—H deformation of the methyl group and splitting of the C—O stretching vibration into two components are observable at 1385, 1261, and 1160cm^{-1}, respectively. The adsorption signal at 1034 cm^{-1} was a result of C—O—C stretching of the ester group. These were similar to the characteristic peaks reported for poly(methacrylic acid) and poly(ethyl

acrylate) (Bajaj *et al.*, 1994). Comparing this spectrum to the one obtained from MNPs (Figure 5-5-b), the appearance of a weak and broad signal at 650cm^{-1} corresponded to the adsorption of magnetite, which confirmed the successful incorporation inside the PMAA-EA scaffold.

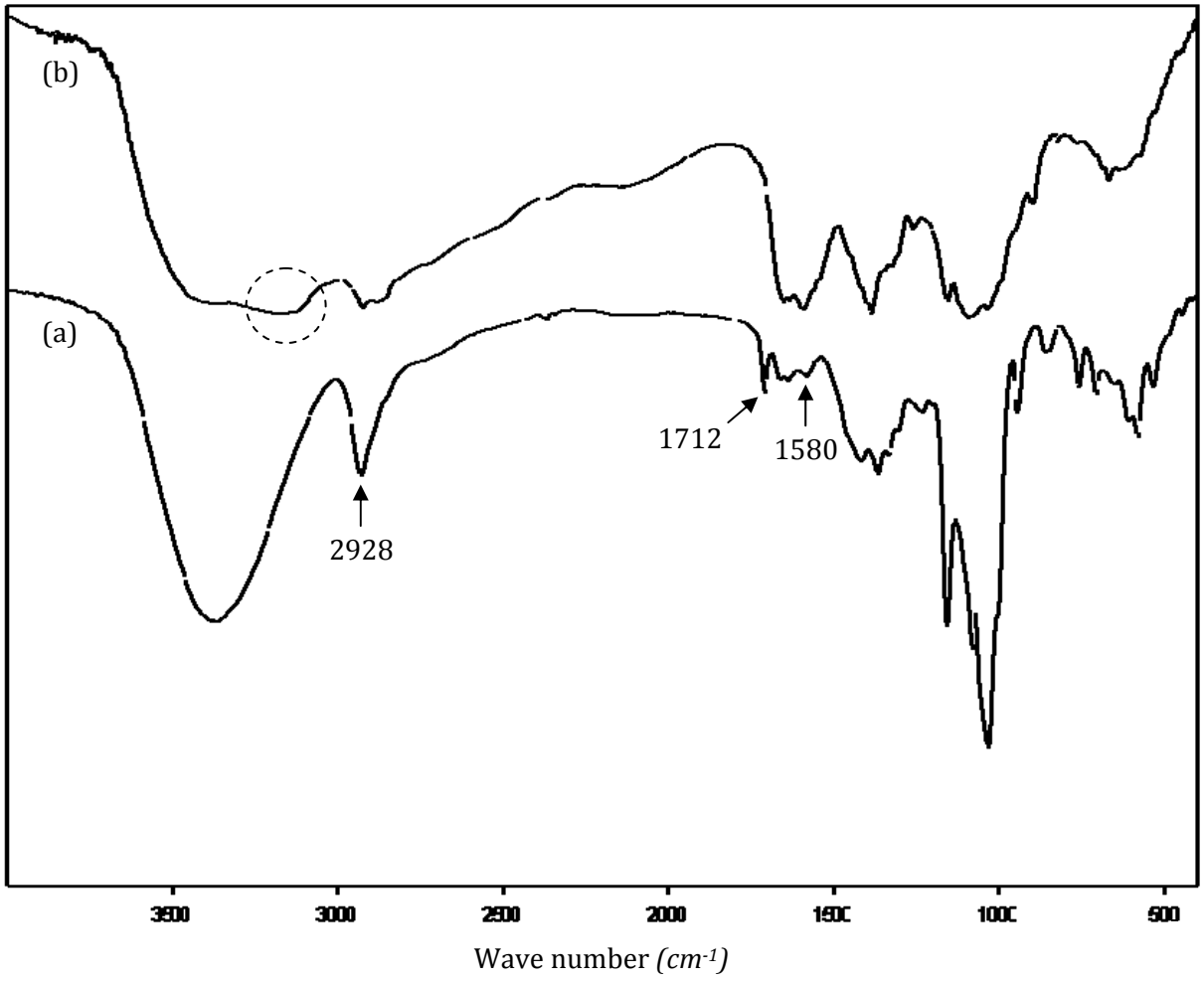

Figure 5-6 FT-IR spectra of βCD-EDA (a) and βCD-CTS (c)

The FT-IR spectrum for βCD-EDA showed the stretching of O—H with a broad peak at 3370cm^{-1} and C—H at 2928cm^{-1} (Figure 5-6-a). Addition of N—H bending signal at 1712cm^{-1} and C—N stretching at 1580cm^{-1} to characteristic signals of β-CD signified the successful grafting. For βCD-CTS, beside the O—H, from both hydroxyl and carboxyl functionalities, the N—H stretching, of primary amine, secondary amine and amide

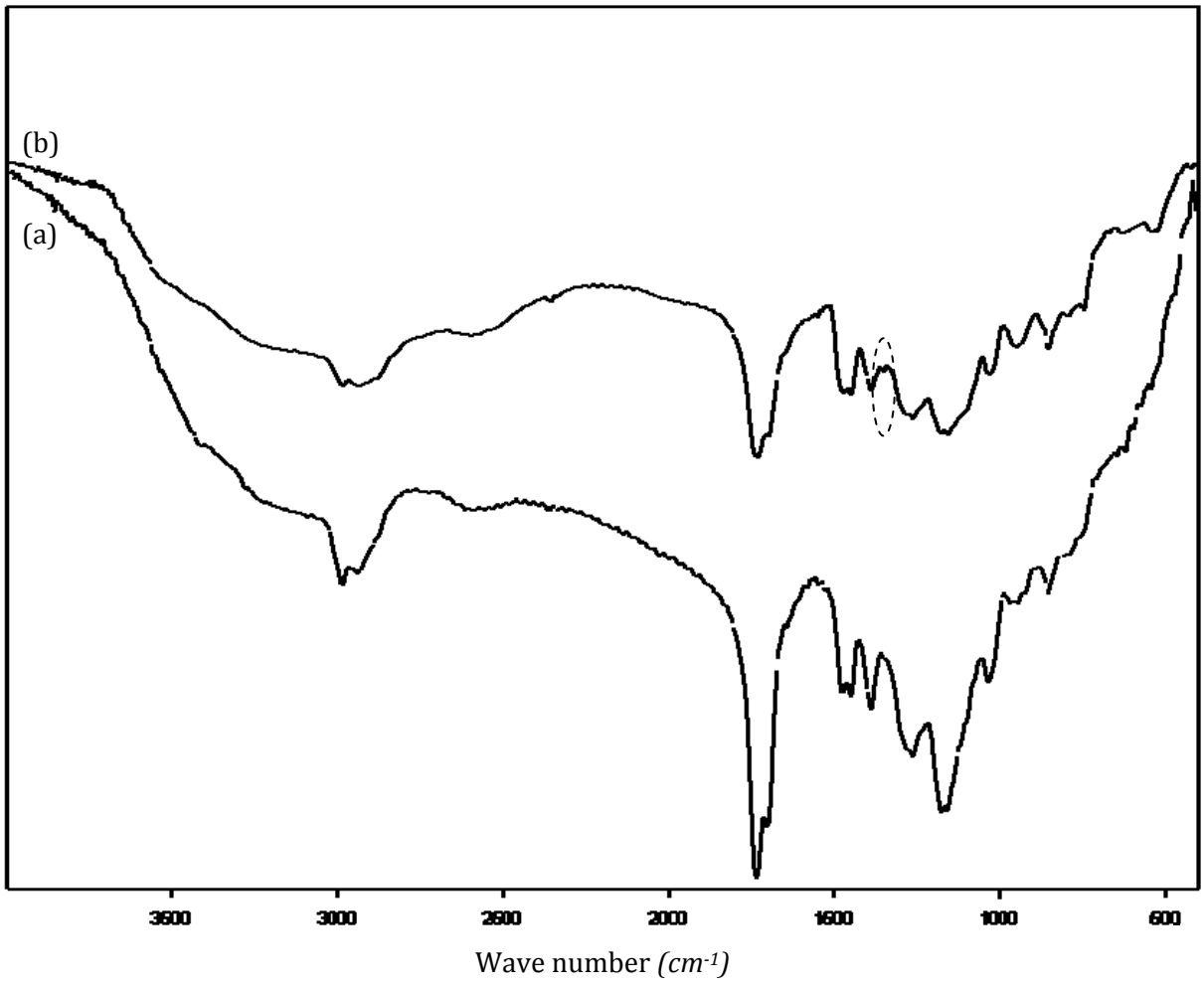

Figure 5-7 FT-IR spectra of PMAA-EA (a) and PMAA-EA-300 (b)

group, resulted in the appearance of another broad peak at 3180cm^{-1} (Figure 5-6-b). The bending peaks of amide were also observed at 1652 and 1638cm^{-1}. The corresponding peak for C=O stretching was noticeable at 1600cm^{-1}, as well. Moreover, the symmetric and asymmetric stretching of C—H in methyl groups of chitosan were detected at 2920 and 2980cm^{-1}.

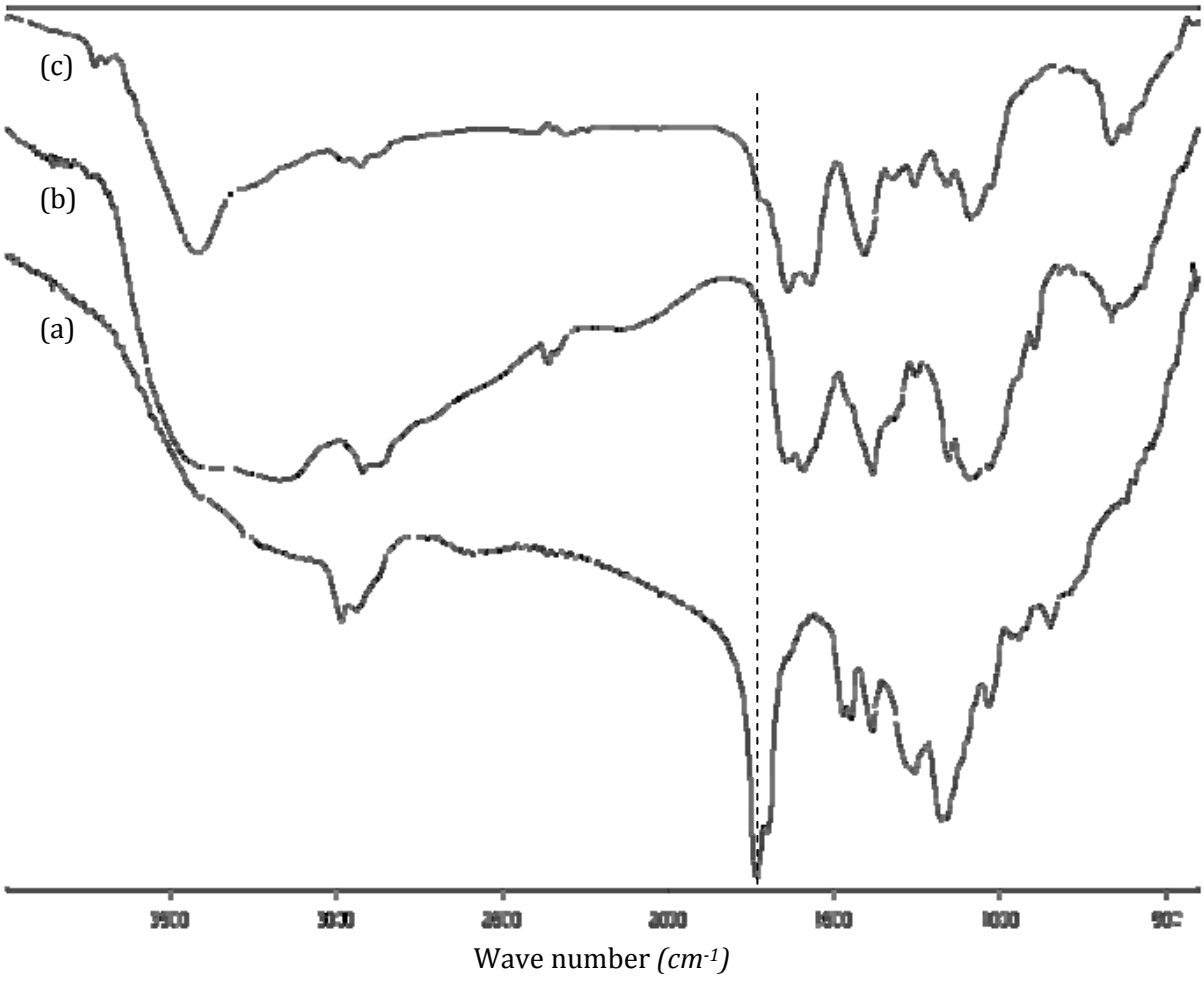

Figure 5-8 FT-IR spectra PMAA-EA (a), βCD-CTS (b), and βCD-MNP2 (c)

When comparing the FT-IR spectra of the PMAA-EA (Figure 5-7-a) to PMAA-EA-300 (Figure 5-7-b), the appearance of a weak adsorption peak at 1351cm^{-1} indicated the ether group on backbone of PEGMA; confirming the success of the grafting polymerization.

The spectra for βCD-MNP2 showed all the characteristic peaks from PMAA-EA and βCD-CTS with minor changes (Figure 5-8). For example the carbonyl stretching peak at 1735cm^{-1} was weakened in the functionalized MNPs. This reduction was caused by the lower carbonyl content of this compound compared to its parent.

5.2 Particle Size Determination

The acquired raw data from Brookhaven software, for each angle and pH were exported to GENDIST in the DOS environment for further analyses. This program converts the correlation functions to the distribution functions using the inverse Laplace transformation. These data were then processed to determine the angle independent size of the particle at each pH.

In Figure 5-9, the pH-responsive nature of the polymer template was noticeable. As the pH increased, the carboxyl group deprotonated; causing an increase in the negative charge on the scaffold. The repulsion between the COO^- ions inside the hydrogel led to an increase in the osmotic pressure and swelling of the scaffold. Comparison between particle size for PMM-EA, PMM-EA-300, and PMM-EA-2080 confirmed the grafting of PEGMA polymer onto the polymer. It is clear from Figure 5-9 that grafting of

PEGMA2080 onto the polymer scaffold increased the particle size by two folds (200%), while PEGMA300 did not affect the particle size significantly, due to its shorter chain length.

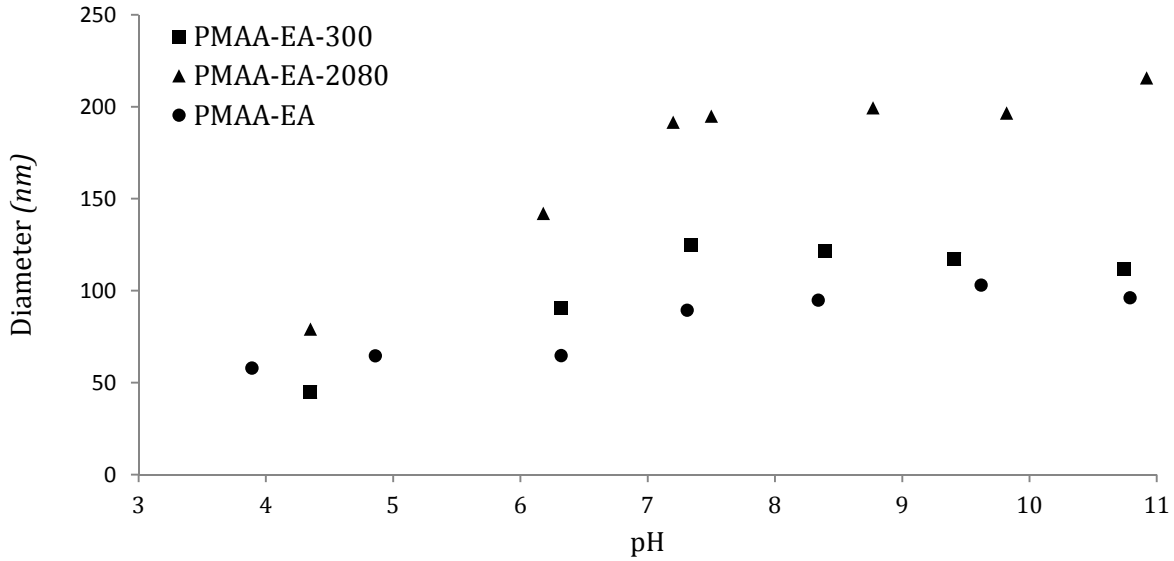

Figure 5-9 Particle size for PMAA-EA and its PEGMA grafted derivatives

increase in the polymer content of MNPs significantly affected their pH-responsiveness. Although both MNP1 and MNP2 possessed similar size at acidic pH, changes in the pH impacts the size of the MNPs. Under alkaline condition (pH>10), the MNP2 size increased by 6 fold, compared to 2.5 for MNP1. The negative surface charge of the magnetite particle at alkaline condition could account for the further swelling of magnetic nanogels, as they repelled the neighbouring deprotonated carboxyl group, compared to their non-magnetic counterpart.

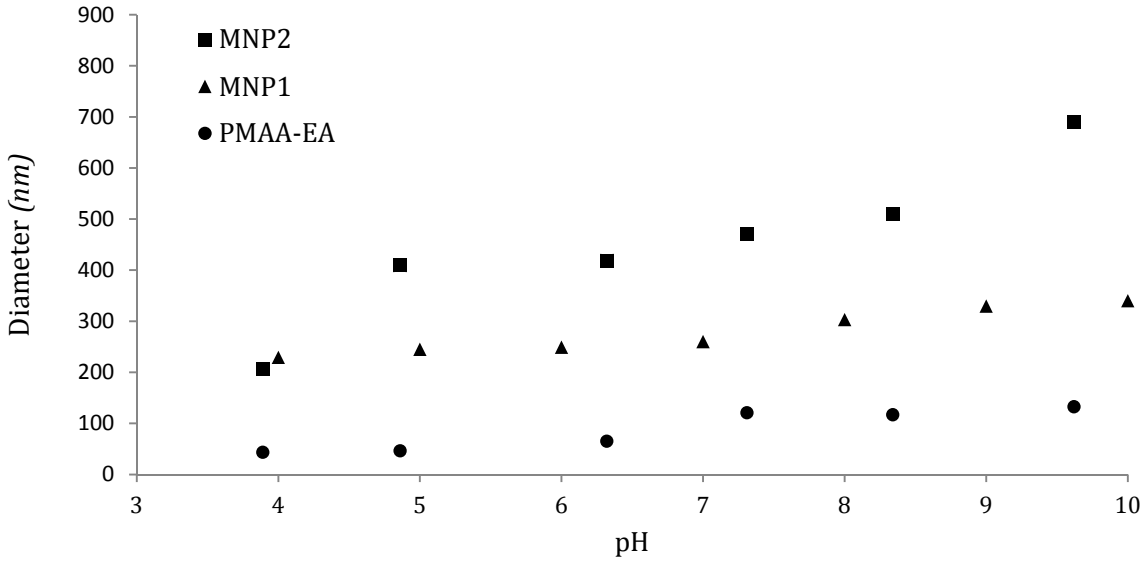

Figure 5-10 Particle size for PMAA-EA and its magnetization products

The DLS measurement revealed that further modification on ferrofluids led to poly disperse products with wide size distribution, as a result of aggregation (Figure 5-11).

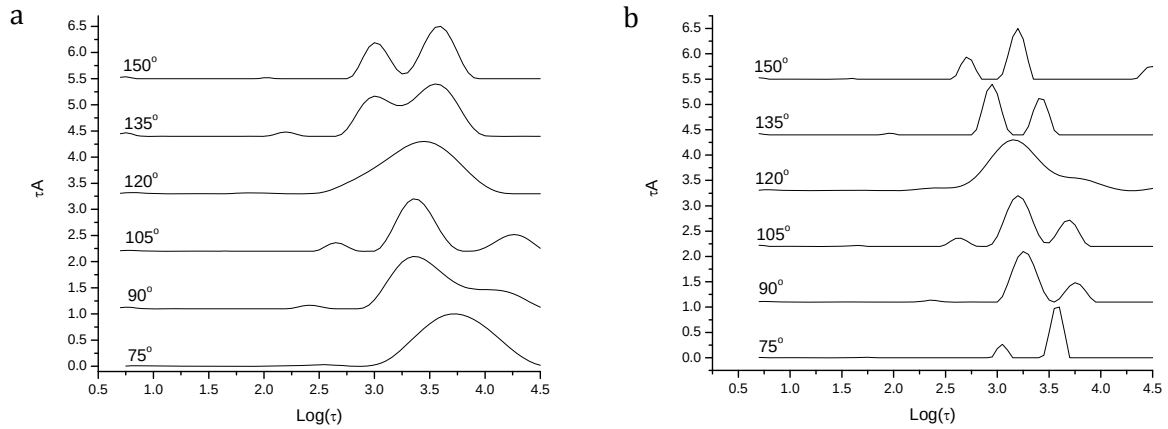

Figure 5-11 Size distribution plot for MNP-PEGMA300 (a) and BCD-MNP2 (b)

5.3 Surface charge measurements

Figure 5-12 displays the changes in the surface charge of polymer nanogels with pH. The initial negative charge was due to the incorporation of 2-sulfoethyl methacrylate onto the gel network during the synthesis. The increase in pH initiated the deprotonation of carboxylic group of methacrylic acid segments of polymer backbone. Deprotonation further increased the negative charge till pH 9. Beyond this point, all the available carboxyl groups were deprotonated, and the anions from the basic medium

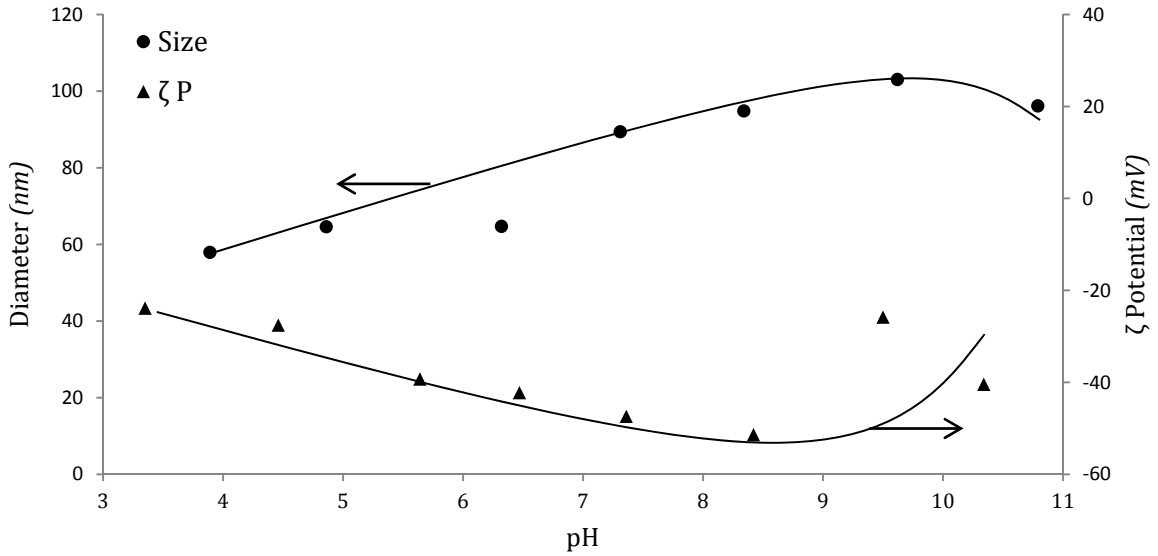

Figure 5-12 pH-responsiveness of PMAA-EA

shielded them from one another. In addition, high concentration of Na^+ can also reverse the deprotonation of carboxyl groups. Therefore, at pH>9 surface charge and particle size were reduced. Therefore, as shown in Figure 5-12, the size of the nanogels decreased slightly at high pH. Measurements were repeated on several samples to confirm occuranse of such behaviour due to nature of the scaffold not errors.

The nanogels loaded with ferric oxides followed similar surface charge trend with a slightly more negative initial value (Figure 5-13). In a stable suspension, the surface charge of suspended particles is often greater than -30mV, in order to prevent aggregation. However, this is not the case for modified MNPs. Figure 5-13 shows that βCD-MNP1 surface charge is less than -30mV at all time which is not large enough to stabilized the particles. It also suggests that although βCD-MNP2 has sufficient charge at pH values greater than 6, during conjugation reaction, at pH=5, its low surface charge promoted rapid agglomeration.

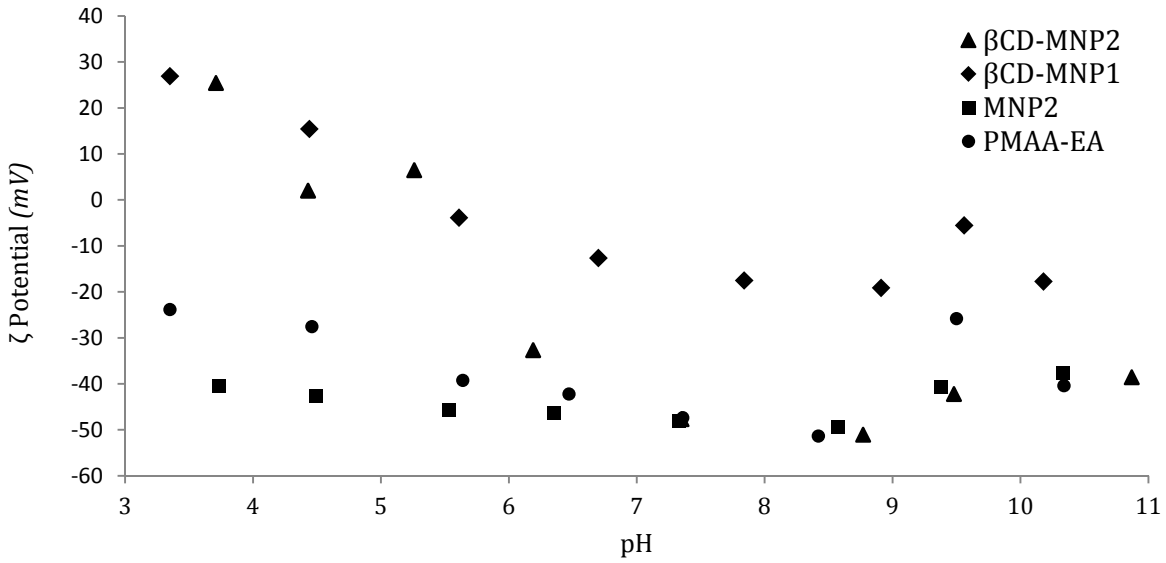

Figure 5-13 Variation of surface charge with pH for PMAA-EA (●), and MNP2 (■), βCD-MNP1 (♦), and βCD-MNP2 (▲)

5.4 Potentiometric measurements

In order to determine the amounts of carboxyl group on PMAA-EA network and MNP, potentiometric titrations were conducted. In a 50ml jacketed reaction vessel, 0.1wt % of the PMAA-EA solution in 10mM NaCl was prepared and its pH was adjusted by adding several drops of concentrated HCl solution, 3M. The mixture was then stirred under N_2 purge at 25°C for 30min. Afterward it was titrated with 10mM NaOH solution. The conductiometry and pH measurements were recorded simultaneously during titration (Figure 5-14). A similar procedure was carried out for the MNPs, where a 50ml solution of 0.1wt% MNP in 10mM NaCl was prepared and several drops of 1M NaOH were added to it. This mixture was then left to stir in a jacketed flask at 25°C under nitrogen purge. Then, back titration was performed with 10mM HCl solution.

It is clear from the conductivity graphs that the titration can be divided into three different regions (Figure 5-14). The first region corresponded to the neutralization of excess HCl resulting in the reduction of the conductivity. When all the excess HCl was neutralized, further addition of NaOH initiated Phase II. During this stage the carboxylic groups on the polymer template were deprotonated according to following reaction:

$$-\mathrm{COOH} \rightleftharpoons -\mathrm{COO}^- + \mathrm{H}^+$$

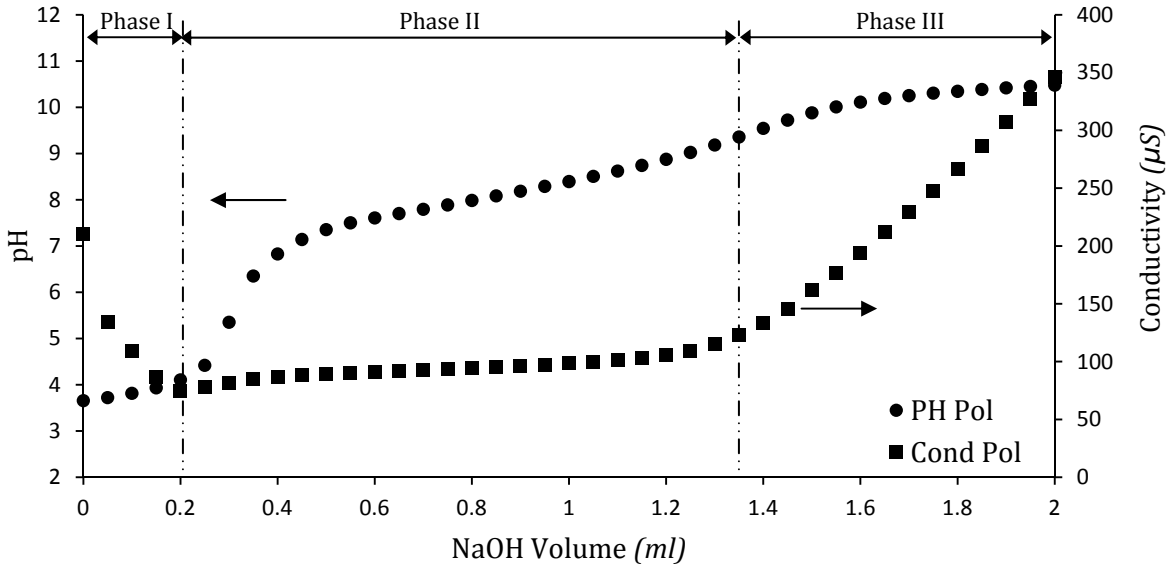

Figure 5-14 Simultaneous potentiometric (●) and contiometric (■) curves for PMAA-EA

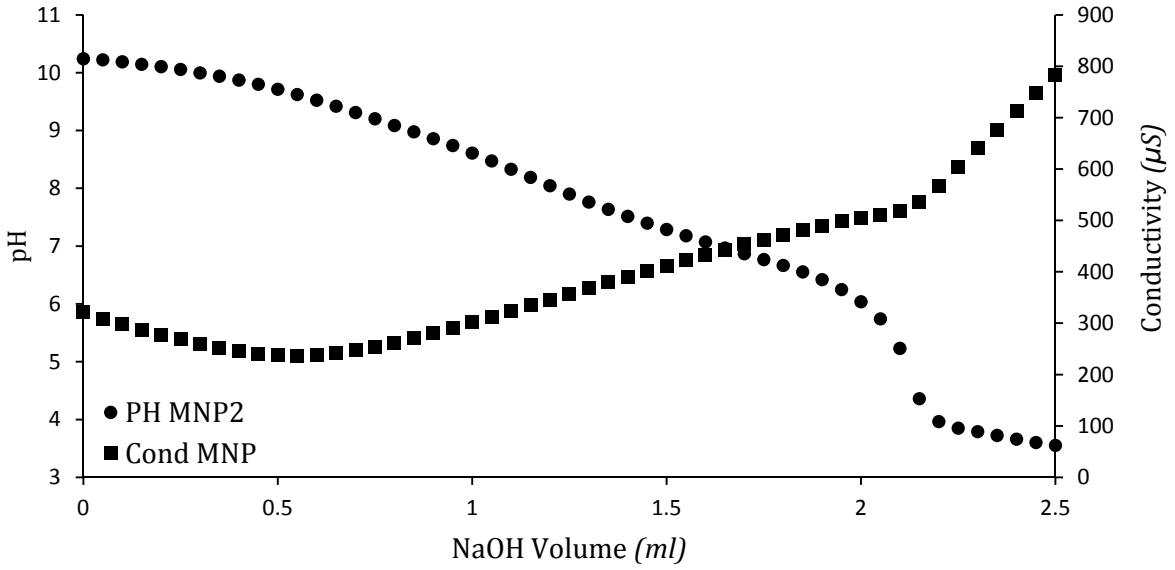

Figure 5-15 Simultaneous potentiometric (●) and contiometric (■) curves for MNP2

Consequently, the above equilibrium proceeded toward ionization to compensate for reduction of [H^+]. However, NaOH is a very strong acid compared to organic carboxylic acid. Hence, although in this phase neutralization was still progressing, the conductivity increased. It is noteworthy that due to pH-responsive nature of MAA-EA copolymer, the scaffold swelled during titration. Therefore, carboxyl groups that were burried inside the network come in contact with bulk solution and the amount of COOH increased from its initial value. Contribution of newly deprotonated carboxyl groups to [H^+] was sufficient to almost match the complete ionization of NaOH. Hence, the conductivity graph followed a logarithmic increase toward the more basic condition.

When all the carboxyl groups on the copolymer network were deprotonated, neutralization process completely ended and phase three began. In this phase further addition of NaOH led to linear increase in the conductivity.

The backward titration of the magnetic solution showed similar behaviour (Figure 5-15). By performing simple titration calculation:

$$N_1V_1 = N_2V_2$$

the carboxyl content of the each solution was determined to be 2.3 and 3.16 mmol/g polymer for PMAA-EA and MNPs, respectively. The increase in the amount of calculated [COOH] for magnetic solution was potentially due to oxidation of magnetite to 3 valence iron ion (Fe^{+3}).

5.5 Stability Studies

To examine the stability of the magnetic solution, pH and ionic strength tests were carried out. For the determination of the upper limit of particles stability in ionic solution, 1ml solution to 1ml solution of NaCl at different concentration, 20µL of the bulk magnetic solution was added with Eppendorf micropipettes. Figure 5-16 shows that the particles experienced partial stability loss at NaCl concentration of 0.75. Further increase in the ionic strength of the solution to 1M, clearly led to instability of the particles and their subsequent precipitation.

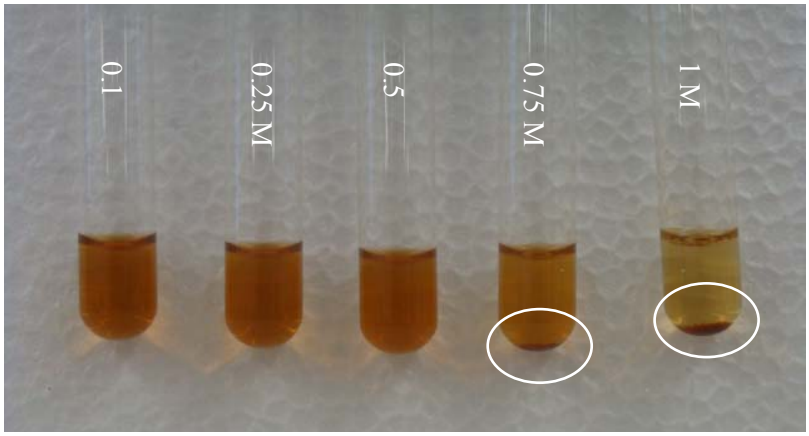

Figure 5-16 Ionic strength stability samples containing 20µl 0.01wt% MNP1 in 1ml of salt solution

The pH stability tests were conducted on a 2ml of 0.01wt% solution of magnetic particles (Figure 5-17). In order to prevent instability caused by introducing salt, buffer solutions were not used and the pH was adjusted by addition of acid or base. To minimize the dilution effect, suitable concentration of HCl and NaOH were used

accordingly for each sample. This test showed that at pH below 6, the nanoparticles started aggregating and hence the turbidity of solution increased. In lower pH most of the magnetic particle precipitated at the bottom of the test vial.

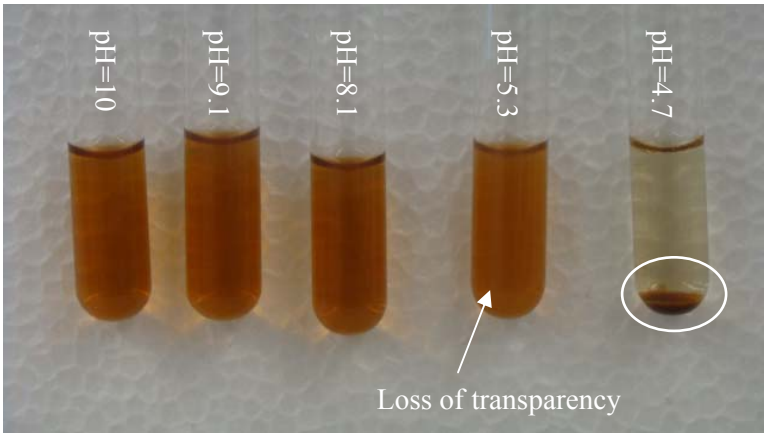

Figure 5-17 pH stability experiment samples containing 2ml of 0.01wt% MNP1 and minimum amount of acid or base

Chapter 6– Interaction Between β-CD and PHC

The focus of this chapter is on preliminary studies performed on the complexation of procaine hydrochloride (PHC), as a model organic contaminant, with β-cyclodextrin (β-CD), as removal agent. Complexation studies were performed using ion-selective electrode with a membrane that has selective permeability to PHC. Furthermore, micro-calorimetry studies were performed to gain better understanding on the nature of the interaction.

6.1 β-cyclodextrin

6.1.1 Introduction

As briefly discussed earlier in Section 4.3.4, cyclodextrins are macrocyclic oligomers of glucose. The three major cyclodextrins, α, β, and γ-cyclodextrins (also referred to as native or common parent cyclodextrins) consist of 6, 7, and 8 α-D-glucopyranoside units, respectively, that are connected through α-1,4-linkage (Figure 6-1a). They are crystalline, homogeneous (purity over 99.5%), nonhygroscopic dextrorotatory enantiomers that are chemically stable. Because of the $^4C_1$ chair conformation of glucopyranoside units, the molecules have hollow conical cylinder shape, often referred to as doughnut or hollow truncated cone (Figure 6-1-b). Table 3 lists the main physical characteristics of these three cyclodextrins. The parent cyclodextrins are soluble in polar solution and moderately soluble in water, with β-CD having the lowest aqueous solubility (8- and 13-fold lower than α-and γ-cyclodextrin, respectively).

Table 3 Characteristics of α -, β-, and γ-cyclodextrin

Property	α	β	γ
Number of glucose units	6	7	8
Molecular weight	972	1135	1297
Solubility in water, g/L (at 25° C)	145	18.5	232
Cavity diameter, Å	4.7-5.3	6-6.5	7.5-8.3
Torus height, Å	7.9	7.9	7.9
Approximate volume of cavity, $Å^3$	174	262	427

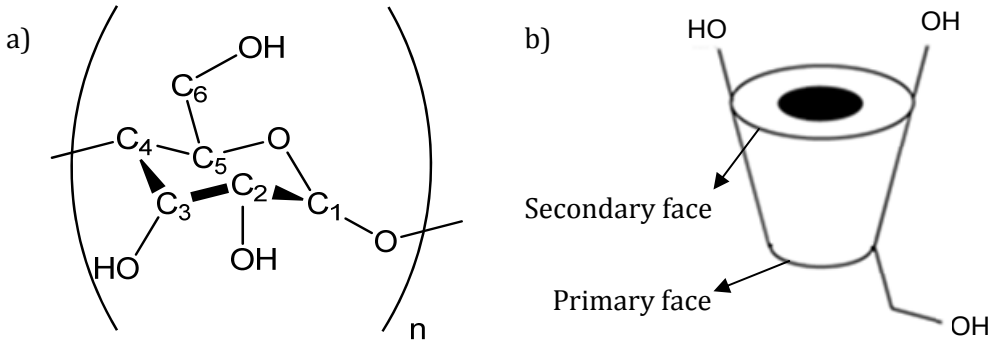

Figure 6-1 a) Cyclodextrin n=6: α, n=7: β, and n=8: γ; b) primary hydroxyl group at C_6 is located on narrow side (primary surface) while the two secondary hydroxyl groups at C_2 and C_3 are on the wide side (secondary surface)

While their outer surface is hydrophilic, due to the accumulation of alcoholic hydroxyl groups, position of skeletal carbons (C_3 and C_5) and ethereal oxygen (glycosidic oxygen bridges) of the glucose residues in the central cavity leads to hydrophobic nature of the central cavity. Hence, it provides a lipophilic environment into which low molecular weight hydrophobic molecules, of proper size, can penetrate and reside. Thus, cyclodextrins were among the first molecules, whose potential to bind with organic compounds, to became the focus of several studies (Cramer, 1954; Bender, 1978; Szejtli, 1988). Therefore, their ability to form inclusion complex, without the formation or destruction of covalent bonds, has made them desirable for many applications, from pure research to applied technologies (such as in the pharmaceutical, food, chemical, cosmetics and other industries (Bender, 1978; Szejtli, 1985; Szejtli, 1988; Szejtli, 1988).

For a number of reasons, such as price and availability, along with suitable cavity dimensions (compared to smaller cavity of α- cyclodextrin, which can only encapsulate aliphatic chains, and larger cavity of γ- cyclodextrin, which results in a loose fit) (Takisawa *et al.*, 1993), β-CD is the most widely used and studied in the family of cyclodextrins (Szejtli, 1994). Moreover, it is the prime product of cyclodextrin-producing enzymes, accounting for at least 95% of cyclodextrin production (Flaschel *et al.*, 1982). However, the low aqueous solubility of β-CD (18 g/l) and low solubility of some of its complexes has resulted in the synthesis of chemically modified compounds with enhanced hydrophilicity (Szejtli, 1994).

6.1.2 Inclusion Complexation

In supermolecular chemistry, inclusion complex, also known as host-guest system, is a form of complex that involves weak noncovalent forces, such as hydrogen bonding, van der Waals forces, and π–π stacking interactions. In a simple 1:1 host-guest system, the host compound has enough available internal space (or cavity) in which the guest can reside (Figure 6-2); resulting in stealth presence of the guest in the medium, protecting it from unfavourable reactions, and improving its stability in the desired environment.

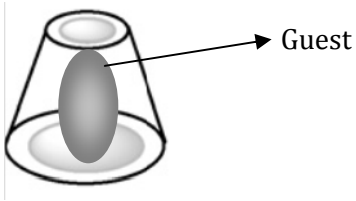

Figure 6-2 1:1 inclusion complex

Cyclodextrins' inclusion complexes have been studied for several decades (Cramer, 1954; Bender, 1978; Rekharsky and Inoue, 1998; Schneider *et al.*, 1998). They are most widely applied for enhancing the presence of hydrophobic compounds in aqueous environment. The most likely manner of cyclodextrin complexation involves the inclusion of less hydrophilic part of the guest inside the cavity, while the more hydrophilic part of it is in contact with the polar solvent (Bergeron, 1984; Szejtli, 1988; Takisawa *et al.*, 1993).

6.1.3 Inclusion Applications of Cyclodextrins

Since the development of cyclodextrins, their applications have become very significant in a variety of industries. Their ability to form inclusion complexes has played a major role in this matter. It has improved drugs solubility in aqueous media, enhanced gene delivery of cationic polymer, protected the flavour in food industry, masked odours and improved selective separation of compounds. Consequently, they are currently implemented in pharmaceutical, (medicine and drug delivery), food, and personal care products industries.

6.1.3.1 Enzymatic Modelling

Cyclodextrin can bind to a substrate and form an enhanced host-guest system, referred to as enzyme substrate system. Such structure displays selectivity for both substrate and product. In this arrangement, cyclodextrin either catalyzes the reactions or mimics a step in catalytic sequence (Breslow and Dong, 1998; Loftsson and Duchêne, 2007).

6.1.3.2 Pharmaceutical Industries

Pharmaceutical compounds can incorporate inside the cavity of cyclodextrins; leading to increased solubility of otherwise insoluble or poorly soluble compounds. Therefore, they can enhance bioavailability and pharmacological effects of pharmaceuticals. As a result, the prescribed or administered dosage of drugs decreases, resulting not only in lower cost of treatment but also, fewer side effects (Uekama *et al.*, 1998a; Uekama, 2002; Loftsson and Duchêne, 2007; Prabaharan and Gong, 2008).

Functionalization of cationic polymers, which are utilized for gene delivery, with cyclodextrin not only reduces the latter's cytotoxicity, but it also provides an opportunity for the modified polymer to form inclusion complex with DNA; therefore, improving the gene transfection (Mellet *et al.*, 2011). Recently, the inclusion complexation of adamantine with β-CD was used in the production of charge-tunable supermolecular dendritic polymers with high transfection efficiency, where adamantine branches on adamantane-modified hyper-branched polyglycerol were guests to β-CD hosts (Dong *et al.*, 2011).

6.1.3.3 Waste Treatment

Cyclodextrins have offered a simple mean for selective separation of organic compounds in liquid or gas phase. They show removal efficiency as high as 95% for elimination of toluene from waste gas stream (Blach *et al.*, 2008). Fluctuations in pH and salt concentration of waste gas have no significant effect on adsorption capacity of the process, which makes it suitable for industrial application. As mentioned in Section 1.1, one of the most effective treatment methods for the removal of organic compounds from wastewater streams, industrial or domestic, is biodegradation by means of activated sludge system. In this process, biological entities present in the sludge, such as yeast or bacteria, degrade the toxic organic substances. However, this process has its limitation with regards to the wastewater of certain industries, like pesticide and pharmaceutical manufacturing. Beside the potential resistance of these compounds to such mean of degradation, when the biological "degraders" are overwhelmed, beyond

their toxic concentration tolerance level, they lose their functionality; leading to irreversible reduction in the activity of sludge. To avoid such damage, cyclodextrins can be used to form inclusion complex with toxic compounds and protect the degraders (Olah *et al.*, 1988; Mamba *et al.*, 2007; Mhlanga *et al.*, 2007; Salipira *et al.*, 2007).

6.1.3.4 Personal Care Products and Food Industries

The ability of cyclodextrins and their derivatives to suppress volatility, stabilize, and control odour has gained them recognition in cosmetics and personal care. Nowadays, they are one of the ingredients in toothpastes, air fresheners, detergents, perfumes, creams, fabric softeners, etc.

Moreover, cyclodextrins ability to form inclusion with most natural and artificial flavours, which are usually volatile oils or liquids, present in food formulation has favoured them over conventional encapsulation methods for protection and deliverance of flavours (Hedges, 1998; Uekama *et al.*, 1998b).

6.2 Ion Selective Membrane Preparation

The procaine-permeable membrane was prepared according to Tan and Tam (Tan and Tam, 2007). In this process 0.5 g of carboxylated PVC (Sigma Aldrich) was first dissolved in 30 ml of solvent (tetrahydrofuran, THF, Sigma Aldrich). This solution, then, was, gradually, added into distilled de-ionized water and THF mixture of ratio 1:9 containing of 0.955 g dissolved procaine hydrochloride (PHC, Sigma Aldrich). The final mixture was added dropwise into a large volume of DI water in order to precipitate

carboxylated PVC–PHC complex. The precipitate was collected and filtered through a 20–25μm filter paper and was washed repeatedly with distilled de-ionized water to remove impurities. Finally it was left to dry at room temperature for one day.

The prepared PVC–PHC complex, poly(ethylene-co-vinyl acetate-co-carbonmonoxide) (PE-co-PVA-co-CO, polymeric plasticizer, Sigma Aldrich), and sodium tetraphenylborate (NaTPB, ion-exchanger, Sigma Aldrich) were dissolved in 30ml of THF with a weight ratio of 38:62:2 totalling 0.3g. The final solution was poured into a petric dish of 55mm in diameter and left under the hood for the solvent to evaporate at room temperature for several days. When the membrane was completely dry a 12mm-diameter disk was cut and fixed onto the Teflon tubing of the drug selective electrode that was moistened with THF.

6.3 Results and Discussion

Procaine hydrochloride (a local anesthetic drug, PHC) is an ester of the *p*-aminobenzoic acid, 4-aminobenzoic acid diethylaminoethyl ester (Figure 6-3). It exists as an ionized form in aqueous solution (Li *et al.*, 2003). Its benzene ring diameter is approximately 6.7–6.8 Å, which makes it a suitable candidate to form a stable inclusion complex with β-CD, unlike α- and γ-cyclodextrin. PHC enters the β-CD cavity via the wider ring, ethylene groups first, up to the aromatic benzene ring with stoichiometry molar ratio of 1:1 (Gu and Pan, 1999; Merino *et al.*, 2000). Therefore, PHC is a good candidate for studying the β-CD potential as removal agent for water treatment. What follows in this

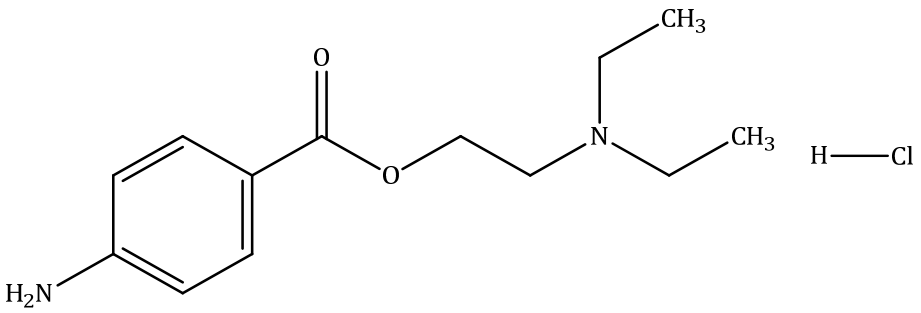

Figure 6-3 Procaine hydrochloride

section is the initial results for β-CD/PHC host-guest system investigation, all performed at neutral pH (between 6 –7).

6.3.1 Host-Guest Thermodynamics

Due to acidity nature of PHC solutions, for the purpose of these experiments, the pH of titrant (PHC solution) was matched with the sample cell (β-CD solution) to avoid the effects of ionic strength or mixing heats.

In one experiment, different concentrations of PHC solution were titrated into the sample cell containing 10mM solution of β-CD. Injection volume rages from 5 to 10 μL. The cell feedback signal measurements for one of the experiment are show in Figure 6-4. Integration of the thermogram yields the enthalpy of host-guest Interaction. Figure 6-5 shows the enthalpy of complexation and suggest that the reaction is exothermic. It is noteworthy to point out that when [PHC] in sample cell equals [β-CD] (10 mM) the

enthalpy curve becomes and straight line; confirming the 1:1 stoichiometry ration of this inclusion complexation is (Figure 6-5-d).

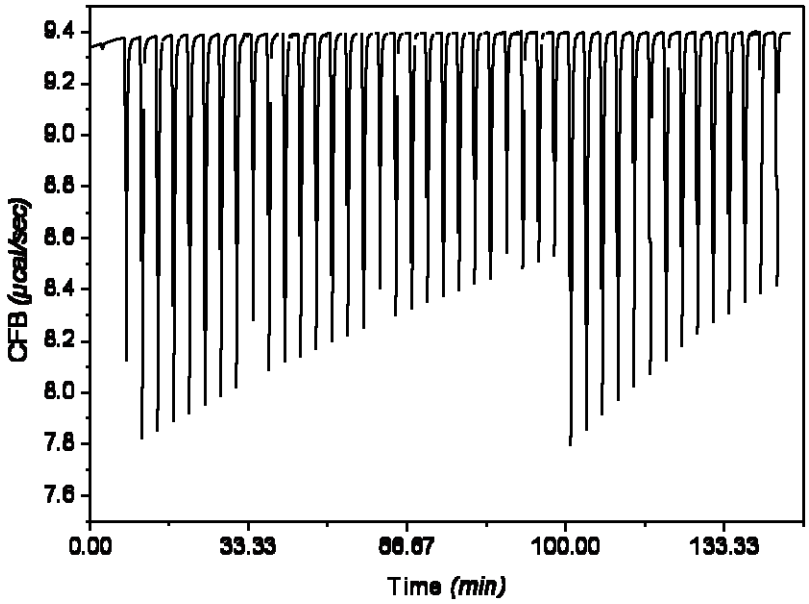

Figure 6-4 Thermogram for titration of 1 mM PHC into 1 mM B-CD

Nonlinear fitting of Figure 6-5-d with single binding site model (Figure 6-6) determines the thermodynamic values of enthalpy, ΔH_{com}, and equilibrium constant, k_{com}, for this Substitution of these values in:

$$\Delta G = \Delta H - T\Delta S = -RT \ln k$$

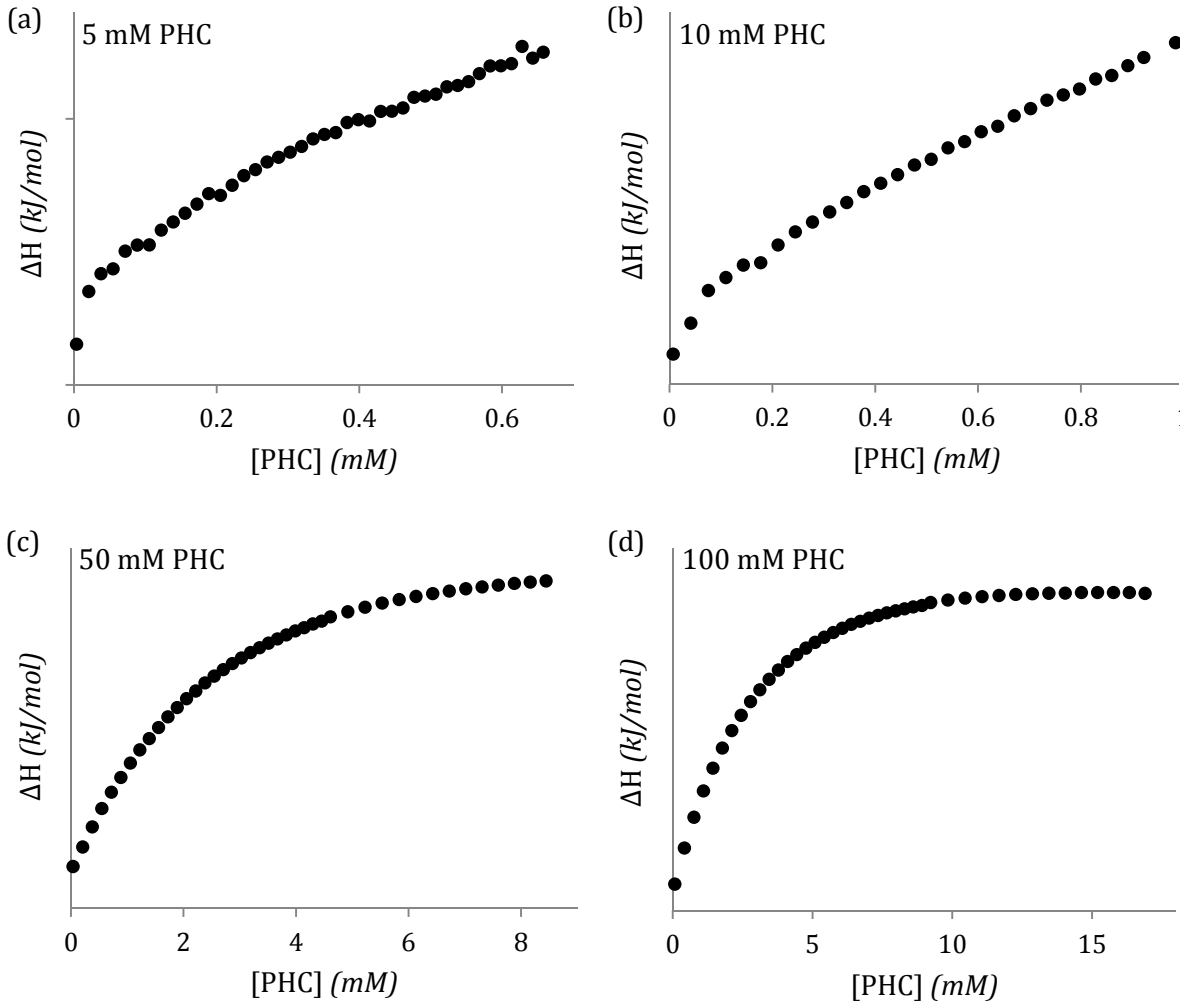

Figure 6-5 Enthalpy of complexation with various concentration of titrant

provide the rest of the value: k_{com}= 395, ΔH_{com}= -22.64, ΔG_{com}= -14.82, and $T\Delta S_{com}$= -7.82 kJ mol^{-1}. These value agree with the ones reported elsewhere (Takisawa *et al.*, 1993).

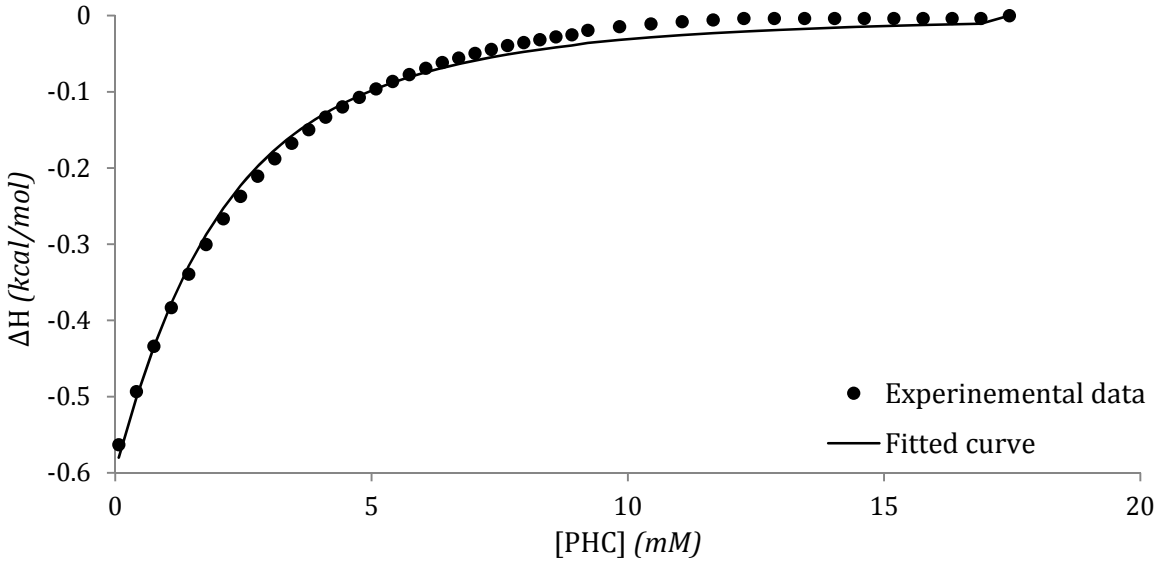

Figure 6-6 Single binding site model fitting model for determination of *ΔH* and *k* of reaction

6.3.2 Effects of Concentration on Host-Guest System

To a 50 ml solutions of PHC at different concentrations, desired amount of β-CD were added. In all measurements, a sudden decrease in the drug concentration is observed. This could be due to rapid increase in the amount of available β-CD to form inclusion complex with PHC, while it is dissolving. By the time β-CD is completely dissolved, most of it has already formed the complex, therefore, the rate of complex formation reduces and further inclusion complexes are formed gradually over time.

As shown in Figure 6-7, increase in the concentration of PHC slightly affects the initial complexation rate. Along with the sharper drop in PHC concentration, while β-CD is dissolving, an increase in PHC concentration yielded further reduction in drug concentration and final drug content of the solution. For example, the fraction of

unbounded PHC in solution decreases from 0.82 for 0.1mM solution to 0.75 for 0.2 mM solution. Consequently, it is clear that at higher initial PHC concentration, more inclusion complexes are formed.

Increase in the amount of added β-CD affects the amount complex formation in the same manner (Figure 6-8). However, the initial slope of the graph is higher for 2 mM β-CD compared to 1 mM β-CD solution. As a result, it could be concluded that concentration of β-CD has a greater effect on the complexation rate. Clearly, an increase in the amount of host in solution has also resulted in the formation of more complex that decreases the unbounded drug concentration. Studying the result reveals that although the concentration of β-CD is larger than initial concentration of PHC, not all the

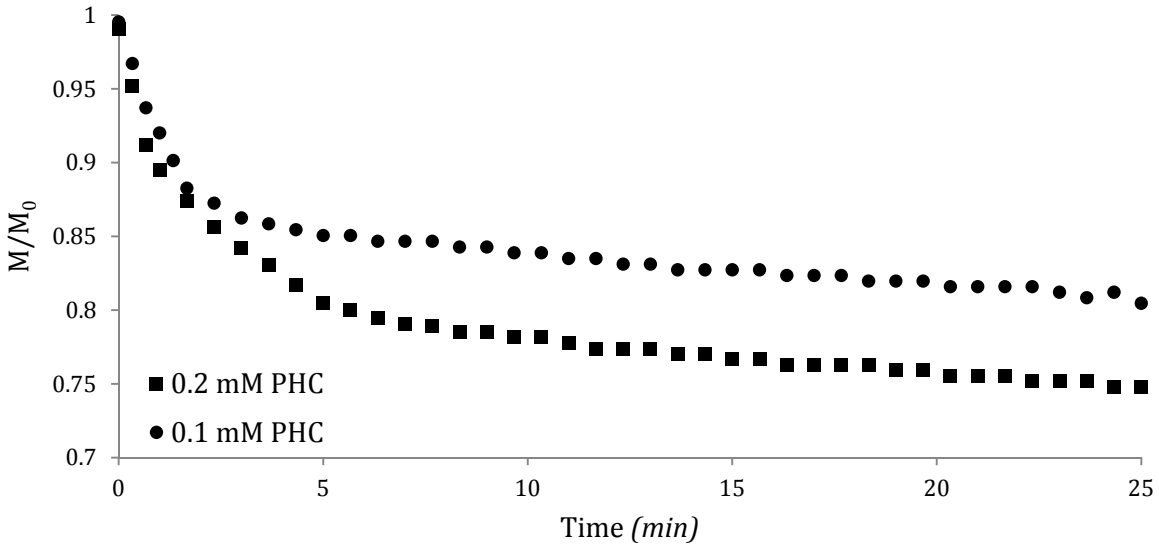

Figure 6-7 Effect of PHC concentration, 0.1mM (●) and 0.2mM (■), on reaction

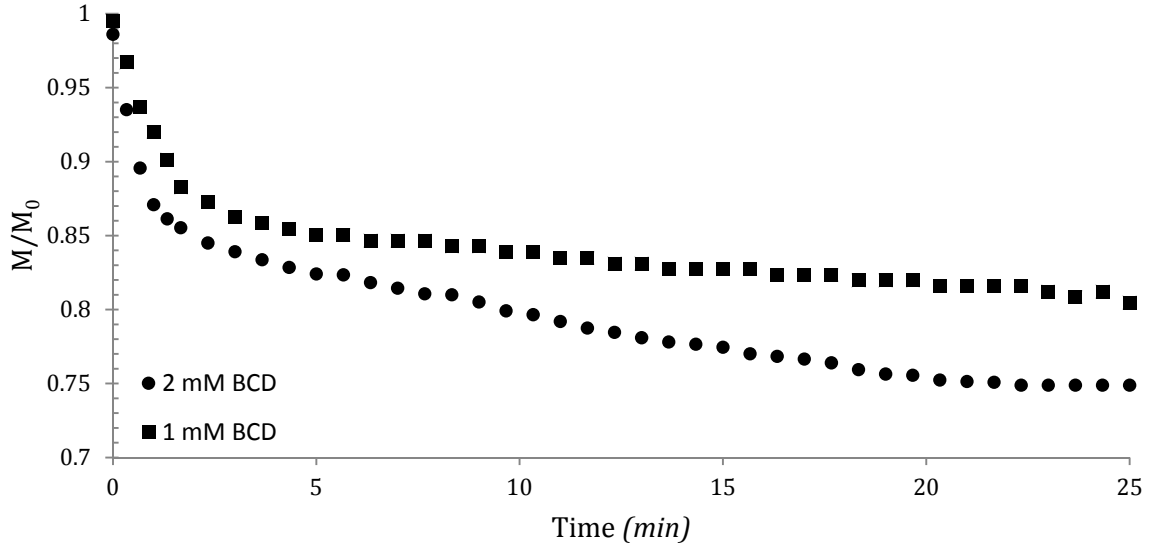

Figure 6-8 Effect of β-CD concentration, 1mM (■) and 2mM (●), on inclusion reaction

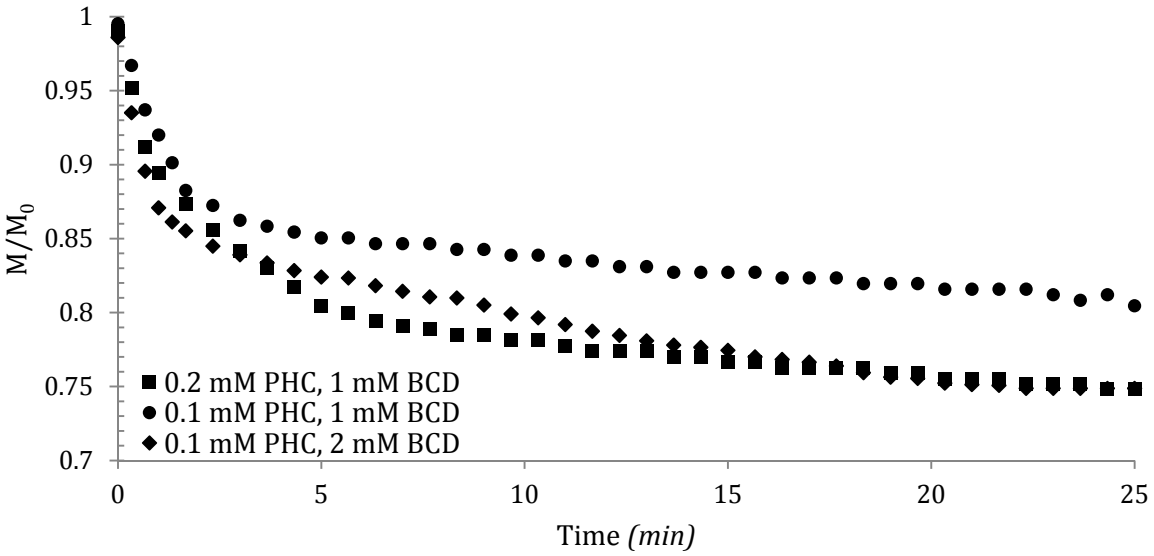

Figure 6-9 Effect of concentration variation on complexation

available PHC form inclusion complex with β-CD. Thus, in all the tests, the final concentration of unbounded drug reaches a plateau value. Also, an increase in β-CD and PHC concentration by same factor leads to same final unbounded drug concentration (Figure 6-9); hence assumption of 1:1 host to guest ratio is valid.

Chapter 7– Conclusion & Future Works

In this study the possibility of functionalization of magnetic nanoparticles, for the purpose of removal of endocrine disrupting compounds from contaminated water streams, was explored. The parent MNPs have reasonable surface charge to maintain a stable homogeneous solution. However, any further modification failed to yield stable suspension.

Template-based MNPs are suitable for biological and medical applications, because their size and polydispersity can be easily controlled. However, the pH-responsive nature of the developed coating may be one of the reasons that further surface modifications have unstabilized the particles. This could be due to its sensitivity to pH and ionic strenght of the solution. The nature of this scaffold demands close monitoring of these parameters during any further reactions. Hence, other types of templates may provide better platforms for the preparation of suitable magnetic particles.

The length of the stabilizers can also contribute to aggregation problem. Chitosan and PEGMA large molecular weight result in long linear polymer that can easily stimulate aggregation, especially because they contain active site on their structure. For PEGMA, double bonds are likely able to bridge individual particles. They also provide active binding sites during magnetization of PEGMA-bearing nanogels; which leads to covalent attachment of iron cations to the grafted PEGMA. While chitosan's high degree of de-acetylation along with its lenghty linear chain cause extensive aggregation.

Since β-cyclodextrin easily interacts with most organic compounds, it is a suitable candidate to bind to endocrine disrupting compounds from contaminated water by forming inclusion complex. Hence, it would be worthwhile to explore other possible pathways to graft it to the polymeric coating of MNPs. Utilization of lower molecular chitin derivative, such as chitosan oligosaccharide, has the potential to address the bridging problem, due to having shorter chain and lower amine content. In another approach, polymer scaffold can be modified in a way that just enough amounts of amine binding sites are introduced and present on its surface. This way, aggregation will be less likely to occur.

References

Aherne, G. W., Hardcastle, A., Nield, A. H., 1990. Cytotoxic drugs and the aquatic environment: Estimation of bleomycin in river and water samples, Journal of Pharmacy and Pharmacology 42(10), 741-742.

Aherne, G. W., Briggs, R., 1989. The relevance of the presence of certain synthetic steroids in the aquatic environment, Journal of Pharmacy and Pharmacology 41(10), 735-736.

Aherne, G. W., English, J., Marks, V., 1985. The role of immunoassay in the analysis of microcontaminants in water samples, Ecotoxicology and environmental safety 9(1), 79-83.

Alexiou, C., Schmid, R., Jurgons, R., Bergemann, C., Arnold, W. A., Parak, F., 2003. Targeted Tumor Therapy with "Magnetic Drug Targeting": Therapeutic Efficacy of Ferrofluid Bound Mitoxantrone, in: Odenbach, S. (Ed), Ferrofluids, Springer Berlin / Heidelberg, pp. 233-251.

Altintaş, E. B., Uzun, L., Denizli, A., 2007. Synthesis and characterization of monosize magnetic poly(glycidyl methacrylate) beads, China Particuology 5(1-2), 174-179.

Arica, M. Y., Yavuz, H., Patir, S., Denizli, A., 2000. Immobilization of glucoamylase onto spacer-arm attached magnetic poly(methylmethacrylate) microspheres: characterization and application to a continuous flow reactor, Journal of Molecular Catalysis B: Enzymatic 11(2-3), 127-138.

Babincová, M., Čičmanec, P., Altanerová, V., Altaner, Č., Babinec, P., 2002. AC-magnetic field controlled drug release from magnetoliposomes: design of a method for site-specific chemotherapy, Bioelectrochemistry 55(1-2), 17-19.

Bacri, J. -., Perzynski, R., Salin, D., Cabuil, V., Massart, R., 1990. Ionic ferrofluids: A crossing of chemistry and physics, Journal of Magnetism and Magnetic Materials 85(1-3), 27-32.

Badruddoza, A. Z. M., Tay, A., Tan, P., Hidajat, K., Uddin, M., 2010. Carboxymethyl-[beta]-cyclodextrin conjugated magnetic nanoparticles as nano-adsorbents for removal of copper ions: Synthesis and adsorption studies, Journal of hazardous materials 185(2-3), 1186.

Bajaj, P., Goyal, M., Chavan, R. B., 1994. Synthesis and characterization of methacrylic acid–ethyl acrylate copolymers, Journal of Applied Polymer Science 53(13), 1771-1783.

Barrera, C., Herrera, A. P., Rinaldi, C., 2009. Colloidal dispersions of monodisperse magnetite nanoparticles modified with poly(ethylene glycol), Journal of colloid and interface science 329(1), 107-113.

Bart, H. L., Fentress, J. A., Steele, S. L., 2006. Reproductive Disruption in Wild Longear Sunfish (Lepomis megalotis) Exposed to Kraft Mill Effluent, Environmental Health Perspectives 114(1), 40-45.

Baselt, D. R., Lee, G. U., Natesan, M., Metzger, S. W., Sheehan, P. E., Colton, R. J., 1998. A biosensor based on magnetoresistance technology, Biosensors and Bioelectronics 13(7-8), 731-739.

Bender, M. L., 1978. Cyclodextrin Chemistry. Berlin: Springer-Verlag.

Bergeron, R. J., 1984. Inclusion compounds, in: Atwood, J. L., Davies, J. E. D., MacNicol, D. D. (Eds), . London ; Toronto : Academic Press, 1984, pp. 443.

Blach, P., Fourmentin, S., Landy, D., Cazier, F., Surpateanu, G., 2008. Cyclodextrins: A new efficient absorbent to treat waste gas streams, Chemosphere 70(3), 374-380.

Blums, E., Cebers, A. O., Maiorov, M. M., 1997. Magnetic Fluids. : Walter De Gruyter New York.

Boyd, G. R., Reemtsma, H., Grimm, D. A., Mitra, S., 2003. Pharmaceuticals and personal care products (PPCPs) in surface and treated waters of Louisiana, USA and Ontario, Canada, The Science of the total environment 311(1-3), 135-149.

Breslow, R., Dong, S. D., 1998. Biomimetic Reactions Catalyzed by Cyclodextrins and Their Derivatives, Chemical reviews 98(5), 1997-2012.

Bromberg, L., Hatton, A. T., 2007. Decomposition of toxic environmental contaminants by recyclable catalytic, superparamagnetic nanoparticles, Industrial and Engineering Chemistry Research 46(10), 3296-3303.

Brown, W., 1993. Dynamic Light Scattering: The Method and some Applications. : Oxford University Press, USA.

Bucak, S., Jones, D. A., Laibinis, P. E., Hatton, T. A., 2003. Protein separations using colloidal magnetic nanoparticles, Biotechnology progress 19(2), 477-484.

Bulte, J. W. M., Kraitchman, D. L., 2004. Iron oxide MR contrast agents for molecular and cellular imaging, NMR in biomedicine 17(7), 484-499.

Burke, N. A. D., Stöver, H. D. H., Dawson, F. P., 2002. Magnetic nanocomposites: Preparation and characterization of polymer-coated iron nanoparticles, Chemistry of Materials 14(11), 4752-4761.

Cabuil, V., Hochart, N., Perzynski, R., Lutz, P., 1994. Synthesis of cyclohexane magnetic fluids through adsorption of end-functionalized polymers on magnetic particles, in: Ottewill, R., Rennie, A. (Eds), Trends in Colloid and Interface Science VIII, Springer Berlin / Heidelberg, pp. 71-74.

Camacho-Muñoz, D., Martín, J., Santos, J. L., Aparicio, I., Alonso, E., 2010. Occurrence, temporal evolution and risk assessment of pharmaceutically active compounds in Doñana Park (Spain), Journal of hazardous materials 183(1-3), 602-608.

Carp, O., Patron, L., Culita, D. C., Budrugeac, P., Feder, M., Diamandescu, L., 2010. Thermal analysis of two types of dextran-coated magnetite, Journal of Thermal Analysis and Calorimetry 101(1), 181-187.

Chang, H., Choo, K., Lee, B., Choi, S., 2009. The methods of identification, analysis, and removal of endocrine disrupting compounds (EDCs) in water, Journal of hazardous materials 172(1), 1-12.

Chemla, Y. R., Grossman, H. L., Poon, Y., McDermott, R., Stevens, R., Alper, M. D., Clarke, J., 2000. Ultrasensitive magnetic biosensor for homogeneous immunoassay, Proceedings of the National Academy of Sciences of the United States of America 97(26), 14268-14272.

Chen, S., Wang, Y., 2001. Study on β-cyclodextrin grafting with chitosan and slow release of its inclusion complex with radioactive iodine, Journal of Applied Polymer Science 82(10), 2414-2421.

Chen, Y., Bose, A., Bothun, G. D., 2010. Controlled Release from Bilayer-Decorated Magnetoliposomes via Electromagnetic Heating, ACS nano 4(6), 3215-3221.

Choi, K., Kim, Y., Park, J., Park, C. K., Kim, M., Kim, H. S., Kim, P., 2008. Seasonal variations of several pharmaceutical residues in surface water and sewage treatment plants of Han River, Korea, Science of the Total Environment 405(1-3), 120-128.

Christensen, F. M., 1998. Pharmaceuticals in the environment - A human risk? Regulatory Toxicology and Pharmacology 28(3), 212-221.

Clara, M., Kreuzinger, N., Strenn, B., Gans, O., Kroiss, H., 2005. The solids retention time-a suitable design parameter to evaluate the capacity of wastewater treatment plants to remove micropollutants, Water research 39(1), 97-106.

Cramer, F., 1954. Inclusion Compounds.

Cunningham, V. L., Binks, S. P., Olson, M. J., 2009. Human health risk assessment from the presence of human pharmaceuticals in the aquatic environment, Regulatory Toxicology and Pharmacology 53(1), 39-45.

Dai, Q., Berman, D., Virwani, K., Frommer, J., Jubert, P. -., Lam, M., Topuria, T., Imaino, W., Nelson, A., 2010. Self-assembled ferrimagnet-polymer composites for magnetic recording media, Nano Letters 10(8), 3216-3221.

Dang, F., Enomoto, N., Hojo, J., Enpuku, K., 2009. Sonochemical synthesis of monodispersed magnetite nanoparticles by using an ethanol-water mixed solvent, Ultrasonics sonochemistry 16(5), 649-654.

De Latour, C., Kolm, H., 1975. Magnetic separation in water pollution control - II, Magnetics, IEEE Transactions on 11(5), 1570-1572.

De Latour, C., 1973. Magnetic separation in water pollution control, Magnetics, IEEE Transactions on 9(3), 314-316.

De Vicente, I., Merino-Martos, A., Cruz-Pizarro, L., De Vicente, J., 2010. On the use of magnetic nano and microparticles for lake restoration, Journal of hazardous materials 181(1-3), 375-381.

De Vicente, J., Delgado, A. V., Plaza, R. C., Durán, J. D. G., González-Caballero, F., 2000. Stability of cobalt ferrite colloidal particles. Effect of pH and applied magnetic fields, Langmuir 16(21), 7954-7961.

Deng, Y., Wang, L., Yang, W., Fu, S., Elaïssari, A., 2003. Preparation of magnetic polymeric particles via inverse microemulsion polymerization process, Journal of Magnetism and Magnetic Materials 257(1), 69-78.

Desbrow, C., Routledge, E. J., Brighty, G. C., Sumpter, J. P., Waldock, M., 1998. Identification of estrogenic chemicals in STW effluent. 1. Chemical fractionation and in vitro biological screening, Environmental Science and Technology 32(11), 1549-1558.

Ditsch, A., Yin, J., Laibinis, P. E., Wang, D. I. C., Hatton, T. A., 2006. Ion-exchange purification of proteins using magnetic nanoclusters, Biotechnology progress 22(4), 1153-1162.

Ditsch, A., Lindenmann, S., Laibinis, P. E., Wang, D. I. C., Hatton, T. A., 2005. High-Gradient Magnetic Separation of Magnetic Nanoclusters, Industrial & Engineering Chemistry Research 44(17), 6824-6836.

Dong, R., Zhou, L., Wu, J., Tu, C., Su, Y., Zhu, B., Gu, H., Yan, D., Zhu, X., 2011. A supramolecular approach to the preparation of charge-tunable dendritic polycations for efficient gene delivery, Chemical Communications 47(19), 5473-5475.

Egashira, R., Hatton, T. A., 2005. Process for removal of hydrocarbon from water with magnetic particles, SOLVENT EXTRACTION RESEARCH AND DEVELOPMENT-JAPAN 12, 59-68.

Eichenbaum, G. M., Kiser, P. F., Dobrynin, A. V., Simon, S. A., Needham, D., 1999a. Investigation of the swelling response and loading of ionic microgels with drugs and proteins: the dependence on cross-link density, Macromolecules 32(15), 4867-4878.

Eichenbaum, G. M., Kiser, P. F., Shah, D., Simon, S. A., Needham, D., 1999b. Investigation of the swelling response and drug loading of ionic microgels: The dependence on functional group composition, Macromolecules 32(26), 8996-9006.

Eichenbaum, G. M., Kiser, P. F., Simon, S. A., Needham, D., 1998. pH and ion-triggered volume response of anionic hydrogel microspheres, Macromolecules 31(15), 5084-5093.

El-Sherif, H., El-Masry, M., Emira, H. S., 2010. Magnetic polymer composite particles via in situ inverse miniemulsion polymerization process, Journal of Macromolecular Science, Part A: Pure and Applied Chemistry 47(11), 1096-1103.

Faseur A.; Van Dooren J.; Vanbrabant R.; Goossens W.R.A., 1986, ELECTROMAGNETIC TREATMENT OF WASTEWATERS.1.

Feng, B., Hong, R. Y., Wang, L. S., Guo, L., Li, H. Z., Ding, J., Zheng, Y., Wei, D. G., 2008. Synthesis of Fe3O4/APTES/PEG diacid functionalized magnetic nanoparticles for MR imaging, Colloids and Surfaces A: Physicochemical and Engineering Aspects 328(1-3), 52-59.

Feng, J., Mao, J., Wen, X., Tu, M., 2011. Ultrasonic-assisted in situ synthesis and characterization of superparamagnetic Fe3O4 nanoparticles, Journal of Alloys and Compounds 509(37), 9093-9097.

Fick, J., Soederstrom, H., Lindberg, R. H., Phan, C., Tysklind, M., Larsson, D. G. J., 2009. Contamination of surface, ground, and drinking water from pharmaceutical production, Environmental Toxicology and Chemistry 28(12), 2522-2527.

Flaschel, E.; Landert, J.; Renken, A., 1982, Process development for the production of a-cyclodextrin, 41-49.

Ghosh, S., Jiang, W., McClements, J. D., Xing, B., 2011. Colloidal stability of magnetic iron oxide nanoparticles: Influence of natural organic matter and synthetic polyelectrolytes, Langmuir 27(13), 8036-8043.

Gonil, P., Sajomsang, W., Ruktanonchai, U. R., Pimpha, N., Sramala, I., Nuchuchua, O., Saesoo, S., Chaleawlert-umpon, S., Puttipipatkhachorn, S., 2011. Novel quaternized chitosan containing β-cyclodextrin moiety: Synthesis, characterization and antimicrobial activity, Carbohydrate Polymers 83(2), 905-913.

Groman, E. V., Josephson, L., 1993. Low molecular weight carbohydrates as additives to stabilize metal oxide compositions .

Gu, J., Pan, J., 1999. Determination of the cyclodextrin inclusion constant with the constant current coulometric titration method, Talanta 50(1), 35-39.

Heberer, T., Stan, H. J., 1996. Determination of trace levels of dichlorprop, mecoprop, clofibric acid, and naphthylacetic acid in soil by gas chromatography/mass spectrometry with selected-ion monitoring, Journal of AOAC International 79(6), 1428-1433.

Heberer, T., Stan, H. -., 1997. Determination of Clofibric Acid and N-(Phenylsulfonyl)-Sarcosine in Sewage, River and Drinking Water, International Journal of Environmental Analytical Chemistry 67(1-4), 113-124.

Heberer, T., Schmidt-Bäumler, K., Stan, H. -., 1998. Occurrence and distribution of organic contaminants in the aquatic system in Berlin. Part I: Drug residues and other polar contaminants in Berlin surface and groundwater, Acta Hydrochimica et Hydrobiologica 26(5), 272-278.

Heberer, T., Dünnbier, U., Reilich, C., Stan, H. -., 1997. Detection of drugs and drug metabolites in ground water samples of a drinking water treatment plant, Fresenius Environmental Bulletin 6(7-8), 438-443.

Hedges, A. R., 1998. Industrial Applications of Cyclodextrins, Chemical reviews 98(5), 2035-2044.

Henschel, K. P., Wenzel, A., Diedrich, M., Fliedner, A., 1997. Environmental Hazard Assessment of Pharmaceuticals, Regulatory Toxicology and Pharmacology 25(3), 220-225.

Hignite, C., Azarnoff, D. L., 1977. Drugs and drug metabolites as environmental contaminants: Chlorophenoxyisobutyrate and salicylic acid in sewage water effluent, Life Sciences 20(2), 337-341.

Hilton, M. J., Thomas, K. V., 2003. Determination of selected human pharmaceutical compounds in effluent and surface water samples by high-performance liquid chromatography–electrospray tandem mass spectrometry, Journal of Chromatography A 1015(1-2), 129-141.

Himmelsbach, M., Buchberger, W., Miesbauer, H., 2003. Determination of Pharmaceutical Drug Residues on Suspended Particulate Material in Surface Water, International Journal of Environmental Analytical Chemistry 83(6), 481-486.

Hong, R. Y., Feng, B., Liu, G., Wang, S., Li, H. Z., Ding, J. M., Zheng, Y., Wei, D. G., 2009. Preparation and characterization of Fe3O4/polystyrene composite particles via inverse emulsion polymerization, Journal of Alloys and Compounds 476(1-2), 612-618.

Hong, R. Y., Li, J. H., Li, H. Z., Ding, J., Zheng, Y., Wei, D. G., 2008. Synthesis of Fe3O4 nanoparticles without inert gas protection used as precursors of magnetic fluids, Journal of Magnetism and Magnetic Materials 320(9), 1605-1614.

Horák, D., Chekina, N., 2006. Preparation of magnetic poly (glycidyl methacrylate) microspheres by emulsion polymerization in the presence of sterically stabilized iron oxide nanoparticles, Journal of Applied Polymer Science 102(5), 4348-4357.

Horák, D., Babič, M., Macková, H., Beneš, M. J., 2007. Preparation and properties of magnetic nano- and microsized particles for biological and environmental separations, Journal of Separation Science 30(11), 1751-1772.

Hsu, S. -., Don, T. -., Chiu, W. -., 2002. Free radical degradation of chitosan with potassium persulfate, Polymer Degradation and Stability 75(1), 73-83.

Hu, F., Neoh, K. G., Cen, L., Kang, E. -., 2006. Cellular response to magnetic nanoparticles "PEGylated" via surface-initiated atom transfer radical polymerization, Biomacromolecules 7(3), 809-816.

Jain, N., Wang, Y., Jones, S. K., Hawkett, B. S., Warr, G. G., 2010. Optimized steric stabilization of aqueous ferrofluids and magnetic nanoparticles, Langmuir 26(6), 4465-4472.

Jassal, M., Acharya, B. N., Bajaj, P., 2003. Synthesis, characterization, and rheological studies of methacrylic acid-ethyl acrylate-diallyl phthalate copolymers, Journal of Applied Polymer Science 89(5), 1430-1441.

Jux, U., Baginski, R. M., Arnold, H. G., Kronke, M., Seng, P. N., Detection of pharmaceutical contaminations of river, pond, and tap water from Cologne (Germany) and

surroundings, International journal of hygiene and environmental health 205(5), 393-398.

Khouri, S., 2010, Experimental Characterization and Theoretical Calculations of Responsive Polymeric Systems,.

Kim, J. -., Jang, H. -., Kim, J. -., Ishibashi, H., Hirano, M., Nasu, K., Ichikawa, N., Takao, Y., Shinohara, R., Arizono, K., 2009. Occurrence of Pharmaceutical and Personal Care Products (PPCPs) in Surface Water from Mankyung River, South Korea, JOURNAL OF HEALTH SCIENCE 55(2), 249-258.

Kim, S. D., Cho, J., Kim, I. S., Vanderford, B. J., Snyder, S. A., 2007. Occurrence and removal of pharmaceuticals and endocrine disruptors in South Korean surface, drinking, and waste waters, Water research 41(5), 1013-1021.

Kondo, K., Jin, T., Miura, O., 2010. Removal of less biodegradable dissolved organic matters in water by superconducting magnetic separation with magnetic mesoporous carbon, Physica C: Superconductivity 470(20), 1808-1811.

Kormos, J.; Servos, M. R.; Oakes, K.; Hao, C.; Yang, P., 2006a, Seasonal Variation of Pharmaceuticals and Endocrine Disrupting Chemicals in Southern Ontario Drinking Water Supplies,.

Kormos, J.; Yang, P.; Hao, C.; Kleywegt, S.; Oakes, K.; Cheung, P.; Socha, A.; Whitehead, B.; Servos, M. R., 2006b, Occurrence and Seasonal Variability of Selected Pharmaceuticals in Southern Ontario Drinking Water Supplies,.

Koutsouba, V., Heberer, T., Fuhrmann, B., Schmidt-Baumler, K., Tsipi, D., Hiskia, A., 2003. Determination of polar pharmaceuticals in sewage water of Greece by gas chromatography–mass spectrometry, Chemosphere 51(2), 69-75.

Kumar, A., Xagoraraki, I., 2010. Pharmaceuticals, personal care products and endocrine-disrupting chemicals in U.S. surface and finished drinking waters: A proposed ranking system, Science of the Total Environment 408(23), 5972-5989.

Lapointe, J., Martel, S., 2009. Thermoresponsive hydrogel with embedded magnetic nanoparticles for the implementation of shrinkable medical microrobots and for targeting and drug delivery applications. Conference proceedings : ...Annual International Conference of the IEEE Engineering in Medicine and Biology Society.IEEE Engineering in Medicine and Biology Society.Conference 2009, 4246-4249.

Larsen, T. A., Lienert, J., Joss, A., Siegrist, H., 2004. How to avoid pharmaceuticals in the aquatic environment, Journal of Biotechnology 113(1-3), 295-304.

Lattuada, M., Hatton, T. A., 2007. Functionalization of Monodisperse Magnetic Nanoparticles, Langmuir 23(4), 2158-2168.

Lefebure, S., Dubois, E., Cabuil, V., Neveu, S., Massart, R., 1998. Monodisperse magnetic nanoparticles: Preparation and dispersion in water and oils, Journal of Materials Research 13(10), 2975-2981.

Li, N., Duan, J., Chen, H., Chen, G., 2003. Determination of the binding constant for the inclusion complex between procaine hydrochloride and β-cyclodextrin by capillary electrophoresis, Talanta 59(3), 493-499.

Li, R., Liu, S., Zhao, J., Hideyuki, O., Atsushi, T., 2010. Application of polymerizable surfactant in the preparation of polystyrene/nano-Fe3O4 composite, Journal Wuhan University of Technology, Materials Science Edition 25(2), 184-187.

Li, X. -., Xu, G., Liu, Y., He, T., 2011. Magnetic Fe3O4 nanoparticles: Synthesis and application in water treatment, Nanoscience and Nanotechnology - Asia 1(1), 14-24.

Lin, G. P., Kuo, P. C., Huang, K. T., Shen, C. L., Tsai, T. L., Lin, Y. H., Wu, M. S., 2010. Self-assembled nano-size FePt islands for ultra-high density magnetic recording media, Thin Solid Films 518(8), 2167-2170.

Liu, Z. L., Ding, Z. H., Yao, K. L., Tao, J., Du, G. H., Lu, Q. H., Wang, X., Gong, F. L., Chen, X., 2003. Preparation and characterization of polymer-coated core–shell structured magnetic microbeads, Journal of Magnetism and Magnetic Materials 265(1), 98-105.

Liu, Z., Kanjo, Y., Mizutani, S., 2009. Removal mechanisms for endocrine disrupting compounds (EDCs) in wastewater treatment — physical means, biodegradation, and chemical advanced oxidation: A review, Science of the Total Environment 407(2), 731-748.

Loftsson, T., Duchêne, D., 2007. Cyclodextrins and their pharmaceutical applications, International journal of pharmaceutics 329(1-2), 1-11.

Lu, T., Ren, Q., Sui, J., Ni, Z. -., Chen, M. -., 2008. Study on properties and preparation of PAA-PMMA magnetic microspheres with crosslinking structures, Gongneng Cailiao/Journal of Functional Materials 39(11), 1809-1812.

Lubbe, A. S., Bergemann, C., Huhnt, W., Fricke, T., Riess, H., Brock, J. W., Huhn, D., 1996. Preclinical experiences with magnetic drug targeting: tolerance and efficacy, Cancer research 56(20), 4694.

Mamba, B. B., Krause, R. W., Malefetse, T. J., Nxumalo, E. N., 2007. Monofunctionalized cyclodextrin polymers for the removal of organic pollutants from water, Environmental Chemistry Letters 5(2), 84.

Matsuno, R., Yamamoto, K., Otsuka, H., Takahara, A., 2004. Polystyrene- and poly(3-vinylpyridine)-grafted magnetite nanoparticles prepared through surface-initiated nitroxide-mediated radical polymerization, Macromolecules 37(6), 2203-2209.

McDowell, D. C., Huber, M. M., Wagner, M., Gunten, U. v., Ternes, T. A., 2005. Ozonation of Carbamazepine in Drinking Water: Identification and Kinetic Study of Major Oxidation Products, Environmental science & technology 39(20), 8014-8022.

Meenach, S. A., Anderson, A. A., Suthar, M., Anderson, K. W., Hilt, J. Z., 2009. Biocompatibility analysis of magnetic hydrogel nanocomposites based on poly(N-isopropylacrylamide) and iron oxide, Journal of Biomedical Materials Research - Part A 91(3), 903-909.

Mellet, C. O., Fernández, J. M. G., Benito, J. M., 2011. Cyclodextrin-based gene delivery systems, Chemical Society Reviews 40(3), 1586-1608.

Merino, C., Junquera, E., Jimenez-Barbero, J., Aicart, E., 2000. Effect of the presence of β-cyclodextrin on the solution behavior of procaine hydrochloride. Spectroscopic and thermodynamic studies, Langmuir 16(4), 1557-1565.

Metcalfe, C. D., Miao, X. -., Koenig, B. G., Struger, J., 2003. Distribution of acidic and neutral drugs in surface waters near sewage treatment plants in the lower Great Lakes, Canada, Environmental Toxicology and Chemistry 22(12), 2881-2889.

Mhlanga, S. D., Mamba, B. B., Krause, R. W., 2007. Removal of organic contaminants from water using nanosponge cyclodextrin polyurethanes, Journal of Chemical Technology and Biotechnology 82(4), 382-388.

Michel, S. C. A., Keller, T. M., Fröhlich, J. M., Fink, D., Caduff, R., Seifert, B., Marincek, B., Kubik-Huch, R. A., 2002. Preoperative Breast Cancer Staging: MR Imaging of the Axilla with Ultrasmall Superparamagnetic Iron Oxide Enhancement, Radiology 225(2), 527.

Miège, C., Choubert, J. M., Ribeiro, L., Eusèbe, M., Coquery, M., 2009. Fate of pharmaceuticals and personal care products in wastewater treatment plants – Conception of a database and first results, Environmental Pollution 157(5), 1721-1726.

Mikhailik, O. M., Povstugar, V. I., Mikhailova, S. S., Lyakhovich, A. M., Fedorenko, O. M., Kurbatova, G. T., Shklovskaya, N. I., Chuiko, A. A., 1991. Surface structure of finely

dispersed iron powders I. Formation of stabilizing coating, Colloids and Surfaces 52(C), 315-324.

Mizukoshi, Y., Shuto, T., Masahashi, N., Tanabe, S., 2009. Preparation of superparamagnetic magnetite nanoparticles by reverse precipitation method: Contribution of sonochemically generated oxidants, Ultrasonics sonochemistry 16(4), 525-531.

Moeser, G. D., Roach, K. A., Green, W. H., Hatton, T. A., Laibinis, P. E., 2004. High-gradient magnetic separation of coated magnetic nanoparticles, AICHE Journal 50(11), 2835-2848.

Moeser, G. D., Roach, K. A., Green, W. H., Laibinis, P. E., Hatton, T. A., 2002. Water-based magnetic fluids as extractants for synthetic organic compounds, Industrial & Engineering Chemistry Research 41(19), 4739-4749.

Nakada, N., Shinohara, H., Murata, A., Kiri, K., Managaki, S., Sato, N., Takada, H., 2007. Removal of selected pharmaceuticals and personal care products (PPCPs) and endocrine-disrupting chemicals (EDCs) during sand filtration and ozonation at a municipal sewage treatment plant, Water research 41(19), 4373-4382.

Nappini, S., Bombelli, F. B., Bonini, M., Nordèn, B., Baglioni, P., 2010. Magnetoliposomes for controlled drug release in the presence of low-frequency magnetic field, Soft Matter 6(1), 154-162.

Noggle, J. H., 1996. Physical Chemistry. New York: Harper Collins Publishers.

Odenbach, S., 2002. Ferrofluids : Magnetically Controllable Fluids and their Applications. Berlin ; New York: Springer.

Oetken, M., Nentwig, G., Löffler, D., Ternes, T., Oehlmann, J., 2005. Effects of pharmaceuticals on aquatic invertebrates. Part I. The antiepileptic drug carbamazepine, Archives of Environmental Contamination and Toxicology 49(3), 353-361.

Olah, J., Cserhati, T., Szejtli, J., 1988. Beta-Cyclodextrin Enhanced Biological Detoxification of Industrial Wastewaters, Water research 22(11), 1345-1351.

Olle, B., Bucak, S., Holmes, T. C., Bromberg, L., Hatton, T. A., Wang, D. I. C., 2006. Enhancement of oxygen mass transfer using functionalized magnetic nanoparticles, Industrial and Engineering Chemistry Research 45(12), 4355-4363.

Palmacci, S., Josephson, L., 1993. Synthesis of polysaccharide covered superparamagnetic oxide colloids .

Pankhurst, Q. A., Connolly, J., Jones, S. K., Dobson, J., 2003. Applications of magnetic nanoparticles in biomedicine, Journal of Physics D: Applied Physics 36(13).

Panneerselvam, P., Morad, N., Aik, T. K., 2011. Magnetic nanoparticle (Fe3O4) impregnated onto tea waste for the removal of nickel (II) from aqueous solution, Journal of hazardous materials 186(1), 168.

Pardoe, H., Chua-anusorn, W., St. Pierre, T. G., Dobson, J., 2001. Structural and magnetic properties of nanoscale iron oxide particles synthesized in the presence of dextran or polyvinyl alcohol, Journal of Magnetism and Magnetic Materials 225(1-2), 41-46.

Peng, S., Wang, C., Xie, J., Sun, S., 2006. Synthesis and stabilization of monodisperse Fe nanoparticles, Journal of the American Chemical Society 128(33), 10676-10677.

Perret, D., Gentili, A., Marchese, S., Greco, A., Curini, R., 2006. Sulphonamide residues in Italian surface and drinking waters: A small scale reconnaissance, Chromatographia 63(5), 225-232.

Petričenko, O., Cebers, A., Maiorov, M. M., Plotniece, A., 2010. Properties of dextran coated magnetic nanoparticles, Magnetohydrodynamics (3), 309-316.

Pich, A., Bhattacharya, S., Lu, Y., Boyko, V., Adler, H. -. P., 2004. Temperature-sensitive hybrid microgels with magnetic properties, Langmuir 20(24), 10706-10711.

Prabaharan, M., Gong, S., 2008. Novel thiolated carboxymethyl chitosan-g- beta - cyclodextrin as mucoadhesive hydrophobic drug delivery carriers, Carbohydrate Polymers 73(1), 117-125.

Purdom, G.; Mistry, P., 1994, Effect of household chemicals on municipal solid waste (MSW) digestion, Institution of Chemical Engineers Symposium Series , 34-36.

Raloff, J., 1998. Drugged Waters: Does It Matter That Pharmaceuticals Are Turning Up In Water Supplies? Science News 153(187), 189.

Ramírez, L. P., Landfester, K., 2003. Magnetic polystyrene nanoparticles with a high magnetite content obtained by miniemulsion processes, Macromolecular Chemistry and Physics 204(1), 22-31.

Ray, S. C., Bhattacharyya, S., Wu, S. L., Ling, D. C., Pong, W. F., Giorcelli, M., Bianco, S., Tagliaferro, A., 2010. High coercivity magnetic multi-wall carbon nanotubes for low-dimensional high-density magnetic recording media, Diamond and Related Materials 19(5-6), 553-556.

Reimers, G. W., Khalafalla, S. E., 1972. PREPARING MAGNETIC FLUIDS BY A PEPTIZING METHOD. U S Bur Mine .

Rekharsky, M. V., Inoue, Y., 1998. Complexation Thermodynamics of Cyclodextrins, Chemical reviews 98(5), 1875-1918.

Richardson, M. L., Bowron, J. M., 1985. The fate of pharmaceutical chemicals in the aquatic environment, Journal of Pharmacy and Pharmacology 37(1), 1-12.

Robinson, B. J., Hui, J. P. M., Soo, E. C., Hellou, J., 2009. Estrogenic compounds in seawater and sediment from Halifax Harbour, Nova Scotia, Canada, Environmental Toxicology and Chemistry 28(1), 18-25.

Rodriguez, B. E., Wolfe, M. S., Fryd, M., 1994.
Nonuniform swelling of alkali swellable microgels, Macromolecules 27(22), 6642-6647.

Sahingr, N., Ilsin, P., 2010. Soft core-shell polymeric nanoparticles with magnetic property for potential guided drug delivery, Current Nanoscience 6(5), 483-491.

Sakaguchi, F., Akiyama, Y., Izumi, Y., Nishijima, S., 2009. Fundamental study on magnetic separation of aquatic organisms for preservation of marine ecosystem, Physica C: Superconductivity 469(15-20), 1835-1839.

Sakaguchi, F., Mishima, F., Akiyama, Y., Nishijima, S., 2010. Fundamental Study on Magnetic Separation of Aquatic Organisms Using a Superconducting Magnet, IEEE Transactions on Applied Superconductivity 20(3), 969-972.

Salipira, K. L., Mamba, B. B., Krause, R. W., Malefetse, T. J., Durbach, S. H., 2007. Carbon nanotubes and cyclodextrin polymers for removing organic pollutants from water, ENVIRONMENTAL CHEMISTRY LETTERS 5(1), 13-17.

Santos, L. H. M. L. M., Araújo, A. N., Fachini, A., Pena, A., Delerue-Matos, C., Montenegro, M. C. B. S. M., 2010. Ecotoxicological aspects related to the presence of pharmaceuticals in the aquatic environment, Journal of hazardous materials 175(1-3), 45-95.

Schneider, H., Hacket, F., Rüdiger, V., Ikeda, H., 1998. NMR Studies of Cyclodextrins and Cyclodextrin Complexes, Chemical reviews 98(5), 1755-1786.

Senyei, A., Widder, K., Czerlinski, G., 1978. Magnetic guidance of drug-carrying microspheres, Journal of Applied Physics 49(6), 3578-3583.

Servos, M. R., Smith, M., Mclnnis, R., Burnison, K., Lee, B. -., Seto, P., Backus, S., 2007a. The Presence of Selected Pharmaceuticals and Personal Care Products in Drinking Water in Ontario, Canada, Water Quality Research Journal of Canada 42(2), 130-137.

Servos, M. R., Smith, M., Mclnnis, R., 2007b. The Presence of Selected Pharmaceuticals and the Antimicrobial Triclosan in Drinking Water in Ontario, Canada, Water Quality Research Journal of Canada 42(2), 130-137.

Sharma, A. K., Mishra, A. K., 2010. Microwave induced β-cyclodextrin modification of chitosan for lead sorption, International journal of biological macromolecules .

Shimoiizaka, J., 1978a, Method for preparing a water base magnetic fluid and product (4094804).

Shimoiizaka, J., 1978b. Method for preparing a water base magnetic fluid and product, Method for preparing a water base magnetic fluid and product .

Smyth, S. A., Lishman, L. A., McBean, E. A., Kleywegt, S., Yang, J. -., Svoboda, M. L., Lee, H. -., Seto, P., 2008. Seasonal occurrence and removal of polycyclic and nitro musks from wastewater treatment plants in Ontario, Canada, Journal of Environmental Engineering and Science 7(4), 299-317.

Song, J., Kong, H., Jang, J., 2011. Adsorption of heavy metal ions from aqueous solution by polyrhodanine-encapsulated magnetic nanoparticles, Journal of colloid and interface science .

Stumm-Zollinger, E., Fair, G. M., 1965. Biodegradation of Steroid Hormones, Journal of Water Pollution Control Federation 37(11), 1506-1510.

Stumpf, M., Ternes, T. A., Wilken, R., Silvana, V. R., Baumann, W., 1999. Polar drug residues in sewage and natural waters in the state of Rio de Janeiro, Brazil, The Science of the total environment 225(1-2), 135-141.

Szejtli, J., 1994. Medicinal applications of cyclodextrins, Medicinal research reviews 14(3), 353-386.

Szejtli, J., 1988. Cyclodextrin Technology. : Dordrecht ; Boston: Kluwer Academic Publishers.

Szejtli, J., 1985. Cyclodextrins: A new group of industrial basic materials, Food/Nahrung 29(9), 911-924.

Tabak, H. H., Quave, S. A., Mashni, C. I., Barth, E. F., 1981. Biodegradability studies with organic priority pollutant compounds, Journal (Water Pollution Control Federation) 53(10), 1503-1518.

Tabatabaei, S. N.; Lapointe, J.; Martel, S., 2009, Hydrogel encapsulated magnetic nanoparticles as hyperthermic actuators for microrobots designed to operate in the vascular network, 2009 IEEE/RSJ International Conference on Intelligent Robots and Systems, IROS 2009 , 546-551.

Takisawa, N., Shirahama, K., Tanaka, I., 1993. Interactions of amphiphilic drugs withα-,β-, andγ-cyclodextrins, Colloid and Polymer Science 271(5), 499-506.

Tan, B. H., Tam, K. C., Lam, Y. C., Tan, C. B., 2005. Microstructure and rheology of stimuli-responsive microgel systems—effect of cross-linked density, Advances in Colloid and Interface Science 113(2-3), 111-120.

Tan, J. P. K., Tam, K. C., 2007. Application of drug selective electrode in the drug release study of pH-responsive microgels, Journal of Controlled Release 118(1), 87-94.

Tataru, G., Popa, M., Desbrieres, J., 2011. Magnetic microparticles based on natural polymers, International journal of pharmaceutics 404(1-2), 83-93.

Ternes, T. A., Meisenheimer, M., McDowell, D., Sacher, F., Brauch, H. J., Haist-Gulde, B., Preuss, G., Wilme, U., Zulei-Seibert, N., 2002. Removal of Pharmaceuticals during Drinking Water Treatment, Environmental science & technology 36(17), 3855-3863.

Ternes, T. A., 2001a. Analytical methods for the determination of pharmaceuticals in aqueous environmental samples, TrAC - Trends in Analytical Chemistry 20(8), 419-434.

Ternes, T. A., 2001b, Pharmaceuticals and metabolites as contaminants of the aquatic environment, ACS Symposium Series 791, 39-54.

Ternes, T. A., Hirsch, R., 2000. Occurrence and behavior of X-ray contrast media in sewage facilities and the aquatic environment, Environmental Science and Technology 34(13), 2741-2748.

Ternes, T. A., Stumpf, M., Mueller, J., Haberer, K., Wilken, R. -., Servos, M. R., 1999. Behavior and occurrence of estrogens in municipal sewage treatment plants — I. Investigations in Germany, Canada and Brazil, The Science of the total environment 225(1-2), 81-90.

Thünemann, A. F., Schütt, D., Kaufner, L., Pison, U., Möhwald, H., 2006. Maghemite nanoparticles protectively coated with poly(ethylene imine) and poly(ethylene oxide)-block-poly(glutamic acid), Langmuir 22(5), 2351-2357.

Trellenkamp, T., Ritter, H., 2010. Poly (N-vinylpyrrolidone) Bearing Covalently Attached Cyclodextrin via Click-Chemistry: Synthesis, Characterization, and Complexation Behavior with Phenolphthalein, Macromolecules 43(13), 5538-5543.

Tsipi, D., Hiskia, A., Heberer, T., Stan, H. -., 1998. Determination of Acidic Pesticides in the Drinking Water of Greece Using Capillary Gas Chromatography-Mass Spectrometry, Water, air, and soil pollution 104(3-4), 259-268.

Tudorachi, N., Chiriac, A., 2008. Magnetic composite based on vinylic template, Journal of Applied Polymer Science 108(6), 3690-3695.

Uekama, K., 2002. Recent aspects of pharmaceutical application of cyclodextrins, Journal of Inclusion Phenomena 44(1-4), 3-7.

Uekama, K., Hirayama, F., Irie, T., 1998a. Cyclodextrin Drug Carrier Systems, Chemical reviews 98(5), 2045-2076.

Uekama, K., Hirayama, F., Irie, T., 1998b. Cyclodextrin Drug Carrier Systems, Chemical reviews 98(5), 2045-2076.

Utkan, G., Sayar, F., Batat, P., Ide, S., Kriechbaum, M., Pişkin, E., 2011. Synthesis and characterization of nanomagnetite particles and their polymer coated forms, Journal of colloid and interface science 353(2), 372-379.

Vogt, C., Toprak, M. S., Muhammed, M., Laurent, S., Bridot, J. -., Müller, R. N., 2010. High quality and tuneable silica shell-magnetic core nanoparticles, Journal of Nanoparticle Research 12(4), 1137-1147.

Wacker, F. K., Reither, K., Ebert, W., Wendt, M., Lewin, J. S., Wolf, K. J., 2003. MR Image–guided Endovascular Procedures with the Ultrasmall Superparamagnetic Iron Oxide SH U 555 C as an Intravascular Contrast Agent: Study in Pigs, Radiology 226(2), 459.

Wang, C., Tam, K. C., Jenkins, R. D., Baselt, D. R., 2000. Potentiometric titration and dynamic light scattering of hydrophobically modified alkali soluble emulsion (HASE) polymer solutions, Physical Chemistry Chemical Physics 2(9), 1967-1972.

Wang, W. -., Neoh, K. -., Kong, E. -., 2006. Surface functionalization of Fe3O4 magnetic nanoparticles via RAFT-mediated graft polymerization, Macromolecular Rapid Communications 27(19), 1665-1669.

Webb, S., Ternes, T. A., Gibert, M., Olejniczak, K., 2003. Indirect human exposure to pharmaceuticals via drinking water, Toxicology letters 142(3), 157-167.

Widder, K. J., Morris, R. M., Poore, G. A., Howard, D. P., Senyei, A. E., 1983. Selective targeting of magnetic albumin microspheres containing low-dose doxorubicin: total remission in Yoshida sarcoma-bearing rats, European Journal of Cancer and Clinical Oncology 19(1), 135-139.

Widder, K. J., Senyel, A. E., Scarpelli, G. D., 1978. Magnetic microspheres: a model system of site specific drug delivery in vivo, Proceedings of the Society for Experimental Biology and Medicine.Society for Experimental Biology and Medicine (New York, N.Y.) 158(2), 141-146.

Willard, M., Kurihara, L., Carpenter, E. E., Calvin, S., Harris, V., 2004. Chemically prepared magnetic nanoparticles, International Materials Reviews, 49 3(4), 125-170.

Windle, P., Popplewell, J., Charles, S., 2002. The long term stability of mercury based ferromagnetic liquids, Magnetics, IEEE Transactions on 11(5), 1367-1369.

Wiseman, T., Williston, S., Brandts, J. F., Lin, L. -., 1989. Rapid measurement of binding constants and heats of binding using a new titration calorimeter, Analytical Biochemistry 179(1), 131-137.

Xu, R., 2001, Equilibrium studies of aqueous surfactant systems containing additives , PQDT - UK & Ireland .

Yallapu, M. M., Foy, S. P., Jain, T. K., Labhasetwar, V., 2010. PEG-functionalized magnetic nanoparticles for drug delivery and magnetic resonance imaging applications, Pharmaceutical research 27(11), 2283-2295.

Yang, S., Liu, H., Zhang, Z., 2008. A facile route to hollow superparamagnetic magnetite/polystyrene nanocomposite microspheres via inverse miniemulsion polymerization, Journal of Polymer Science, Part A: Polymer Chemistry 46(12), 3900-3910.

Yangde, Z., Zhaowu, Z., Weihua, Z., Xingyan, L., Zhenfa, L., Jun, L., Jianfeng, X., Yulin, L., Tiehui, H., Yifeng, P., 2008. The roles of hydrochloric acid and polyethylene glycol in magnetic fluids, Journal of Magnetism and Magnetic Materials 320(7), 1328-1334.

Yavuz, C. T., Prakash, A., Mayo, J. T., Colvin, V. L., 2009. Magnetic separations: From steel plants to biotechnology, Chemical Engineering Science 64(10), 2510-2521.

Yoon, Y., Westerhoff, P., Snyder, S. A., Wert, E. C., 2006. Nanofiltration and ultrafiltration of endocrine disrupting compounds, pharmaceuticals and personal care products, Journal of Membrane Science 270(1-2), 88-100.

Zborowski, M., Chalmers, J. J., 2008. Magnetic Cell Separation. Amsterdam ; Boston: Elsevier.

Zhang, J., Xu, S., Kumacheva, E., 2004. Polymer microgels: Reactors for semiconductor, metal, and magnetic nanoparticles, Journal of the American Chemical Society 126(25), 7908-7914.

Zins, D., Cabuil, V., Massart, R., 1999. New aqueous magnetic fluids, Journal of Molecular Liquids 83(1-3), 217-232.